UNIVERSITY OF MODENA AND REGGIO EMILIA
Department of Biomedical, Metabolic and Neural Sciences

Ph.D. School in Neurosciences
XXVI Cycle

A new strategy to fool the blood-brain barrier: *in vivo* study of uptake, distribution and transport of CNS-targeted nanoparticles within the brain

Ph.D. School Director: Prof. MICHELE ZOLI

Supervisor: Prof. MICHELE ZOLI

Co-supervisor: Dr. GIOVANNI TOSI

PhD Student
Dr. ANTONIETTA VILELLA

ACADEMIC YEAR 2013/14

INDEX

pag.

LIST OF PAPERS 4
ABBREVIATIONS 5
INTRODUCTION 10

1. BARRIERS TO CNS DRUG DELIVERY 12
1.1 Blood-brain barrier 12
1.2 Blood-cerebrospinal fluid barrier 15

2.NANOCARRIERS FOR BRAIN DELIVERY 16
(i) Liposomes 16
(ii) Solid lipid nanoparticles 17
(iii) Polymeric nanoparticles 17
(iv) Nanogels 17
(v) Dendrimers 17
(vi) Carbon nanotubes 18
(vii) Quantum dots 18

3.STRATEGIES TO ENHANCE CNS DRUG PENETRATION 18
(i)Carrier mediated transport 19
(ii)Receptor-mediated endocytosis 19

4.ALTERNATIVE ROUTES TO CNS DRUG DELIVERY 21

5. BRAIN DRUG DELIVERY USING NPs: PLGA NANOPARTICLES 23
5.1 Biodegradation 23
5.2 Biodistribution 23
5.3 Therapeutic applications of PLGA-NPs 24
5.4 BBB-crossing PLGA-NPs: g7 peptide 25

AIM OF THE THESIS 27

METHODS 28
1.Formulation and purification of NPs 28
2.Preparation of antibody-modified R-g7-NPs: NCAM-R-g7-NPs and CD44-R-g7-NPs 28
2.1 Determination of molecule loading 29

3. Characterization of NPs: morphology, particle size and surface analysis 30
3.1 Evaluation of NPs-stability 31
4. Animal procedures and sample preparation for BBB-crossing and BBB-integrity studies 31
4.1 Intraperitoneal administration of g7-NPs 31
4.2 Intranasal administration of g7-NPs 31
4.3 Oral administration of g7-NPs 32
4.4 Assessment of BBB-integrity 32
5. Animal procedures and sample preparation for injection of modified- and unmodified-g7-NPs 32
6. Immunohistochemistry of brain sections 33
7. In vivo endocytosis inhibition 34
8. Quantification of nanoparticles and Rab5 immunoreactivity 34
9. Cell-to-cell exchange of nanoparticles 34

RESULTS 35
1. Routes of g7-NP administration 35
1.1 Intraperitoneal administration of g7-NPs 35
1.2 Intranasal administration of g7-NPs 36
1.3 Oral administration of g7-NPs 36
1.4 BBB integrity 37
2.g7-NP accumulation in brain areas and cell types: in vivo evidence 37
3. Time-course and dose-response study: in vivo evidence 39
4. Nanoparticle uptake mechanisms 42
5. Cell-to-cell exchange of nanoparticles 46
6. Engineered Ab-modified g7-NP accumulation in brain areas and cell types: in vivo evidence 48

DISCUSSION 50
REFERENCE LIST 71

LIST OF PAPERS

In this thesis the following papers will be discussed.

1. Tosi G., Ruozi B., Belletti D.,**Vilella A**., Zoli M., Vandelli M.A., Forni F.
Brain-targeted polymeric nanoparticles: in vivo evidence of different routes of administration in rodents. Nanomedicine (Lond). 2013 Sep;8(9):1373-83

2. **Vilella A**., Tosi G., Grabrucker A.M., Ruozi B., Belletti D., Vandelli M.A., Boeckers T.M., Forni F., Zoli M.
Insight on the fate of CNS-targeted nanoparticles. Part I: Rab5-dependent cell-specific uptake and distribution. Journal of Controlled Release. 2014 Jan28:174:195-201

3. Tosi G., **Vilella A.**, Chhabra R., Schmeisser M.J., Boeckers T.M., Ruozi B., Vandelli M.A., Forni F., Zoli M., Gracrucker A.M.
Insight on the fate of CNS-targeted nanoparticles. Part II: Intercellular neuronal cell-to-cell transport. Journal of Controlled Release. 2014 Jan11:177C:96-107

ABBREVIATIONS

5hmC	5-hydroxymethylcytosine
5mC	5-methylcytosine
6-OHDA	6-hydroxydopamine
aCSF	Artificial cerebrospinal fluid
AD	Alzheimer's disease
AFM	Atomic force microscopy
AMPA	α-Amino-3-hydroxy-5-methyl-4-isoxazolepropionic acid
ApoB	Apoliprotein B
ApoE	Apoliprotein E
ApoR	Apoliprotein receptor
APP	Amyloid precursor protein
ATP	Adenosine triphosphate
Aβ	Amyloid-beta peptide
BBB	Blood brain barrier
BBBD	Blood brain barrier disruption
BCB	Blood-cerebrospinal fluid barrier
BFCN	Basal forebrain cholinergic neuron
bFGF	Basic fibroblast growth factor
BPD	Bipolar disease
BSA	Bovine serum albumin
C-NP	Control nanoparticle
CA	Cornu Ammonis
CAT1	Cationic amino acid transporter
CB	Calbindin
CC	Corpus callosum
CD44-g7-NP	CD44-g7-nanoparticle
Cg	Cingulate cortex
CLIC	Clathrin- and dynamin-independent carrier
CMT	Carrier-mediated transport
CNS	Central nervous system
CNT2	Nucleoside transporter 2
CP	Choroid plexus
CR	Calretinin
CRH	Corticotrophin releasing hormone
CSF	Cerebrospinal fluid
CVO	Circumventriculat organ
Cx	Cerebral cortex

DA	Dopamine
DAPI	4',6-diamidino-2-phenylindole
DDS	Drug delivery system
DG	Dentate gyrus
DMSO	Dimethyl sulfoxide
DNMT1	DNA-methyltransferase 1
DNMT3a	DNA-methyltransferase 3a
EDC	1-Ethyl-3-(3-dimethylaminopropyl)-carbodiimide
EE	Early endosome
EEA1	Early endosome antigen 1
EEC	Early endosomal compartment
EEN	Early endosomal network
ELP	Endosomal-lysosomal pathway
EMA	European Medicine Agency
ERK	Extracellular signal-regulated kinase
ESCA	Electron spectroscopy for chemical analysis
Eto-PLGA-NP	Etoposide-loaded PLGA NP
FGF	Fibroblast growth factor
g7	Glycopeptide H2N-Gly-L-Phe-D-Thr-Gly-L-Phe-L-Leu-L-Ser(O-β-D-glucose)-CONH2
g7-NP	g7-nanoparticle
g7-NP-NHS	g7-N–hydroxy-succinimide nanoparticle
GA	Glycolic acid
GABA	γ-Aminobutyric acid
$GABA_A$	γ-Aminobutyric acid-A receptor
$GABA_B$	γ-Aminobutyric acid-B receptor
GAD	Glutamic acid decarboxylase
GDNF	Glial cell derived neurotrophic factor
GEEC	Glycosyl-phosphatidylinositol-anchored protein-enriched early endosomal compartment
GFAP	Glial fibrillary acid protein
GFP	Green fluorescent protein
GluA1	Glutamate receptor A1
GluA2	Glutamate receptor A2
GLUT	Glucose transporter
GPI	C-terminal glycophosphatidyl-inositol
Gr	Granular layer of hippocampus
GTPase	Guanidine triphosphatase
HD	Huntington’s disease
Hil	Hilus
hIR	Human insulin receptor

HSA-NP	Human serum albumin nanoparticle
i.c.v.	Intracerebroventricular
i.n.	Intranasal
i.p.	Intraperitoneal
i.t.	Intrathecal
i.v.	Intravenous
iba1	Ionized calcium-binding adapter molecule 1
IF	Immunofluorescence histochemistry
IGFI	Insulin like growth factor-I
IGFII	Insulin like growth factor-II
ir	Immunoreactive
IR	Insulin receptor
LA	Lactic acid
LAT1	Large amino acid transporter 1
LDH	Lactate dehydrogenase
LDH-NP	Layered double hydroxide-nanoparticle
LDL	Low density lipoprotein
LDLr	Low density lipoprotein receptor
LEC	Late endosomal compartment
LE	Late endosome
Lf	Lactoferrin
Lf-NP	Lactoferrin nanoparticle
LMol	Stratum lacunosum-moleculare
Lop	Loperamide
LPS	Lipopolysaccharide
Lps	Liposome
LTD	long-term depression
LTP	long-term potentiation
LV	Lateral ventricle
MAP	Mitogen-activated protein kinases
MCT1	Monocarboxylic acid transporter
MES	2-(N-morpholino)ethanesulfonic acid
MGE	Medial ganglionic eminence
MPTP	1-methyl-4-phenyl-1,2,3,6,tetrahydropyridine
mRNA	Messenger ribonucleic acid
MTf	Melanotransferrin
MTT	3-(4,5-dimethylthiazol-2yl)-2,5-diphenyltetrazolium bromide
MW	Molecular weight
NCAM-g7-NP	Neural cell adhesion molecule1-g7-nanoparticle
NCAM1	Neural cell adhesion molecule 1

NeuN	Neuronal nuclei
NFT	Neurofibrillary tangle
NGF	Nerve growth factor
NHS	N–hydroxy-succinimide
NP	Polymeric nanoparticle
NPY	Neuropeptide Y
Nrf2	Nuclear erythroid 2-related transcription factor
NS	Normal serum
o.a.	Oral administration
PBCA-NP	Polymeric n-butyl-2-cyanoacrylate nanoparticle
PCA-NP	Polycyanoacrylate nanoparticle
PCS	Photon correlation spectroscopy
PD	Parkinson's disease
PEG	Polyethylenglycol
PEG-PHDCA-NP	PEG-n-hexadecylcyanoacrylate nanoparticle
PEG-PLA-NP	PEG-polylactic acid nanoparticle
PEG-PLGA-NP	PEG-Poly(lactic-co-glycolic acid) nanoparticle
PEI	Polyethyleneimine
PFC	Prefrontal cortex
Pgp	P glycoprotein
PIK3	Phosphoinositide 3-kinase
PLGA	Poly(lactic-co-glycolic acid)
PLGA-NP	Poly(lactic-co-glycolic acid)-nanoparticle
PS	Polystyrene
PS-NP	Polystyrene-nanoparticle
PV	Parvalbumin
PVA	Polyvinyl alcohol
PVP	Polyvinyl pyrrolidone
Pyr	Pyramidal layer of hippocampus
qD	Quantum dot
Reln	Reelin
RES	Reticuloendothelial system
Rhod	Rhodamine 123
RME	Receptor mediated endocytosis
RT	Room temperature
SA	Sialic acid
SAM	S-adenosyl-methionine
SFO	Subfornical organ
siRNA	Small interfering ribonucleic acid
SLN	Solid lipod nanoparticle
SLT	Solanum tuberosum lectin

SN	Substantia nigra
SS	Somatostatin
STL-PEG-PLGA NP	Solanum tuberosum lectin-PEG-PLGA nanoparticle
SZ	Schizophrenia
TEM	Transmission electron microscopy
TeNT	H_c tetanus toxin heavy chain
Tf-NP	Transferrin nanoparticle
TfR	Transferrin receptor
TGN	Trans-Golgi network
TH	Tyrosine hydroxylase
TNFαip2	Tumor necrosis factor−α induced protein 2
TNT	Tunneling nanotube
TrkA	Neurotrophin tyrosine kinase receptor type 1
UCN	Urocortin
US FDA	American Food and Drug Administration
VEGF	Vascular endothelial growth factor
VIP	Vasoactive intestinal peptide

INTRODUCTION

In the last decades, a growing number of publication at the intersection between nanotechnology and drug delivery contributed to the development of a new branch of science named nanomedicine, in which drug administration, pharmacokinetics and pharmacodynamics are affected by the use of materials organized in nanoscale structures to generate new strategies for drug delivery and targeting (Tosi et al 2013).

Nanomedicine started when scientists, working on pharmacologically active substances, understood that a main problem of such molecules was represented by their wide and non-specific biodistribution resulting in the increase of toxicity and in the decrease in compliance of patients and benefit-risk ratio, after administration to human body. In this view, the development of new drug delivery systems (DDS), able to improve the pharmacokinetics profile of drugs, protect the body from the exposure to a large amount of drugs, and decrease the circulating dose, represents a most innovative improvement of pharmaceutical research.

Notwithstanding nanomedical research started 20 years ago, still a limited number of new technology-based pharmaceutical products is available on the market (Wagner et al 2006) nowadays for different applications, especially in the field of cancer and infection, though an increasing number of phase I-II studies is currently on-going.

The success of the applications of this new “synthetic” strategy has prompted the interest in many scientists to develop nanotechnological approaches also in basic and clinical neuroscience. Despite enormous advances in brain research, central nervous system (CNS) disorders remain the world’s leading cause of disability and the treatment of neurological diseases represents one of the most difficult challenges in medicine.

A main limitation of therapies for neuropsychiatric diseases is the inability of the majority of drugs to reach the brain parenchyma, when intravenously administered. Many existing pharmaceutical agents are ineffective in the treatment of cerebral diseases due to the inability to be effectively delivered into the brain. The clinical failure of many potentially effective therapeutic agents is often not due to the lack of drug potency but rather to shortcomings in the methods by which the drug is delivered.

Unfortunately, the same mechanism that protects the brain against intrusive chemicals can also frustrate therapeutic interventions. In this regard, the first problem to solve to more effectively deliver a drug to the brain for treating specific neurological disorders such as meningitis, encephalitis, degenerative diseases like Alzheimer's (AD), and Parkinson's (PD) disease and tumors as glioblastoma is to overcome the blood brain barrier (BBB). Engineered nanoparticles are an important tool to realize a number of these applications.

In the following chapters, different categories of nanocarriers will be discussed, preceded by an introductory section focused on the most important biological features of the natural CNS protective barriers, i.e., the BBB and the blood cerebrospinal fluid barrier (BCB), and the strategies to enhance CNS drug delivery.

1. BARRIERS TO CNS DRUG DELIVERY

1.1 *Blood-brain barrier*

It is well established that the BBB is a unique membranous barrier that tightly segregates the brain from the circulating blood. The BBB is formed by the endothelial cells of cerebral microvessels and creates the critical interface regulating the molecular fluxes between blood and brain (Patabendige et al 2013). Differently from blood capillaries in other tissues, CNS capillaries generate a permeability barrier between the blood and the extracellular fluid in brain tissue (Fig.1).

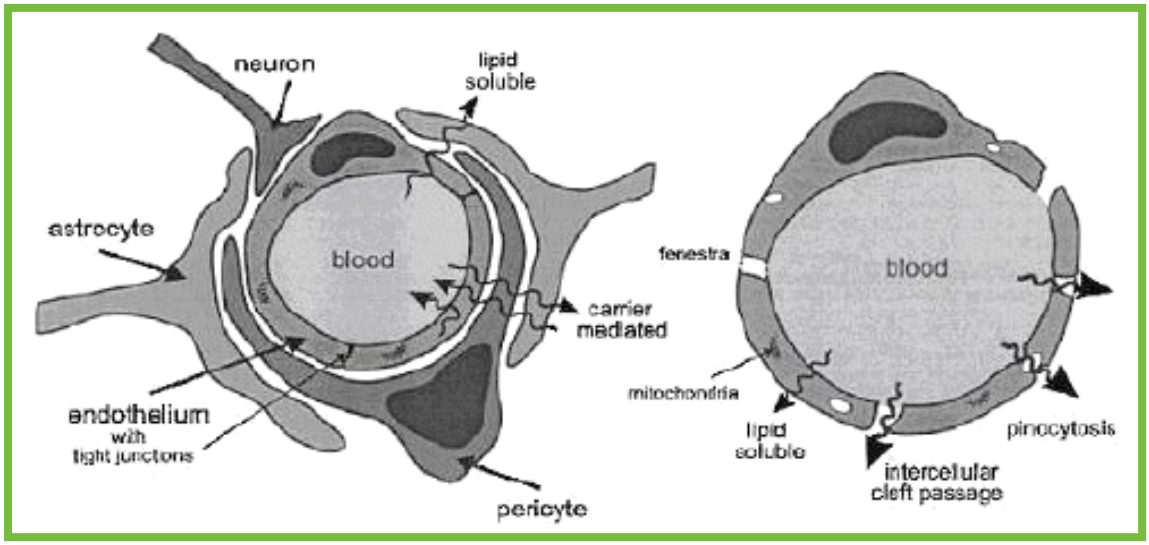


Fig.1: Schematic comparison between general (right) and brain (left) capillaries. (From Misra et al 2003)

Capillaries of the vertebrate brain and spinal cord lack the small pores that allow rapid movement of solutes from circulation into other organs and vice versa; CNS capillaries are lined with a layer of special endothelial cells that lack pores or fenestrations and are sealed with tight junctions (Fig.2).

Glial cells are of three types. Astrocytes form the structural framework for the neurons and control their biochemical environment. Astrocyte foot processes or limbs encapsulate the capillaries and form the external layer of the BBB. Oligodendrocytes are responsible for the formation and maintenance of the myelin sheath, which surrounds axons and is essential for the fast transmission of

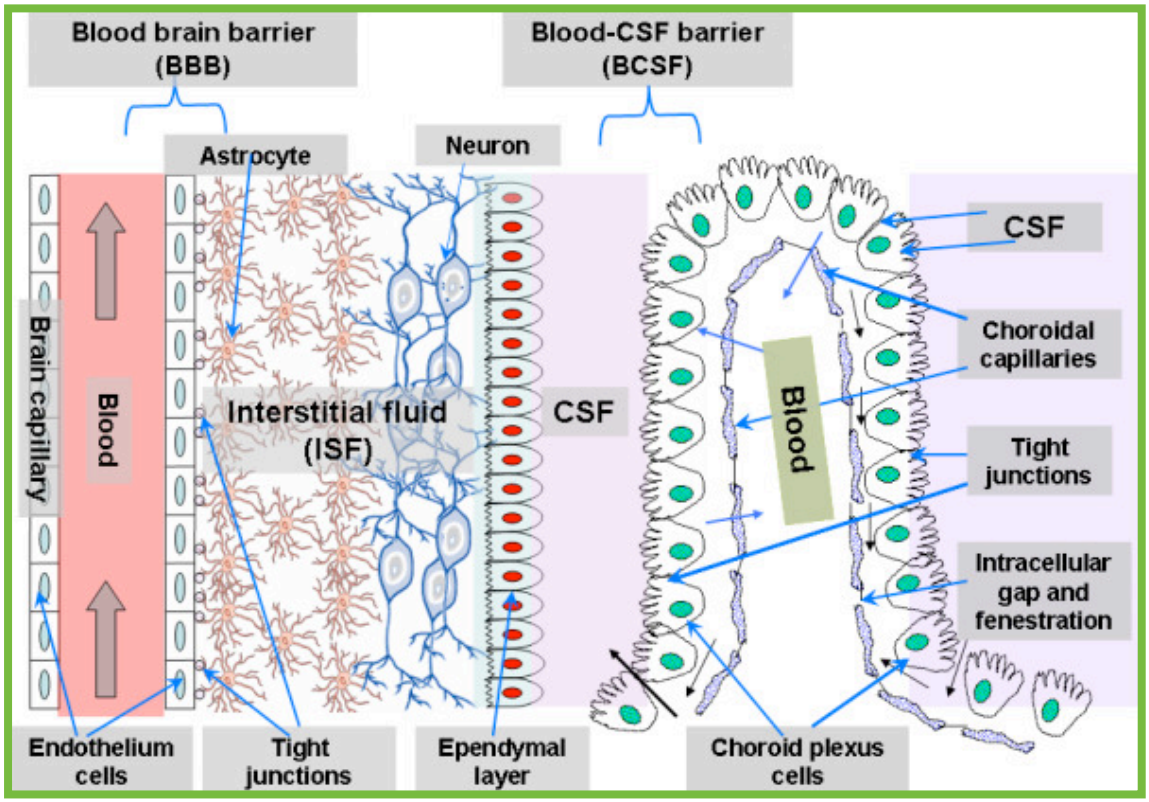


Fig.2: Overview of the two main barriers of the CNS, blood-brain barrier (BBB) and blood cerebrospinal fluid barrier (BCB). ISF: Interstitial Fluid. CSF: Cerebrospinal fluid **(From Bhaskar et al 2010)**

action potentials by saltatory conduction. Microglia are blood- or brain-borne mononuclear macrophages.

Microvessels make up an estimated 95% of the total surface area of the BBB, and represent the principal route by which chemicals enter the brain. Vessels in brain were found to have somewhat smaller diameter and thinner wall than vessels in other organs.

In CNS capillaries, intercellular cleft, pinocytosis, and fenestrae are virtually nonexistent; blood-brain exchange must pass trans-cellularly. Therefore, only lipid-soluble solutes that can freely diffuse through the capillary endothelial membrane may passively cross the BBB. In capillaries of other parts of the body, such exchange is overshadowed by other nonspecific exchanges. Despite the estimated total length of 650 km and total surface area of 12 m^2 of capillaries in human brain, this barrier is very efficient and makes the brain practically inaccessible to lipid-insoluble compounds such as polar molecules and small ions. As a consequence, the therapeutic value of many promising drugs is

diminished, and cerebral diseases have proved to be most refractory to therapeutic interventions.

Some regions of the CNS do not express the classical BBB, but have microvessels similar to those of peripheral organs. These areas are the choroid plexus (CP) and the circumventricular organs (CVOs). The CVOs include the median eminence, the neurohypophysis, the pineal gland, the organum vasculosum of the lamina terminalis, the subfornical organ (SFO), the subcommissural organ and the area postrema. In the CVO regions and CP the capillaries are more permeable to solute and endothelial cells contain fenestrated. In detail, the epithelium of CP is polarized with the basolateral side facing the blood, whereas the apical part contains microvilli that are in direct contact with the CSF. All solutes are transported through the BBB and BCB to the brain interstitial fluid and CSF, respectively. The cells forming these barriers transport essential nutrients, metals and pharmaceuticals into the brain in a controlled manner (Begley 1996).

The BBB has an additional enzymatic aspect. Solutes crossing the cell membrane are subsequently exposed to degrading enzymes present in large numbers inside the endothelial cells that contain large densities of mitochondria, metabolically highly active organelles. BBB enzymes also recognize and rapidly degrade most peptides, including naturally occurring neuropeptides (Witt et al 2001).

Finally, the BBB is further reinforced by a high concentration of P-glycoproteins (Pgp), active-drug-efflux-transporter protein expressed by the luminal membranes of the cerebral capillary endothelium. This efflux transporter actively removes a broad range of drug molecules from the endothelial cell cytoplasm before they cross into the brain parenchyma. Fig.1 gives a schematic representation of all these BBB properties comparing brain and general capillaries.

1.2 *Blood-cerebrospinal fluid barrier*

The BCB represents the second barrier that a systemically administered drug may encounter before entering the CNS. The BCB strictly regulates the passage of blood-borne molecules into the CSF. Since the CSF can exchange molecules with the interstitial fluid of the brain parenchyma, the BCB indirectly protects brain from blood-borne molecules. Physiologically, the BCB is found in the epithelia of the CP and the arachnoid membrane (Fig.2).

On the external surface of the brain the ependymal cells fold over onto themselves to form a double layered structure, which lies between the dura and pia mater, that is called the arachnoid membrane. Within the double layer is the subarachnoid space, which participates in CSF drainage. Passage of substances from the blood through the arachnoid membrane is prevented by tight junctions (Nabeshima et al 1975). The arachnoid membrane is generally impermeable to hydrophilic substances, and its role in forming the BCB is largely passive.

The CP forms the CSF and actively regulates the concentration of molecules in the CSF. The CP consists of highly vascularized, "cauliflower-like" masses of pia mater tissue that dip into pockets formed by ependymal cells. The majority of CP is distributed throughout the fourth ventricle near the base of the brain and in the lateral ventricles inside the right and left cerebral hemispheres. The cells of the CP epithelium are modified and have epithelial characteristics. These ependymal cells have microvilli on the CSF side, basolateral interdigitations, and abundant mitochondria. The ependymal cells, which line the ventricles, form a continuous sheet around the CP. While the capillaries of the CP are fenestrated, non-continuous and have gaps between the capillary endothelial cells allowing the free-movement of small molecules, the adjacent choroidal epithelial cells form tight junctions preventing most BCB passage of macromolecules (Brightman 1968).

2. NANOCARRIERS FOR BRAIN DELIVERY

An ideal method for the delivery of therapeutic agents across the BBB should have the following characteristics:

✤ it should be controlled

✤ it should not damage the barrier

✤ the carrier system should be degradable and non-toxic

✤ transport of drugs across the BBB should be selective

✤ systemic delivery should be targeted to the BBB and the site of intended action in the brain

✤ the loaded drug transported through the BBB should be adequate for reaching therapeutic concentrations in the brain

✤ therapeutic concentration should be maintained for a sufficient duration of time for the desired efficacy.

Among the available approaches, nanobiotechnology-based delivery methods provide the best prospects for achieving this ideal. In fact, the use of nanomaterials to deliver drugs to the brain across the BBB may provide a significant advantage over currently used strategies, without any damage to the BBB.

Several nanoparticles have been used for drug delivery to various organs by a variety of methods, but only those relevant for the BBB will be briefly discussed in this section.

Depending on the biomaterial and morphology of the DDS, different categories of nanocarrier can be identified: (i) liposomes (Lps), (ii) solid lipid nanoparticles (SLNs), (iii) polymeric nanoparticles (NPs), (iv) nanogels, (v) dendrimers, (vi) carbon nanotubes and (vii) quantum dots (qDs).

(i) Lps, which are obtained starting from phospholipids, represent the first generation of the novel colloidal carriers (Bawarski et al 2008, Costantino et al 2009), and consist of one or more phospholipid bilayers surrounding an aqueous space. According to their size and number of bilayers, Lps can be classified into three categories: unilamellar (10–50 nm), multilamellar (20–100 nm) and large unilamellar (50–1000 nm) vesicles. Water-soluble drugs can be included within the aqueous compartment while lipophilic and amphiphilic molecules can be

associated with lipid bilayers (Ricci-Junior & Marchetti 2006). These structures have long been used as carriers for the delivery of therapeutic agents because of their easy preparation, good biocompatibility, low toxicity, and commercial availability. Main limitations of these systems are low physico-chemical stability, short *in vivo* life and fast release of encapsulated drugs, thus hampering their parenteral application in chronic affections.

(ii)SLNs are made of lipids which remain solid at room temperature (RT). Important advantages include high drug loading capacity, the possibility to control drug release and targeting, and to increase long-term stability during storage. SLNs have been investigated as possible carriers for modified drug delivery and targeting after intravenous administration or as oral drug carriers to overcome administration problems of drugs that are unstable in the gastrointestinal tract or are inadequately absorbed (Yang et al 1999). Furthermore, the possibility to produce SLNs in a large scale at low cost and with excellent reproducibility performing high pressure homogenization method is of great value towards a scale up and industrial production (Bondi & Craparo 2010, Denora et al 2009).

(iii) NPs are colloidal systems in the size range of 1-300 nm, realized with polymers of different nature, which can consist of biocompatible and biodegradable copolymers with low water solubility (Kumari et al 2010, Prokop & Davidson 2008). Long lasting *in vivo* life and higher stability are advantages of NPs over Lps. On the other hand, since use of organic solvents (to dissolve the polymer) and surfactant (to reduce the interfacial tension during formulation) is requested during the preparation of the carrier, the purification process of NPs is a challenging step. All the techniques of preparation have been recently described in the literature.

(iv) Nanogels are another novel class of nanomaterials (Vinogradov et al 2002) representing hydrogels of cross-linked polymer networks and ionic and nonionic chains such as polyethyleneimine (PEI). Such networks can incorporate charged molecules such as small interfering RNA (siRNA), DNA, oligonucleotides, and low-molecular-mass compounds, which bind to oppositely charged ionic chains.

(v) Dendrimers are repeatedly branched polymer molecules grown from one or several cores with a typical diameter ranging 1-20 nm: the outside surface allows drug loading while shell degradation under physiological conditions

results in drug release (Svenson & Tomalia 2005). Dendritic structures can also be used as building blocks for attachment of various functional moieties to the surface: hydrophobic and hydrophilic polymer blocks can be grafted to the surface resulting in formation of unimolecular micelles (Liu et al 2000, Tsai et al 2006, Wang et al 2005, Yang & Kao 2006) that, unlike conventional ones, are stable upon dilution and do not disintegrate during circulation in the body. Apart from drug delivery applications, dendrimers are being investigated for bacterial cell killing, gene transfer agents and trans-membrane transport.

(vi) Carbon nanotubes, fullerenes with cylindrical nanostructure, can be either single or multiwalled and have the potential to act as biopersistent fibers and DDS (Liu et al 2008). Nanotubes have length-to-diameter ratios higher than 100, with lengths of several μm and diameters of 0.7 to 1.5 nm for single-walled carbon nanotubes or 2 to 50 nm for multiwalled carbon nanotubes. Concerns have been raised about *in vivo* toxicity affecting cardiovascular and pulmonary systems (Lam et al 2004, Warheit et al 2004).

(vii) qDs are a heterogeneous group of NPs (for review see Hardman 2006), ranging from 2.5 to 100 nm, depending on coating thickness, with cell or cell organelle specific targeting after bioactive coating (Akerman et al 2002, Dahan et al 2003, Howarth et al 2008).

3. STRATEGIES TO ENHANCE CNS DRUG PENETRATION

To circumvent the barriers limiting CNS penetration by potential therapeutic agents, numerous drug delivery strategies have been developed (Lo et al 2001, Siegal & Zylber-Katz 2002). These strategies fall into one or more of the following three categories: manipulating drugs (lipophilic analogs, prodrugs), disrupting the BBB (an invasive strategy for enhanced CNS drug delivery involving the systemic administration of drugs in conjunction with transient BBB disruption (BBBD)) and finding alternative approaches for drug delivery as *molecular Trojan horse*.

Despite advances in rational CNS drug design and BBBD, many potentially efficacious drug molecules still cannot penetrate into the brain parenchyma at therapeutic concentrations. A winning strategy might consist in mimicking strategies used by the endothelial cells of BBB to exchange nutrients between CNS and blood in physiological conditions: the so called *molecular Trojan horse*.

Briefly, a specific ligand can be bound onto the nanocarrier surface in order to enhance the CNS delivery (De Rosa et al 2012).

Two main transport routes (see also schematic representation in Fig.3) have been exploited to actively target BBB: (i) carrier-mediated transport (CMT) and (ii) receptor-mediated endocytosis (RME).

(i) CMT is a form of active or passive diffusion, depending on the context, and accounts for the unidirectional transport of molecules from the blood to the brain. It is involved in the transport of vital nutrients required for normal brain homeostasis. These transporters are responsible for the brain delivery of substrates such as D-glucose (GLUT, glucose transporter), large neutral amino acids (the LAT1 large neutral amino acid transporter, the CAT1 cationic amino acid transporter), carboxylic acids (the MCT1 monocarboxylic acid transporter) and nucleosides (the CNT2 nucleoside transporter) into the brain. CMT can be used for targeting of CNS. From a general point of view, nutrients or their analogues, for which specific transporters exist on BBB endothelium, can be bound to the nanovector surface. By this strategy, the ligand transport into the CNS lumen leads also to the transport of the nanocarrier bearing the ligand on its surface. Into the brain tissue, the nanovectors can release their cargo by different mechanisms depending on the type of carrier used.

(ii) RME or clathrin-dependent endocytosis is a highly specific and energy mediated transport enabling eukaryotic cells to selectively uptake macromolecules as specific cargo. The BBB receptor-specific ligands have also been shown to be very effective to transport endogenous peptides like insulin, insulin like growth factor-I (IGF-I), insulin like growth factor-II (IGF-II), transferrin (Tf), albumin, and opioid peptides e.g. deltorphins, [D-penicillamine 2,5] enkephalin and deltorphin II (Fiori et al 1997, Roberts et al 1993, Tabernero et al 2002, Witt et al 2000). That is why receptor-mediated drug delivery, is also a promising approach for the release of therapeutic agents into neuronal cells, and tissues; nanocarriers conjugated to different types of ligands for cell surface receptors expressed on brain endothelial cells, can accumulate and eventually be internalized by cells on the vascular side of the brain through the mechanism of RME. Several receptors have been investigated, such as transferrin (TfR), insulin (IR), thiamine, apolipoprotein receptors, beyond some peptides. OX-26 and 8D3mAb (respectively,

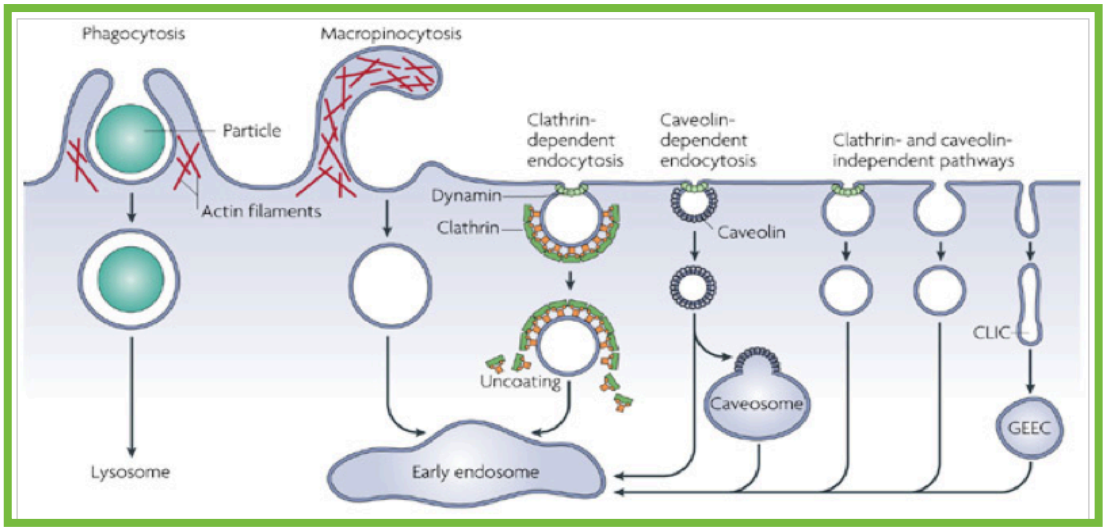


Fig.3: Pathways of entry into cells. Large particles can be taken up by phagocytosis, whereas fluid uptake occurs by macropinocytosis. Numerous cargos can be endocytosed by mechanisms that are independent of the coat protein clathrin and the fission GTPase, dynamin. Most internalized cargos are delivered to the EEC via vesicular (clathrin- or caveolin-coated vesicles) or tubular intermediates known as clathrin- and dynamin-independent carriers (CLICs) that are derived from the plasma membrane. Some pathways may first traffic to intermediate compartments, such as the caveosome or glycosyl phosphatidylinositol-anchored protein-enriched early endosomal compartments (GEEC), en route to the EEC (From Parton & Simons 2007).

monoclonal antibody to rat and mouse TfR) conjugated nanocarriers have proven to deliver drug molecules or exogenous genes to the brain (Huwyler et al 1996, Pang et al 2008, Shi et al 2001, Shi & Pardridge 2000). Lps coupled to 83-14mAb, a murine monoclonal antibody to the human IR (hIR), have successfully delivered messenger RNA (mRNA), siRNA or green fluorescent protein (GFP) into rat brain (Zhang et al 2003a, Zhang et al 2003b, Zhang et al 2004). Apolipoproteins B (ApoB) and E (ApoE) have been suggested to be mainly involved in the transport of polysorbate 80 coated NPs-bound drugs into the CNS: absorption of Apo from the blood after injection of surfactant-coated NPs is likely to mimic lipoprotein particles that could be taken up by the brain capillary endothelial cells via RME.

One group of proteins which are necessary for efficient intracellular membranous trafficking, including endocytosis, are Rab GTPases together with their effector proteins (Grant & Donaldson 2009, Zerial & McBride 2001). In their active states, Rabs-GTP bound forms are distributed on the cytosolic face of specific membrane compartments where they regulate vesicle formation, motility, docking and fusion (Vandersluijs et al 1991). For example, Rab4, Rab5, and Rab11 are localized to EE and serve different functions. Rab4 has been

shown to be involved in the regulation of recycling from the EE and, in particular, TfR recycling. Rab5 is important in the homotypic fusion between EE as well as in the transport to the early endosomal compartment (EEC) (Bucci et al 1992, Gorvel et al 1991, Stenmark et al 1994). In addition, it seems to be also necessary for budding of vesicles from the plasma membrane and has been suggested to regulate transport beyond EEC (McLauchlan et al 1998). Rab11, on the other hand, has been demonstrated to function in transport through the recycling compartment (Ullrich et al 1996, Wilcke et al 2000). Two Rabs are localized to the late endosomal compartment (LEC): Rab7 has been shown to control LE trafficking (Feng et al 1995, Vitelli et al 1997) while Rab9 regulates transport from LEC to the TGN (Lombardi et al 1993) (Fig.4).

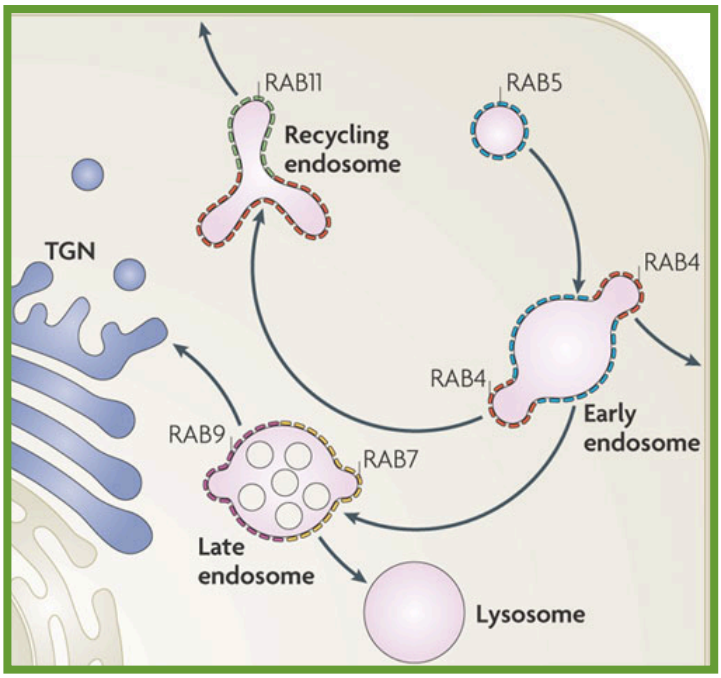


Fig.4: Rab domains. EE contain separate domains enriched in Rab5 (blue) and Rab4 (red), which are involved in endosome fusion and endocytic recycling, respectively. The recycling endosome contains domains enriched in Rab4 and Rab11 (green), which are involved in vesicle trafficking from the EE and to the plasma membrane, respectively. Late endosomes (LEs) contain domains enriched in Rab7 (yellow) and Rab9 (purple), which mediate trafficking to lysosomes and the trans-Golgi network (TGN), respectively (From Stenmark 2009).

4. ALTERNATIVE ROUTES TO CNS DRUG DELIVERY

A third class of strategies aimed at enhancing CNS penetration of drug molecules is composed of delivery methodologies that do not rely on the cardiovascular system (intravenous (i.v.) administration of drugs and DDS). These alternative routes for controlled CNS drug delivery obviate the need for the drug manipulation to enhance BBB permeability and/or BBBD by circumventing the BBB altogether.

One strategy to bypassing the BBB that has been studied extensively in both laboratory and clinical trials is the intralumbar injection or

intracerebroventricular (i.c.v.) infusion of drugs directly into the CSF. Theoretically, intra-CSF drug administration has several advantages: the drug bypasses the BCB and directly results in high CSF drug concentrations. Since the drug is somewhat contained within the CNS, a smaller dose can be used, potentially minimizing systemic toxicity. Furthermore, drugs in the CSF encounter lower protein binding and decreased enzymatic activity in comparison with drugs in plasma, leading to longer drug half-life in the CSF. Finally, since the CSF freely exchanges molecules with the extracellular fluid of the brain parenchyma, delivering drugs into the CSF could theoretically result in therapeutic CNS drug concentrations. Intrathecal (i.t.) and intracerebral (i.c.) drug administration differs fundamentally from systemic drug administration in terms of pharmacokinetic characteristics in that 100% of the available dose reaches the target organ. However, there can be large gradients inside the tissue with very high local concentrations at the site of administration (the ventricular surface or tissue site of injection) and zero concentration at some distance. In the case of macromolecules that have low diffusion coefficients, the gradients will be even steeper than what has been measured for small molecular weight (MW) drugs (Blasberg et al 1975). After i.c.v. injection, the rate of elimination from the CNS compartment is dominated by CSF dynamics.

An alternative CNS drug delivery strategy that has received relatively little attention is the intranasal route (i.n.). Drugs delivered intranasally are transported along olfactory sensory neurons to yield significant concentrations in the CSF and olfactory bulb. The difficulties that have to be overcome include an enzymatically active, low pH nasal epithelium, the possibility of mucosal irritation or the possibility of large variability caused by nasal pathology, such as a common cold. An obvious advantage of this method is that it is non invasive relative to other strategies that avoid the hematic route.

Therefore, the administration route of nanocarriers is an important factor to overcome the physiological barriers of the brain and to achieve high drug concentrations therein (Patel et al 2009, Semmler-Behnke et al 2008, Wang et al 2008); the major interest is represented by non-invasive approaches, associated with lower toxicity and sepsis risks and higher patient compliance.

5. BRAIN DRUG DELIVERY USING NPs: PLGA NANOPARTICLES

One of the most commonly used polymers for production of NPs is Poly(lactic-co-glycolic acid) (PLGA) normally used also in several biomedical devices as implants and microparticles in humans, due to its high biodegradability and to its approval by the American Food and Drug Administration (US FDA) and European Medicine Agency (EMA).

5.1 Biodegradation

Within body fluids, PLGA is degraded by non-enzymatic hydrolysis of the ester backbone. The degradation process of PLGA is well known and leads to lactic acid (LA) and glycolic acid (GA), i.e., the main components of PLGA, and finally gives CO_2 and H_2O. One of the main advantages of the use of PLGA in biomedical devices, as well as in NPs, is the possibility of governing the biodegradation rates (from several months to several years) depending on the MW and copolymer ratio.

5.2 Biodistribution

When PLGA nanoparticles (PLGA-NPs) are administered i.v., they are rapidly cleared by the liver and the reticuloendothelial system (RES), with a plasma half-life of 2-3 min.

Chemical-physical modifications of PLGA-NPs such shape, size and surface properties, improve the pharmacokinetics profile of these compounds by reducing opsonization, phagocytosis and clearance by the liver and RES (Newton 2006).

In fact, Yadav and colleagues (2011) demonstrated, after i.v. administration in animal models, the impact of particle size of NPs on the biodistribution and blood clearance of etoposide-loaded PLGA NPs (Eto-PLGA-NPs). The results highlighted that Eto-PLGA-NPs sizing 105 nm were present in the blood at higher concentrations up to 24 h after i.v. injection reducing their uptake by the RES as compared to 160 nm Eto-PLGA-NPs. Moreover, the NPs sizing 105 nm had greater uptake in bone and brain, in which concentration of the 160 nm NPs was negligible. The study concluded that ~100 nm NPs can be used for long-term

circulation without the need of surface modifications due the escape from liver metabolism (Yadav et al 2011).

The same phenomenon was confirmed in other experiments by Nagayama and colleagues (2007) using NPs made of different substances (i.e., gold and polysterene) demonstrating the accumulation in the liver, lung and spleen as a function of particle size. In particular, the smaller NPs were found in almost all organs, including the brain, while 200 nm NPs displayed a high accumulation only in spleen and liver (Nagayama et al 2007).

5.3 Therapeutic applications of PLGA-NPs

The applications of PLGA-NPs comprise many fields of biomedical research as vaccination, regenerative medicine, cardiovascular disease, osteoporosis, infectious disease, neurological disorders and cancer.

In general, two types of targeting strategies can be taken into consideration: active targeting by "*targeting PLGA-NPs*" and passive targeting by "*un-targeted PLGA-NPs*". In the first case, the *molecular Trojan horse* approach (see section **3. STRATEGIES TO ENHANCE CNS DRUG)** is applied; in the second case PLGA-NPs are used exploiting the naturally occurring cellular events (enhanced permeability and retention phenomena).

The passive targeting is particularly exploited in some applications in cancer therapy, in inflammation conditions as colitis (Moulari et al 2008), arthritis (Ye et al 2008), cystic fibrosis (Vij et al 2010) and osteoporosis (Ulbrich & Lamprecht 2010), for the delivery of growth factors in regenerative medicine (glial cell derived neurotrophic factor (GDNF), vascular endothelial growth factor (VEGF) and fibroblast growth factors (FGFs) as examples) (Danhier et al 2012), in cardiovascular diseases (Mulder & Fayad 2008), in diabetes (Clemente-Casares & Santamaria 2014) and in infectious diseases (Sundar & Prajapati 2012).

Several examples of the application of PLGA as starting material for the preparation of DDS are available on market: Lupron Depot® (gonadotropin releasing hormone analog for prostate cancer and endometriosis), Decapetyl®, Suprecur®, Trelstar®, Eligard®, Luprogel®, Nutropin® (for the treatment of growth hormone deficiency), Somatuline® (for the treatment of endocrine tumors), Atridox® and Arestin® (for the delivery of antibiotics for periodontal

diseases). All of these formulations, sometimes administered in bolus, release the drugs over a period of 0.5 to 4 months, allowing a prolonged pharmacological activity.

Even if no product based on PLGA-NPs is on market, several papers investigated the parameters affecting PLGA-NP degradation, such as MW, polydispersity, stability in water or in medium (Makadia & Siegel 2011), polymer composition (Wang et al 2000).

The use of targeted PLGA-NPs is strongly recommended in those pathologies lacking selective drugs able to specifically target the diseased cell population (targeting a specific receptor for example) or by the presence of natural barriers such as the BBB.

5.4 BBB-crossing PLGA-NPs: g7 peptide

A ligand-based procedure represents one of the most intriguing and, maybe, promising approaches to reach an effective CNS targeting. In fact, physiologic vector-based strategies involve the use of existing BBB transport properties to enhance brain entry of a specific drug. This strategy consists in coupling a drug delivery vector, like NPs, to a peptide that is normally transported through the BBB via CMT or RME: that is the SDDs strategy. Different examples of ligand choice for CNS targeting have been published; in most cases, antibodies against TfR or IR expressed by BBB endothelial cells are used demonstrating a low percentage of nanocarriers transported into the brain in both *in vivo* and *in vitro* experiments (Gabathuler 2010).

Peptides are generally polar in nature, do not easily cross the BBB by diffusion and, except for a small number, do not have specific transport systems. Nevertheless, some naturally occurring peptides can effectively cross the BBB by RME. Therefore, the use of peptides, or their fragments, that physiologically cross the BBB for targeting of macromolecules across the BBB became a successful strategy to improve drug delivery to the brain (Kabanov & Batrakova 2004).

On the basis of this knowledge, PLGA-NPs might be used as cargos for peptides that normally cross the BBB. For instance, some opioid-derived peptides able to cross the BBB have been intensively investigated (Costantino et al 2005).

In order to improve BBB crossing, the conjugation of a synthetic peptide, known to be membrane-permeable, on the surface of PLGA-NPs was tested. The leading peptides [H2N–Gly-L-Phe-D-Thr-Gly-L-Phe-L-Leu-L-Ser-(O-β-D-glucose)-CONH2, g7] were obtained by substituting Tyr at the N-terminus with Phe in the synthetic opioid peptide MMP-2200 [H2N-L-Tyr-D-Thr-Gly-L-Phe-Leu-L-Ser(-O-B-D-lactose)-CONH2] to avoid any potential opioid activity, since the presence of Tyr is essential for the nociceptive effect (Beddell et al 1977).

g7-coupled NPs (g7-NPs) produced by nanoprecipitation procedure have proved to enter into the brain (Costantino et al 2006). NPs loading with two model drugs per se unable to enter the BBB, namely Loperamide (Lop) (Sadeque et al 2000) and Rhodamine-123 (Rhod) (Fontaine et al 1996) demonstrated the efficacy of CNS targeting. The peak of Lop anti-nociceptive action was elicited 240 min after i.v. administration in rats, with a calculated active dose in the CNS that is higher than 10% of the dose injected peripherally (Vergoni et al 2009). Similarly, Rhod, a fluorescent dye used in cerebral studies, was loaded into targeted NPs in this way delivering up to 15% of injected dose into the brain.

Furthermore, the substitution of the g7 sugar moiety with a different carbohydrate was tested by the Lop-loaded g7-NPs antinociceptive activity: glucose proved to be the most active substitution, defining H2N-Gly-L-Phe-D-Thr-Gly-L-Phe-L-Leu-L-Ser(O-β-D-glucose)-CONH2 as the best CNS-targeting peptide to be further investigated.

AIM OF THE THESIS

NPs are being extensively investigated as sustained drug delivery devices and as specific carriers for gene delivery, vaccines and therapeutic drugs. These systems have a promising future as DDSs that could allow an efficient and site-specific transport of drugs to the target tissue affected by a disease.

DDSs for the treatment of neurological and psychiatric disorders must have the characteristic to pass the unique membrane that restricts the entry of peripheral molecules into the brain: the BBB. Thus, if nanocarriers are to be translated into the clinic, the capability to pass the BBB, their distribution within the brain and interaction with CNS cells must be assessed accurately. In this context, we had four principal aims:

- ✤ To assess the capability of g7-NPs, designed for brain delivery, to cross the BBB after administration by different routes: from common i.v. and intraperitoneal (i.p.) to uncommon i.n. injection.
- ✤ To study the g7-NP cell-specific uptake and biodistribution within the brain, after i.p. injection in mice, in a dose and time-dependent manner.
- ✤ To investigate the possible mechanisms of cell-to-cell transport of g7-NPs after *in vivo* administration in mice.
- ✤ To investigate the possibility of differential cell targeting by engineering g7-NPs with antibodies (Ab) against cell-type specific markers.

METHODS

1. Formulation and purification of NPs

NPs were prepared in accordance to nanoprecipitation procedure (Fessi et al 1989) to obtain a matrix-like system where a hydrophobic bead of drug and polymer are entrapped. To obtain labelled g7-NPs, a mixture composed by g7-PLGA (20 mg w/w), Rhod-PLGA (10 mg w/w) and PLGA (70 mg w/w) was dissolved in acetone (8 mL). The organic phase was then added dropwise into deionised water (25 mL) containing 100 mg of poloxamer 188 (Pluronic F68®, Sigma Aldrich). After stirring at RT for 10 min, the organic solvent was removed at 30°C under reduced pressure (10 mmHg).

The final volume of the suspension was adjusted to 10 mL with deionised water. To purify NPs from excess of loaded molecules, surfactant and polymer not assembled, all the g7-NP preparations were purified by gel-filtration chromatography (Sepharose CL 4B gel, 160 mL, column 50×2 cm, Sigma Aldrich), using water as the mobile phase and freeze-dried (Lyovac GT-2, Leybold-Heraeus, Hanau, Germany) without any cryoprotector. At least 3 batches of g7-NP samples were prepared and purified to be tested in cell cultures and for *in vivo* experiments.

2. Preparation of antibody-modified R-g7-NPs: NCAM-R-g7-NPs and CD44-R-g7-NPs

Ab-modified g7-NPs were prepared starting from g7-NPs, obtained as described in upper point 1, and applying well known methodologies for Ab-surface engineering of NPs. Briefly, there are two approaches to anchor a moiety to the surface of NPs: the ligand can be either attached to the polymer before NPs formulation or linked afterwards. In our case, the second approach was used: in the presence of 1-Ethyl-3-(3-dimethylaminopropyl)-carbodiimide (EDC, 170 mg) and N–hydroxy-succinimide (NHS, 30 mg) to firstly activate g7-NPs (g7-NPs-NHS) and then conjugate the free primary amine groups on the g7-NPs surface with the carboxylic groups of the Ab molecules.

Desired amounts of g7-NPs-NHS (50 mg) were suspended and stirred at RT for 1.5 h in 2-(N-morpholino)ethanesulfonic acid (MES, Sigma Aldrich) buffer with designated volume of Anti-NCAM1 Ab (50 µl of a 1 mg/mL stock solution) or Anti-CD44 Ab (50 µl of a 0.5 mg/mL stock solution) stock solution, in order to obtain, respectively, NCAM-g7-NPs and CD44-g7-NPs.

After the reaction, the suspensions of the Ab-modified NPs (NCAM-g7-NPs or CD44-g7-NPs) were collected by centrifugation and further washed twice by distilled water for purification. Some amounts of Ab-NPs were re-suspended in ultrapure water for further characterization, while other NPs were lyophilized to prepare stocks (trealose, in ratio 1:1 w/w with respect to NPs was added as cryoprotector).

2.1 Determination of molecule loading

As previously established in literature, the efficiency in surface engineering of g7-NPs with Ab moieties was demonstrated by X-ray photoelectron spectroscopy (Electron Spectroscopy for Chemical Analysis, ESCA) analysis performed on a 04-153 X-ray source analysis system (PHI, Uvalca-PHI, Tokyo, Japan) and an EA11 hemispherical electron analyzer (Leybold Optics, Alzenau, Germany) using MgKα1,2 radiations. The spectra were recorded in fixed retardation ratio (FAT) mode with 190 eV pass energy. The pressure in the sample analysis chamber was approximately 10−9 mbar. The data were acquired and processed using the RBD AugerScan 2. 1H-HRMAS NMR spectra were recorded on a Bruker (Billerica, MA, USA) Avance 400 instrument; D2O was added to the sample, which was then spun at 4000 Hz. All experiments were recorded at RT.

In order to further assess the presence of Ab on the NPs surface, we incubated the NCAM-g7-NPs or CD44-g7-NPs with nanogold (mono-sulfo-N-Hydroxy-succinimido Nanogold®, Nanoprobes, Inc., NY 11980-2301 USA), sizing 1.4 nm and able to react with Ab, to provide a qualitative identification of Ab. As control, we performed the same coupling reaction using g7-NPs.

Following the procedures given by the manufacturer, a weighted amount (1 mg) of NPs (g7-NPs, NCAM-g7-NPs, CD44-g7-NPs) was suspended in phosphate buffer (pH 7.8) and added to 300 µl of a resuspension of nanogold, poured to a final volume of 3 mL of solution. After purification, the NPs coupled with nanogold were processed for Transmission Electron Microscopy (TEM) analysis. In particular, negative staining TEM was used for the evaluation of the inner morphology of all batches of NPs. A drop of a water-diluted suspension of the purified NPs (about 0.05 mg/mL) was placed on a 200-mesh formvar copper grid (TABB Laboratories Equipment, Berks, UK), and allowed to adsorb. The surplus was removed by filter paper. A drop of 2% (w/v) aqueous solution of uranyl acetate was added and left in contact with the sample for 5 min (initially,

we tested different concentrations of uranyl acetate solution; the condition applied in this study was the most suitable to maintain the integrity of the sample during the preparation). The surplus water was removed and the sample was dried at RT before the NPs were imaged with a TEM operating at an acceleration voltage of 200 KV (model JEM 2010; JEOL, Peabody, MA).

3. Characterization of NPs: morphology, particle size and surface analysis

All the batches of NPs were characterized regarding their surface, chemico-physical and morphological properties. In particular, for surface properties (size and surface charge), NPs in distilled water were analyzed by photon correlation spectroscopy (PCS) and laser Doppler anemometry using a Zetasizer Nano ZS (Malvern, UK; Laser 4 mW He–Ne, 633 nm, Laser attenuator Automatic, transmission 100% to 0.0003%, Detector Avalanche photodiode, Q.E. > 50% at 633 nm, T = 25°C). The results were normalized with respect to a polystyrene (PS) standard solution.

To evaluate physical properties like the shape and morphology of NPs, a scanning electron microscope (SEM) (XL-40; Philips, Eindhoven, The Netherlands) operating at 8 kV was used. NPs were re-suspended in distilled water after at least 3 washing with water, and a drop of the suspension was placed onto a SEM sample holder and dried under vacuum (10–2 mmHg). The dried samples were coated under argon atmosphere with a 10 nm gold palladium thickness (Emitech K550 Super Coated; Emitech Ltd, Ashford, Kent, UK) to increase electrical conductivity. The NPs were then processed for the evaluation of their morphology and shape by analyzing images at different magnifications (13,000× to 16,000×).

Moreover, Atomic Force Microscopy (AFM) was used for morphological assessments and surface properties. In particular, an AFM (Park Instruments, Sunnyvale, CA, USA) at RT (about 20°C) at atmospheric pressure (760 mmHg) operating in air and in non-contact mode using a commercial silicon tip-cantilever (tip diameter ≅ 5-10 nm) with stiffness about 40 Nm-1 and a resonance frequency around 150 kHz. A little amount of each NP sample was dispersed in deionised water (about 40 μL) on a small freshly cleaved mica disk (1 cm x 1 cm). After 2 min from the deposition, the excess of deionised water was removed by a blotting paper and the sample was observed. Two kinds of images were obtained: the first one is a topographical image and the second one is the 3D

elaboration. The AFM images were obtained with a scan rate of 1 Hz and processed using a ProScan Data Acquisition software developed under Windows 95.

3.1 Evaluation of NPs-stability

To assess the stability of NPs, we incubated a fixed amount of Control-NPs (C-NPs), g7-NPs, NCAM-g7-NPs and CD44-g7-NPs (1 mg) in 1 mL of saline solution, artificial cerebrospinal fluid (aCSF, i.e Ringer) solution or serum solution. The incubation was performed under stirring at 37°C over 24 h. At fixed times (10, 30 or 60 min, 2, 6 or 24 hr), a sample of each NPs suspension was analyzed for size determination, surface charge, dye-stability and tests on the maintenance of the functionality of g7-NPs *in vivo*.

4. Animal procedures and sample preparation for BBB-crossing and BBB-integrity studies

To determine the capability of g7-NPs, designed for brain delivery, to cross the BBB following different routes administration, a total of 9 mice were injected.

4.1 Intraperitoneal administration of g7-NPs

An exact amount of g7-NPs (3 mg), suspended in saline solution (0.05 mL), was injected i.p. in mice (n=3). Then the animals were sacrificed 90 min after the administration. This time was selected as the transport of g7-NPs from the peritoneum to the brain is hampered by the peritoneal barrier (Flessner 2005), delaying the appearance of a remarkable amount of g7-NPs in the CNS respect to the time (60 min) usually used after i.v. administration.

4.2 Intranasal administration of g7-NPs

An exact amount of g7-NPs, suspended in saline solution (0.05 mL), were administered to mice (3 mg/animal; n=3). Briefly, the animals were anesthetized with an i.p. injection of a saline solution of xylazine (4.0 mg/Kg) and ketamine (100 mg/Kg). Then, the animals were positioned on their backs, with a rolled up 4x4 gauze under the dorsal neck. Drops of 5-6 µL of the g7-NPs suspensions were administered using a Hamilton microsyringe in each noun after having closed the opposite one and the mouth (Thorne et al 1995). A total volume of about 0.05 mL was given in about 2 min alternating the nares. The survival time of the animals was fixed 60 min after administration as for the i.v. administration

tests (Tosi et al 2011). Since the g7-NPs should cross only the nasal epithelium before reaching the brain via an intra-axonal route (Seju et al 2011).

4.3 Oral administration of g7-NPs

An exact amount of g7-NPs suspended in saline buffer (0.5-2 mL) was administered by oral gavage to mice (3 mg/animal; n=3). The rodents were maintained alive for 180 min in order to allow g7-NPs to be absorbed through the gastro-intestinal tract. The 180 min period was selected as it is reasonable to take into account that the presence of the gastro-intestinal wall slows down the entry of g7-NPs in the blood stream respect the i.v. administration.

4.4 Assessment of BBB-integrity

To prove the BBB integrity, a total of 3 mice received a single i.p. injection of 300 µl of Evans Blue, an azo dye with a very high affinity for serum albumin (unable to cross the BBB). 30 min after Evans Blue injection, mice were anesthetized (chloral hydrate 400 mg/kg, i.p.) and decapitated. The brains were removed and processed for both macroscopic and confocal analysis (see below).

5. Animal procedures and sample preparation for injection of modified- and unmodified-g7NPs

C-NPs, g7-NPs, NCAM-g7-NPs or CD4-g7-NPs suspended in saline solution were injected i.p. in C57Bl6 mice. After 10 min, 30 min, 1 h, 2 h, 6 h, or 5 days, animals were sacrificed. For histological processing, animals were anesthetized with chloral hydrate (400 mg/kg, i.p.). Intracardial perfusion was performed with 4% paraformaldehyde and 0.2% picric acid in Phosphate Buffered Saline (PBS) (70 mL/7 min) preceded by an infusion of 50 mL of 0.9% NaCl saline containing heparin sodium (5000U/L); organs as brain, liver, spleen and kidneys were dissected out. The brains were postfixed in the same solution for 12 h, rinsed in 15% sucrose in PBS for approximately 12 h and then in a 30% sucrose in PBS for 1 day. The brains were frozen using dry ice, and coronal 50 µm thick sections series were cut at a cryotome, washed three times in cold 1x PBS and stored at -20°C in a glycerol-PBS solution until use. As control, also saline solution was i.p. injected with the same procedure.

6. Immunohistochemistry of brain sections

Brain sections were processed for multiple immunofluorescence (IF) histochemistry according to the following protocol. After five washes with 1xPBS pH 7.4 for 10 min, blocking was performed for 1 h at RT in a 1xPBS solution containing 0.1% Triton X100 and 1% bovine serum albumin (BSA). Incubation with primary antibodies diluted in 0.3% Triton X100, 1% normal serum (NS) and 1xPBS was performed overnight at 4°C. After three washes in PBS/0.1% Triton X100, incubation with secondary antibody in 0.2% Triton X100, 1% NS and PBS was carried out for 90 min at RT. After washing three times with PBS for 10 min, brain sections were placed on gelatinised glass slides, dried and, after incubation with 4',6-diamidino-2-phenylindole (DAPI), mounted for confocal microscopy analysis.

Primary Antibody	Diluition
Anti-NeuN Antibody, clone A60, MAB377 Millipore	1:200
Anti Iba1, Polyclonal Antibody, Rabbit, Cat. #019-19741 Wako	1:1000
Anti NPY Polyclonal Antibody Rabbit, Peninsula Laboratories	1:250
Anti GFAP Polyclonal Antibody Rabbit, Dako	1:3000
Anti EEA1 Polyclonal Antibody Rabbit, Cat. #ab50313 abcam	1:200
Anti Rab5 purified mouse, Cat. #610725 BD Biosciences	1:200
Anti Rab5 Polyclonal Antibody Rabbit, Cat. #2143 Cell Signaling	1:200
Anti TNFα-ip2 Polyclonal Antibody Rabbit, Cat. #sc30138 Santa Cruz Biotechnology	1:200
Secondary Antibody	**Diluition**
Alexa Fluor® 488 Donkey Anti-Mouse IgG (H+L) Antibody	1:400
Alexa Fluor® 488 Donkey Anti-Rabbit IgG (H+L) Antibody	1:400

7. *In vivo* endocytosis inhibition

A total of six C57Bl6 mice hippocampi/group were infused unilaterally with 1 μL of chlorpromazine hydrochloride (Sigma-Aldrich) (30 μM) or staurosporine (Sigma-Aldrich) (60 μM) to inhibit clathrin-dependent and caveolin-dependent endocytosis, respectively. The mouse contralateral hippocampi were injected with the respective vehicle: water for chlorpromazine and dimethyl sulfoxide (DMSO):water (50:50) for staurosporine. Mice were fixed to a stereotaxic apparatus and drugs were infused using a Hamilton syringe (0.2 μL/min) for 5 min, leaving the syringe in the brain for 5 more min before withdrawal. Finally, 300 ag of g7-NPs were injected i.p. and 20 min later mice were sacrificed by intracardial perfusion (see above).

8. Quantification of nanoparticles and Rab5 immunoreactivity

Semi-quantitative measurement of NPs and Rab5 immunoreactivity was performed on confocal images by means of an image analysis software (ImageJ) using established protocol (Zoli et al 1992). Briefly, NP or Rab5 immunoreactivity profiles were selected from background using the threshold function and the field area % was calculated. For each treatment, 10 cells/section in 3 animals were analyzed.

9. Cell-to-cell exchange of nanoparticles

To investigate the pathway of NP cell-to-cell transport we took in consideration the recent discovery of tunneling nanotubes (TNTs), a new identified strategy used for intercellular signaling. TNTs are continuous conduits of the plasma membrane that allow direct physical connection of plasma membranes and cytosol among remote cells. They are important for intercellular communication by mediating exchange of cellular components as well as signal transduction molecules.

To visualize TNT in brain mice slides, an antibody against M-Sec also known as tumor necrosis factor−α induced protein 2 (TNFαip2) was used.

g7-NP co-localization with TNFαip2 was evaluated by confocal analysis, in mice injected i.p. with 300 pgr/mouse of NPs. The animals were sacrificed after 48 h following the procedures for intracardial perfusion and IF previously described.

RESULTS

1. Routes of g7-NP administration

To test the capability of brain delivery-designed g7-NPs to cross the BBB and distribute within the brain, after administration through different routes, we injected 3 mg of g7-NPs to 3 mice/group using i.p., i.n. or oral (o.a.) modality of NP administration.

1.1 Intraperitoneal administration of g7-NPs

Red spots of the R-g7-NPs could be observed heterogeneously distributed in the entire CNS, demonstrating the ability of g7-NPs to cross the BBB 90 min after i.p. administration. Here, we provide two representative images of hypothalamus (Fig.5a) and cerebral cortex (Cx) (Fig.5c) sections showing that red spots preferentially decorate the nuclei of neurons (larger with spotted chromatin) and only rarely of glial cells (smaller with compact chromatin).

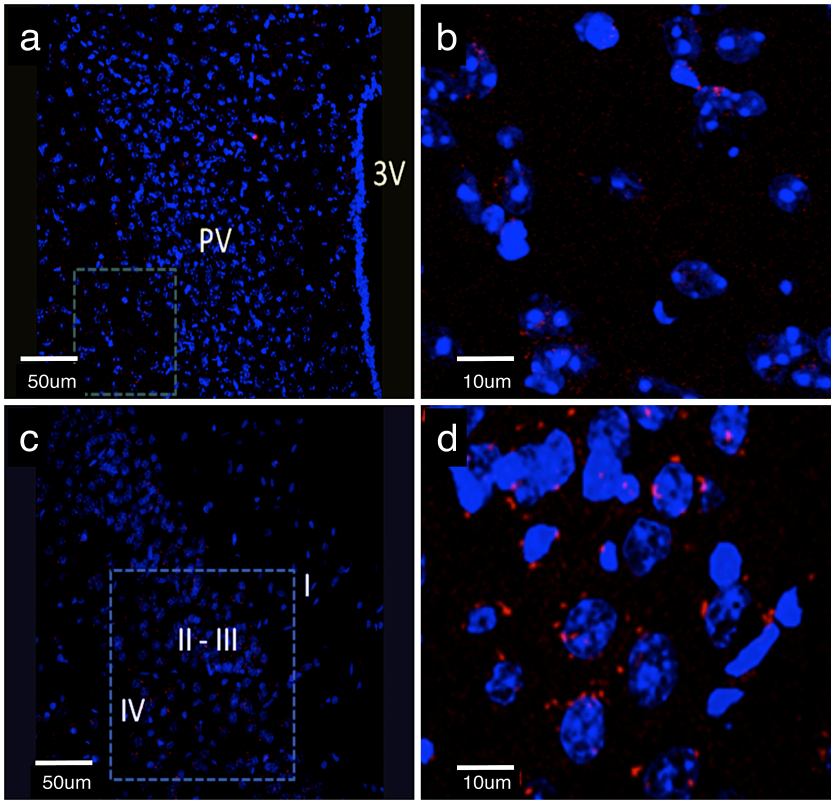


Fig.5 Spatial distribution of g7-NPs in brain paraventricular hypothalamic nucleus (PV) (a) and external pyramidal layers of the somatosensory cortex (c). Confocal microscopy analysis using DAPI (blue) and g7-NPs (red) on brain cryosections obtained from mice sacrificed 90 min after g7-NPs i.p. injection (3 mg/mouse). The right panels report higher magnifications of the dashed squared areas in the left panels. In right panels, it is shown that NPs (red dots) decorate mainly neuronal (large spotted) nuclei and only rarely glial (small homogeneously intense) nuclei. 3V= third ventricle;

1.2 Intranasal administration of g7-NPs

The localization of g7-NPs within the brain was widespread and heterogeneous. We report the distribution of R-g7-NP signal in hippocampal cornu ammonis (CA) 3 field (Fig.6a) and dentate gyrus (DG) (Fig.6b), striatum (Fig.6c) and cingulate cortex (Cg) (Fig.6d). The images highlighted, at regional level, a remarkable accumulation of g7-NPs without a specific tropism to any specific brain area, and, at cellular level, a preferential accumulation of g7-NP signal around neuronal nuclei (see also the high magnification images of Fig.6e-h).

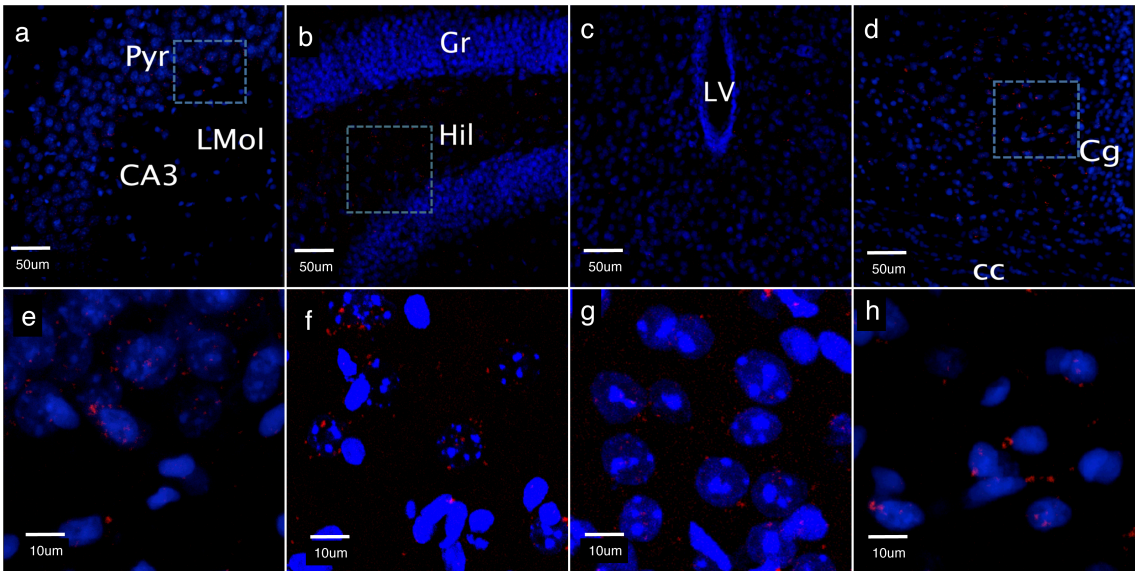


Fig.6 Spatial distribution of* g7-*NPs after intranasal administration in brain cornu ammonis (CA) 3 subfield (a), dentate gyrus (b) of the hippocampus, cindulate cortex (Cg) (c) and striatum (d). Confocal microscopy analysis using DAPI (blue) and g7-NPs (red) on brain cryosections obtained from mice sacrificed 60 min after i.n. g7-NPs administration (3 mg/ mouse). Panels e-h report higher magnifications of the dashed squared areas in panels a-d. It is shown that NPs (red dots) decorate mainly neuronal (large spotted) nuclei and only rarely glial (small homogeneously intense) nuclei. In particular, the neurons whose nucleus is most intensely labeled are interneurons of the stratum lacunosum-moleculare (LMol) (a,e) and hilus (Hil) (b,f). Pyr= pyramidal layer of hippocampus; Gr= granular layer of hippocampus; LV= lateral ventricle; CC= corpus callosum.

1.3 Oral administration of g7-NPs

An exact amount of g7-NPs suspended in saline buffer (0.5-2 mL) was administered by oral gavage to mice (3 mg/animal; n=3). The rodents were maintained alive for 180 min in order to allow g7-NPs to be absorbed through the gastro-intestinal tract. The 180 min period was selected as it is reasonable to take

into account that the presence of the gastro-intestinal wall slows down the entry of g7-NPs in to the blood stream with respect the i.v. administration.

1.4 BBB integrity

Evans Blue is used in neuroscience to assess the permeability of the BBB to macromolecules. Since serum albumin cannot cross the BBB, and serum Evans Blue is bound to albumin, the neural tissue remains unstained by Evans Blue when the BBB is intact. No Evans Blue signal was detected within the brain parenchyma after i.p. g7-NP injection demonstrating that g7-NPs enter the brain without altering BBB permeability.

2. g7-NP accumulation in brain areas and cell types: in vivo evidence

In order to elucidate the possible accumulation of g7-NPs in specific brain areas or cell populations, we injected 300ag/300µL/mouse i.p. of g7-NPs and analyzed samples of different brain areas by confocal microscopy.

Six hours after the injection, g7-NPs were largely distributed across brain regions, with higher concentrations in grey matter areas than in white matter areas (Fig.7a,b Cx vs CC). The ependyma of the CP, an epithelium protruding into the brain ventricles that contributes to the BCB (see Introduction), was less

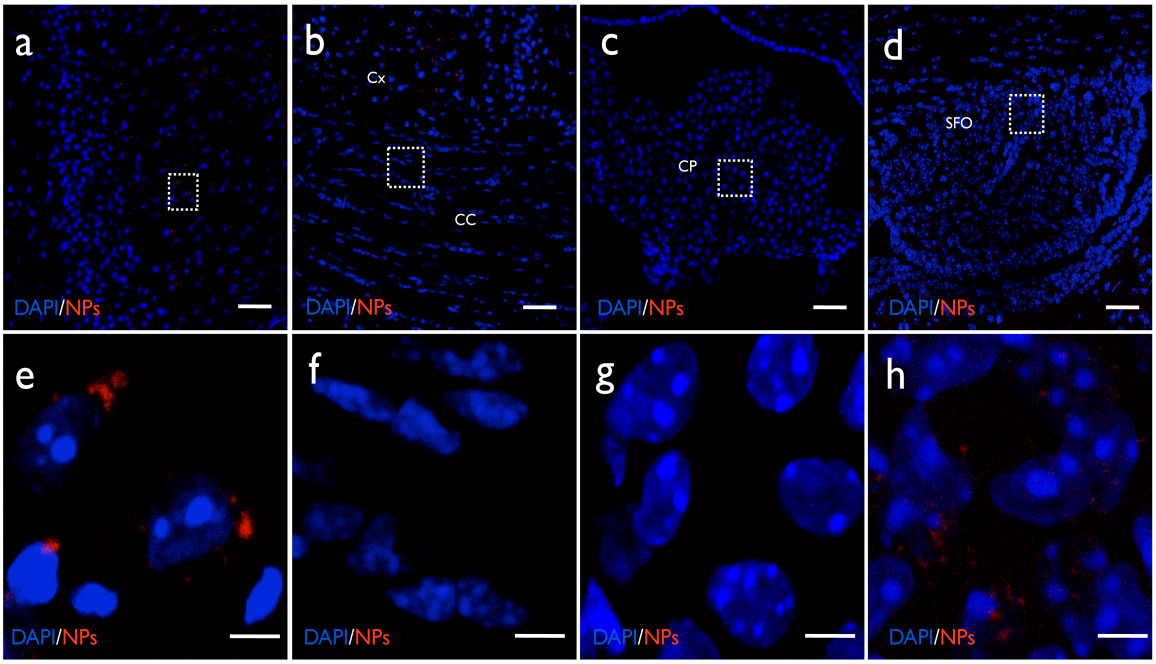


Fig.7 ***g7-NP distribution in different brain regions*** Confocal microscopy images of brain cryosections in mice sacrificed six hours after an i.p. injection of 300ag/300µL/mouse of g7-NPs (red) labeled with DAPI (blue). Low (panels a-d) and high (panels e-h) magnification images of cerebral cortex (Cx, panels a,e), corpus callosum (CC, panels b,f), choroid plexus (CP, panels c,g), and subfornical organ (SFO). Panels e-h show high magnifications of the dashed squares indicated in panels a-d, respectively. Scale bar = 50 µm (a-d), 10 µm (e-h).

intensely labeled than grey matter regions, and the SFO, one of CVOs devoid of BBB, was as intensely labeled as other grey matter regions (Fig.7c,d). Within all these regions, cellular accumulation of g7-NPs appeared to be highly heterogeneous (Fig.7e-h) and did not seem to depend on BBB passage, but rather, on some cell subtype-specific mechanism(s).

Next, to try to identify classes of g7-NP positive cells we performed a detailed analysis within the hippocampal region, using different cell-type specific markers like NeuN, or NPY for neuronal populations, GFAP for astroglia and Iba-1 for microglia. By far the largest population of cells with clear g7-NP accumulation were NeuN-immunoreactive (ir) neurons (Fig.8a). A clear

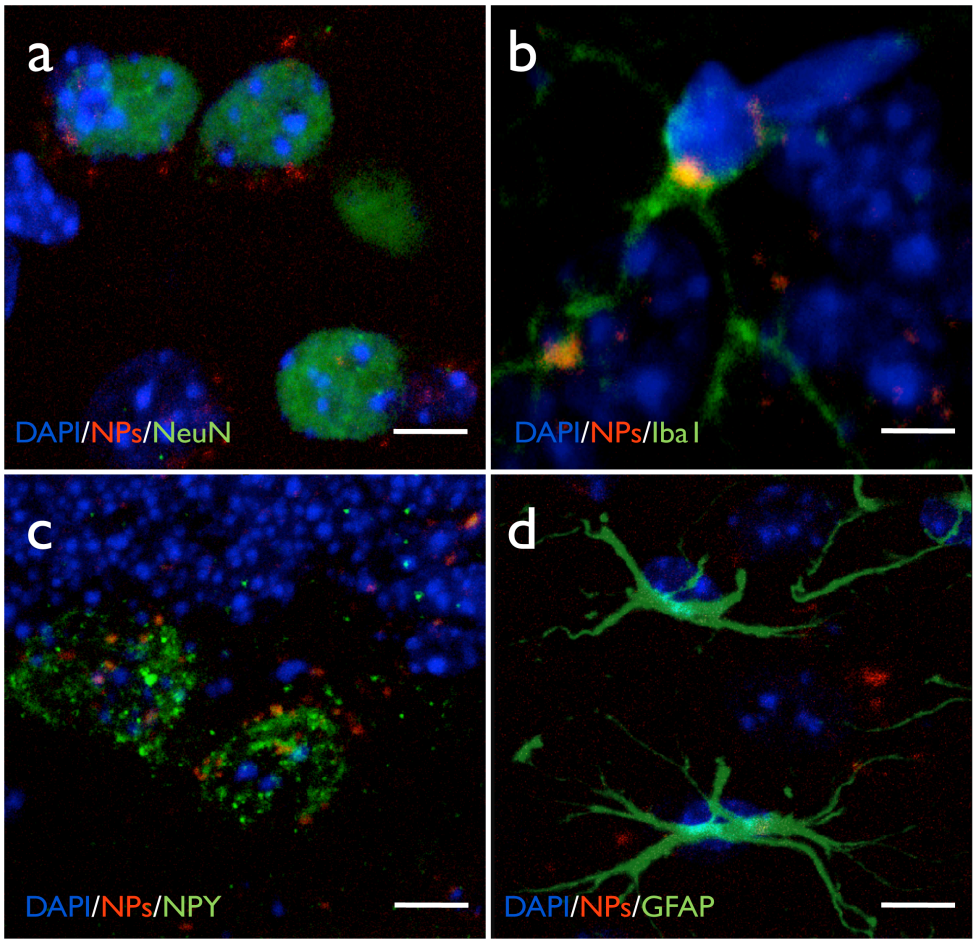


Fig.8 g7-NP distribution in different cell population Confocal microscopy images of brain cryosections in mice sacrificed six hours after an i.p. injection of 300ag/300µL/mouse of g7-NPs labeled with DAPI (blue), g7-NPs (red) and a number of antibodies (green): mouse anti-neuronal nuclear antigen (NeuN, panel a), rabbit anti-neuropeptide Y (NPY, panel c), rabbit anti-ionized calcium binding adaptor molecule 1 (Iba1, panel b), rabbit anti-glial fibrillary acidic protein (GFAP, panel d). High magnification images showing single cells from the hippocampal formation. Green and red co-localization is marked by yellow color, whereas green and blue co-localization is marked by pale blue color.
Scale bar = 50 µm (a-d), 10 µm (e-l).

accumulation of g7-NPs was also observed in some Iba-1-ir microglia (Fig8b), whereas g7-NPs could only rarely be attributed to GFAP-ir astroglia (Fig.8d).

g7-NP neuronal accumulation was heterogeneous, with preferential accumulation in interneurons of the stratum oriens and lacunosum-moleculare of CA subfields as well as of the hilus of DG, especially NPY interneurons (Fig.8c). Regarding the other major classes of hippocampal neurons, the g7-NP labeling was clearly present in CA3 pyramidal neurons, though at a level lower than that in NPY interneurons, but labeling was almost undetectable in granule cells of the DG or CA1 pyramidal neurons.

3. Time-course and dose-response study: *in vivo* evidence

To further characterize the distribution of g7-NPs in the brain after peripheral administration, we performed a time course (10 min to 5 days, Fig.9) and a dose-response study (300ag/300µL/mouse to 300ng/300µL/mouse) (Fig. 10) on the cellular populations of the hippocampal formation using markers for neurons (NeuN, NPY), astroglia (GFAP) and microglia (Iba-1). There was no qualitative change in the cell types accumulating g7-NP signal over time; however, the amount of g7-NP accumulation per cell was time-dependent, with minimal accumulation at 10 min, a peak at 30 min, and a decrease at 2 h. Then the levels remained roughly stable for up to 5 days after administration (Fig.9p). These kinetics were similar in hilar NPY interneurons and CA3 pyramidal neurons.

A quantitative analysis of the dose-response study, performed on hilar NPY interneurons, DG granule cells and CA3 pyramidal neurons, showed that, on the one hand, saturation of g7-NP accumulation was reached at the dose of 300fg/ 300µL/mouse, and, on the other hand, that the rank order of NP accumulation between neuronal cell types (NPY interneurons > CA3 pyramidal neurons >> DG granule cells) was maintained at all NP doses tested (Fig.10g).

These experiments clearly demonstrated that g7-NPs cross the BBB in less than 10 min after an i.p. administration, and accumulate into specific neuronal populations and microglia (Fig.8a,b) regardless of the dose and time after NP administration. Therefore, g7-NPs demonstrate a strong tropism towards certain neuronal subpopulations (Fig.8c). In these neuronal populations, the accumulation of g7-NPs is maximal at the dose of 300fg/300µL/mouse and does not change at higher doses as if the selected neuronal subpopulations capable of accumulating g7-NPs have a saturable uptake system for g7-NPs.

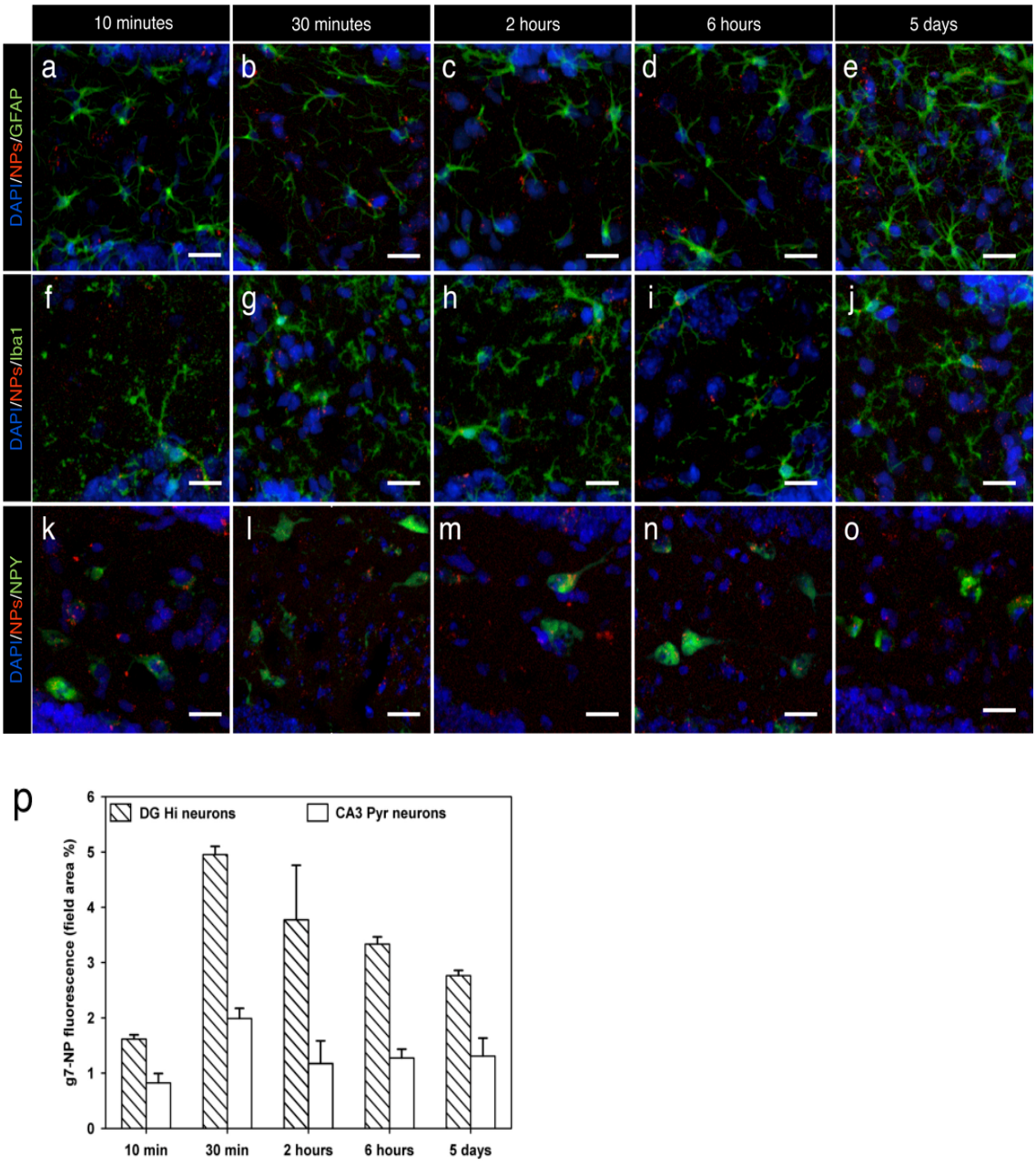


Fig.9 Time course of g7-NP distribution in brain cell subtypes Confocal microscopy images of brain cryosections labelled with DAPI (blue), rabbit anti-glial fibrillary acidic protein (GFAP, green, panels a-e), rabbit anti-ionized calcium binding adaptor molecule 1 (Iba1, green, panels f-j), rabbit anti-neuropeptide Y (NPY, green, panels k-o), and g7-NPs (red) from the hippocampal dentate gyrus of mice sacrificed at different time points (from 10 min to 5 days) after an i.p. injection of 300ag/300µL/mouse of g7-NPs. Starting 10 min after the injection, g7-NPs were accumulated in both microglial cells (f) and NPY cells (k) in the dentate gyrus hilus. This co-localization persisted at the following time points studied. Only rarely GFAP-ir astrocytes were positive at any time point studied. (p) Bar histogram showing the intensity of g7-NP labeling in dentate gyrus hilar (DG Hi) interneurons and CA3 pyramidal (CA3 Pyr) neurons at different time points after an i.p. injection of 300ag/300µL/ mouse of g7-NPs. In both neuronal populations, peak g7-NP labeling was detected at 30 min, followed by a decrease at longer time intervals. Scale bar = 20 µm

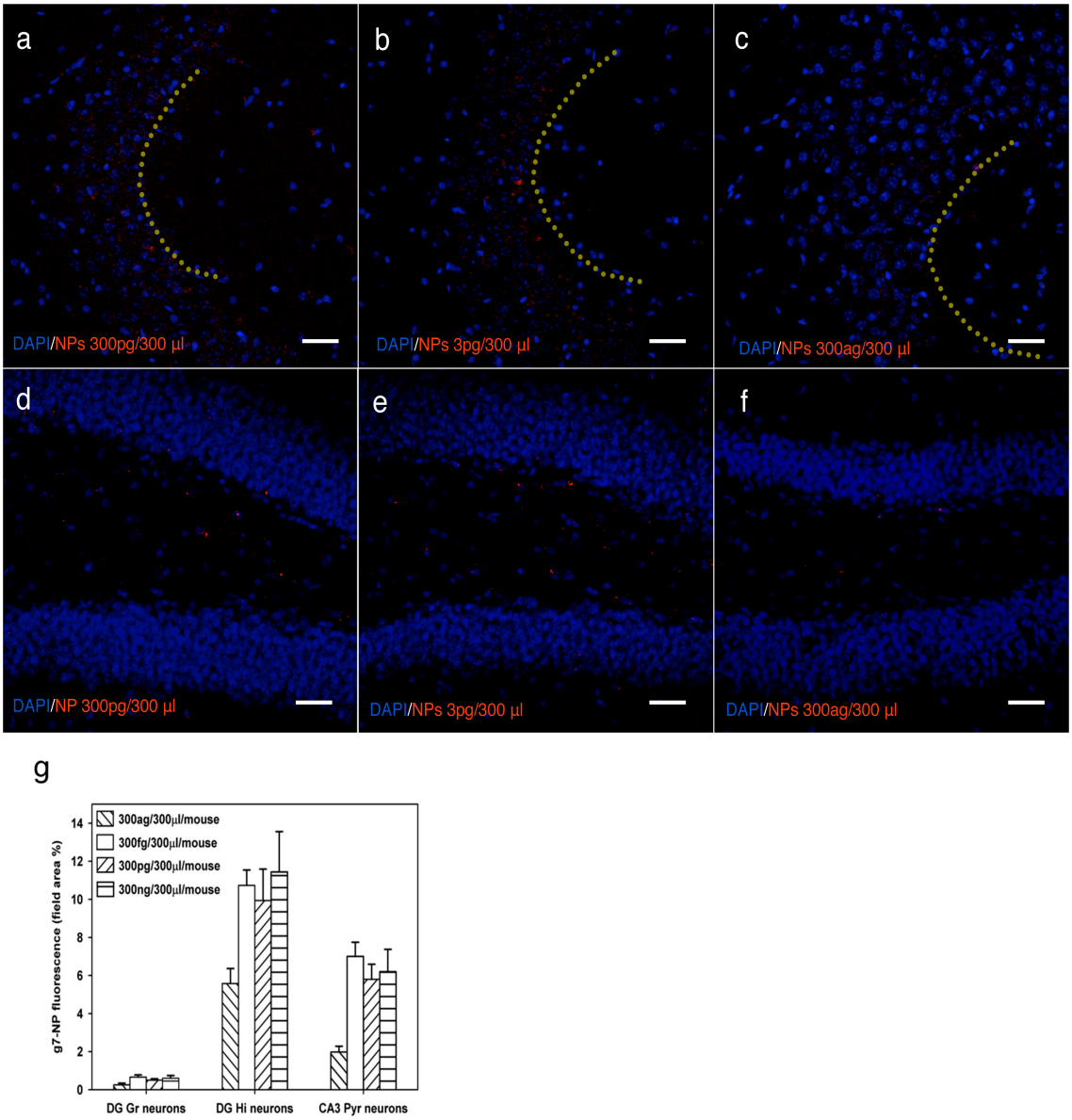


Fig.10 Dose-response of g7-NP labeling in neuronal populations of the hippocampal formation Confocal microscopy images of brain cryosections labelled with DAPI (blue) and g7-NPs (red) from the hippocampal CA3 field (a-c) and dentate gyrus (d-f) of mice sacrificed 6 hr after different doses (from 300 ag to 300ng/300µL/mouse, i.p.) of g7-NPs. The dotted line in panels a-c delimits the internal border of CA3 pyramidal layer. g7-NP cellular accumulation in dentate gyrus hilar (DG Hi) interneurons and CA3 field pyramidal (CA3 Pyr) neurons peaked at the dose of 300fg/300µL/mouse and remained at the same level at higher doses. Low to undetectable g7-NP labeling was present in dentate gyrus granule (DG Gr) neurons at all doses. Scale bar = 50 µm

Remarkably, C-NPs used for control experiments were completely unable to cross the BBB and to reach the brain compartment after i.p. administration in mice, independently from both the time-point chosen (even time-point as long as 5 days) and the dose used (Fig.11).

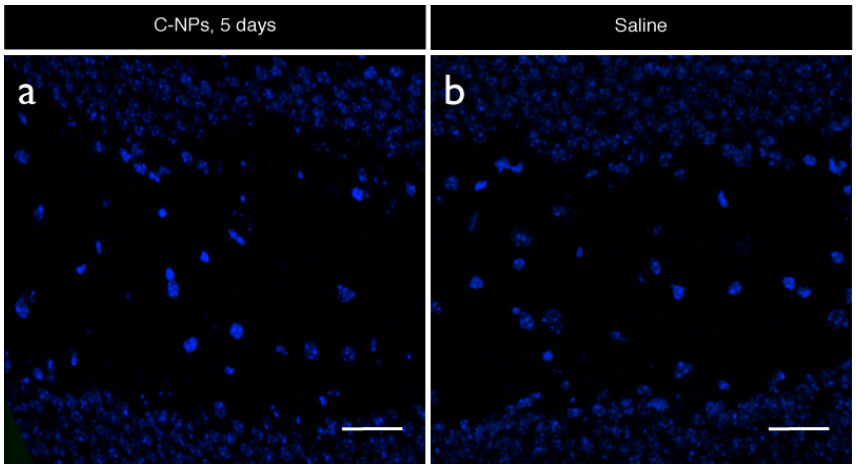


Fig.11 C-NP labeling in the hippocampal formation Representative confocal image showing the dentate gyrus labeling of mice sacrificed 5 days after i.p. injection of 300ag/300µL/mouse of C-Nps (a) and 300µL of saline solution (b). DAPI is represented in blue. No red spots, corresponding to C-NPs were detected within the brain.
Scale bar = 50 µm

4. Nanoparticle uptake mechanisms

Recent studies reported that layered double hydroxide (LDH)-NP internalization in neurons is mediated by clathrin-dependent endocytosis and that NPs are targeted mainly to the clathrin endocytotic machinery (Chang et al 2009, Cleal et al 2013, Shan et al 2011, Zhang et al 2009).

A cellular regulator of vesicular transport in all eukaryotes is represented by the small Rab GTPase family. Rabs, in conjunction with their effectors and regulators, participate in CNS development (Rab23), polarized neurite growth (Rab8 and Rab11), α-Amino-3-hydroxy-5-methyl-4-isoxazolepropionic acid (AMPA) receptor endocytosis in a clathrin-dependent manner (Brown et al 2005) and axonal retrograde transport (Rab5 and Rab7) (Ng & Tang 2008).

Based on *in vitro* data about the uptake mechanism in primary hippocampal cell cultures (Vilella et al 2014), we sought to verify whether the same uptake mechanisms of g7-NPs are active *in vitro* and *in vivo* in the mouse brain upon peripheral g7-NP administration.

First, we studied the possible co-localization of g7-NPs with the clathrin-related Rab5 and caveola-related EAA1 early endosome markers (Fig.12a-d). In

accordance with the *in vitro* data, there was an impressive co-localization of g7-NP and Rab5 signals in hippocampal interneurons (Fig.12a,b), but only minimal co-localization with EAA1 signals in the same cells (Fig.12c,d).

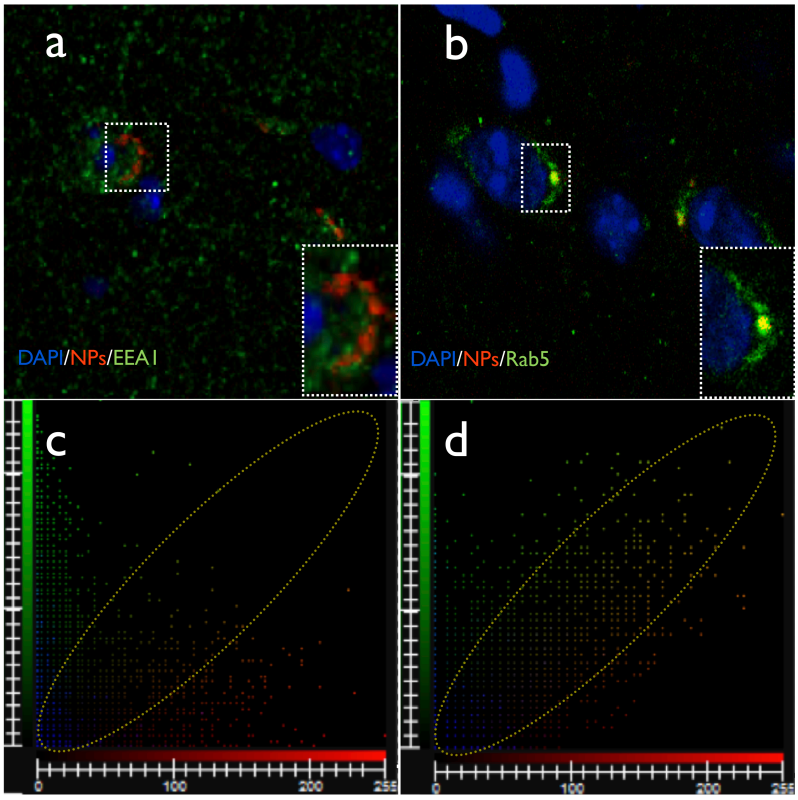


Fig.12 g7-NP uptake in neurons in vivo Colocalization of g7-NPs with markers of EE. Confocal microscopy images of brain cryosections labelled with DAPI (blue), g7-NPs (red) and, in green, rabbit anti-Rab5 (a,b) or rabbit anti-EEA1 (c,d) from the hippocampal dentate gyrus of mice sacrificed 6 hr after an i.p. injection of 300ag/300µL/mouse of g7-NPs. Intracellular g7-NPs co-localized with Rab5 (b) but not with EEA1 (a) immunoreactivity in hippocampal interneurons. Panels c and d represent the plots of the pixels with single (red or green) or double (yellow) labeling. Only Rab5 immunoreactivity shows a high extent of pixels with g7-NP co-localization (d).

Next, we tested whether neuronal uptake of g7-NPs *in vivo* is clathrin-dependent and/or caveolin-dependent. Thus, we infused chlorpromazine hydrochloride or staurosporine, inhibitors of clathrin-dependent and caveolin-dependent endocytosis, respectively, unilaterally within mouse hippocampus and, 15 min later, injected g7-NPs (300ag/300µL/mouse) peripherally. Infusion of the respective vehicles was performed into the contra-lateral hippocampus. As also reported in *in vitro* data (Vilella et al 2014), we observed a marked decrease of g7-NP signal accumulation within hippocampal neurons in chlorpromazine-

treated hippocampus (Fig.13c,d) but not in staurosporine-treated hippocampus (Fig.13a,b).

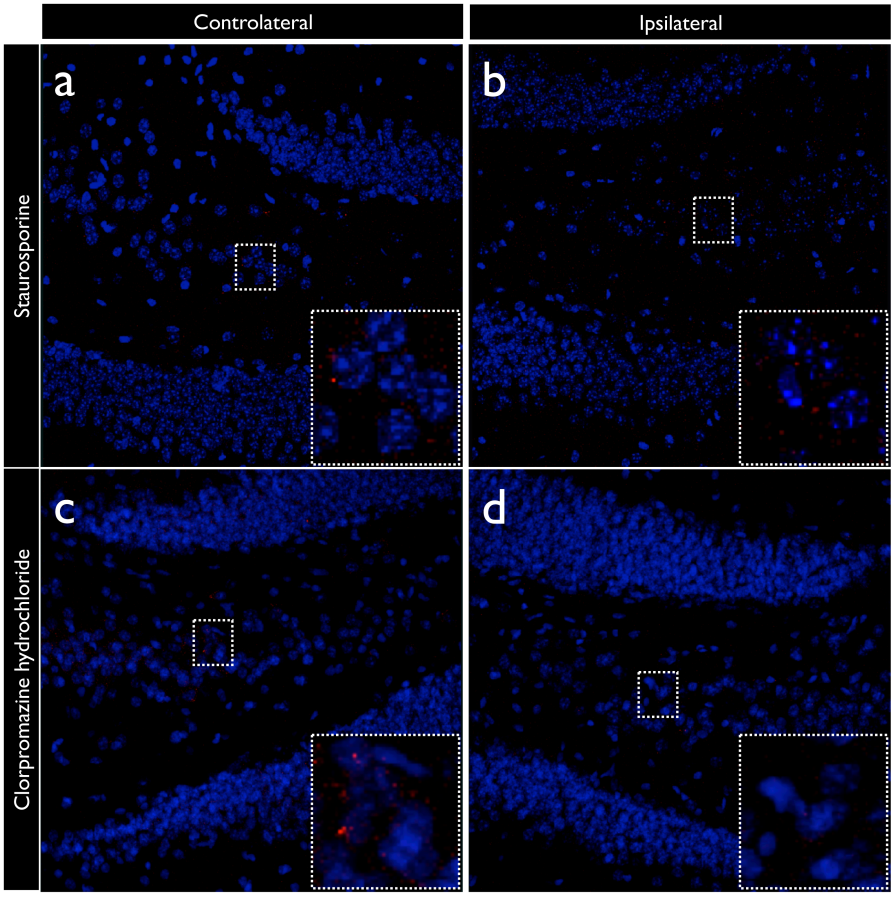


Fig.13 g7-NP uptake in neurons in vivo: Inhibition of endocytotic pathways in vivo Confocal microscopy images of brain cryosections labelled with DAPI (blue) and g7-NPs (red) from the hippocampal dentate gyrus of mice sacrificed 20 min after the local infusion of staurosporine (inhibitor of caveolin-dependent uptake pathway, 1µL of 50µM) or chlorpromazine hydrochloride (inhibitor of clathrin-dependent uptake pathway, 1µL of 30µM) and 15 min after i.p. injection of 300ag/300µl/mouse of g7-NPs. Contralateral sides received a local infusion of the respective vehicle. Panels in the lower right portion of each image report high magnification images of the squared areas indicated within the respective larger images. While staurosporine infusion did not alter g7-NPs distribution in the dentate gyrus, chlorpromazine infusion dramatically reduced the intensity of g7-NPs neuronal labeling.

Although Rab5 immunoreactivity is ubiquitous in the CNS, its intensity is markedly heterogeneous in different neuronal subpopulations. For instance, in the hippocampal DG, a few cells of the hilar region showed high levels of Rab5 immunoreactivity (in green), whereas granule cells demonstrated low Rab5 expression (Fig.14a-f). Likewise, pyramidal neurons in CA3 and CA1 fields showed moderate and low Rab5 immunoreactivity, respectively (Fig.14g-i).

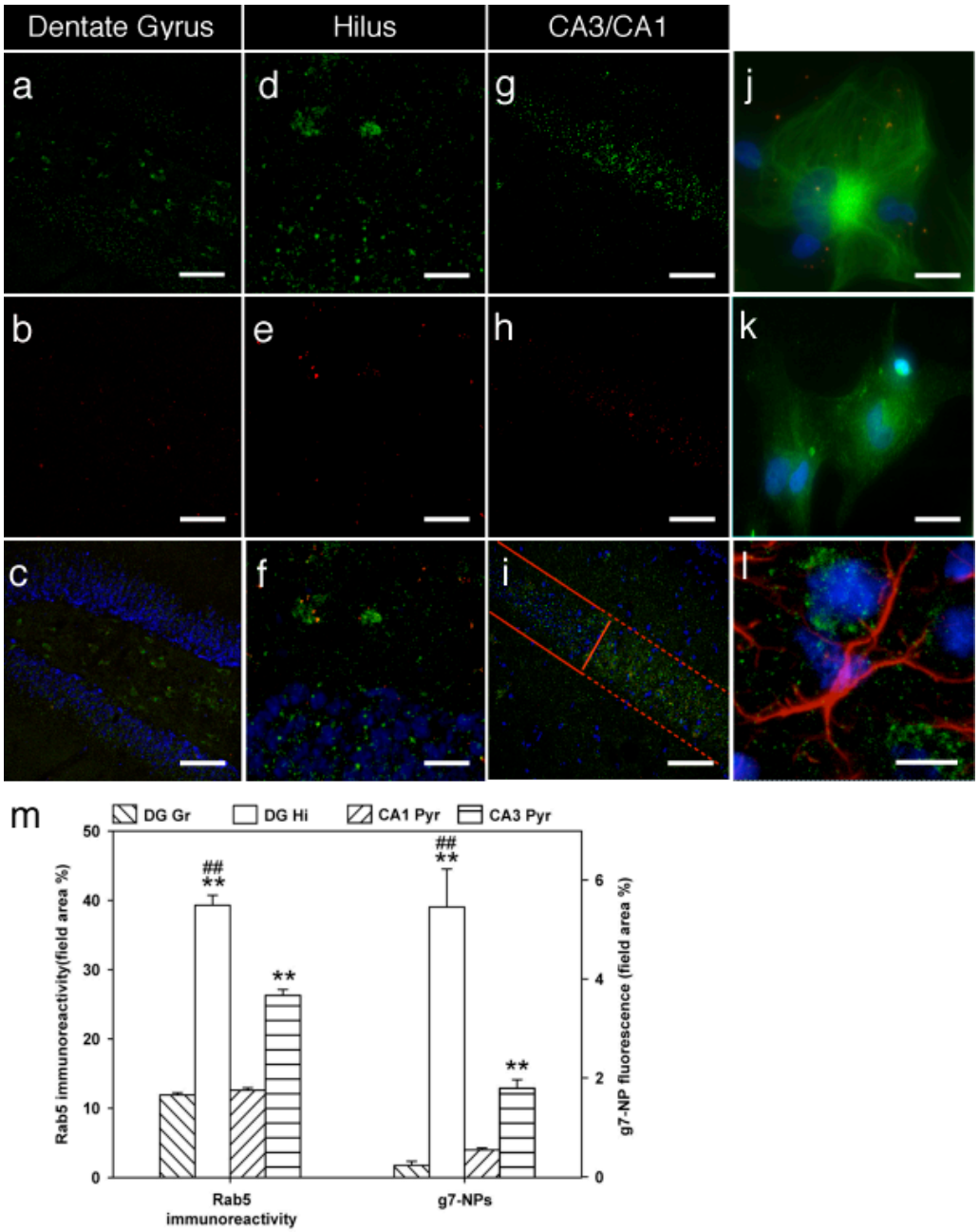


Fig.14 Correlation between Rab5 immunoreactivity and g7-NP labeling Confocal microscopy images of brain cryosections labelled with DAPI (blue), rabbit anti-Rab5 immunoreactivity (green) and g7-NPs (red) of the dentate gyrus (a-c), the hilus (d-f) and the boundary between CA1 and CA3 fields (g-i) from mice sacrificed 6 hr after an i.p. injection of 300ag/300µL/ mouse of g7-NPs.

(m) Bar histogram of the intensity of Rab5 immunoreactivity and g7-NPs labeling in granule cells (Gr) and hilar (Hi) neurons of the dentate gyrus (DG), and pyramidal cells (Pyr) of the CA1 and CA3 field. The rank-order of both Rab5 immunoreactivity and g7-NPs is: Hi > CA3 Pyr > CA1 Pyr ≈ Gr.

(j-l) GFAP (green) and g7-NPs (red) (j) and Rab5 (green) (k) positive astroglial cells from astroglial cell primary culture. GFAP positive astrocyte (red) and Rab5 positive cells (green) in wild type mice (l).

In vitro, astrocytes express Rab5 immunoreactivity and accumulate g7-NPs (j-k) whereas *in vivo* astrocytes neither express Rab5 immunoreactivity nor accumulate g7-NPs (l).

Scale bar = 50 µm (a-c, g-i), 20 µm (d-f), 5 µm (j,k), 10 µm (l)

We performed a high magnification single cell analysis of highly intense Rab5-ir cells in the hilus of DG using confocal microscopy and found that these cells correspond to the interneurons that accumulate the highest levels of g7-NPs (in red) after peripheral administration (Fig.14f). We then performed a semiquantitative analysis of Rab5 immunoreactivity in different neuronal subpopulations of the hippocampal formation. Granule cells of the DG and CA1 field pyramidal neurons had the lowest level of Rab5 immunoreactivity, whereas hilar interneurons had the highest levels, and the pyramidal neurons of the CA3 field showed intermediate levels (Fig.14m).

This nicely corresponds to the rank order of g7-NP accumulation in the same cells. The heterogeneity in the intensity of Rab5 immunoreactivity and g7-NP accumulation after peripheral injection is particularly impressive at the boundary between CA1 and CA3 pyramidal layers, two structures with a relatively similar density of neurons (Fig.14g-i). Interestingly, while in astroglial primary cell cultures, astroglia show high Rab5 immunoreactivity and accumulate high levels of g7-NPs (Fig.14j-k), astroglial cells in the brain express very low levels of Rab5 immunoreactivity and do not accumulate g7-NPs *in vivo* (Fig.14l).

5. Cell-to-cell exchange of nanoparticles

As the application of g7-NPs to cell cultures showed NPs associated with TNT-like structures (Tosi et al 2014), here we investigated whether in the living brain g7-NP labeling co-localizes with M-Sec (a marker of TNTs), also called TNFαip2, immunoreactivity 48 h after a peripheral administration of NPs.

We found that well defined TNFαip2 immunoreactivity spots decorated putative neuronal profiles (recognized by their regional location and nuclear features) in the hippocampal formation (Fig.15c).

A semiquantitative analysis of TNFαip2 immunoreactivity showed that the highest amount of signal was detected on DG hilar cells, whereas CA3 and CA1 pyramidal layers showed a moderate level of immunoreactivity and DG granule layer a low level of immunoreactivity (Fig.15a). In CA1 and CA3 pyramidal layers as well as in DG granule layer, the distribution of TNFαip2 immunoreactivity was heterogeneous. In fact, a restricted sub-population of cells showed a very high level of signal whereas the large majority of cells showed a much lower and substantially homogeneous level of signal.

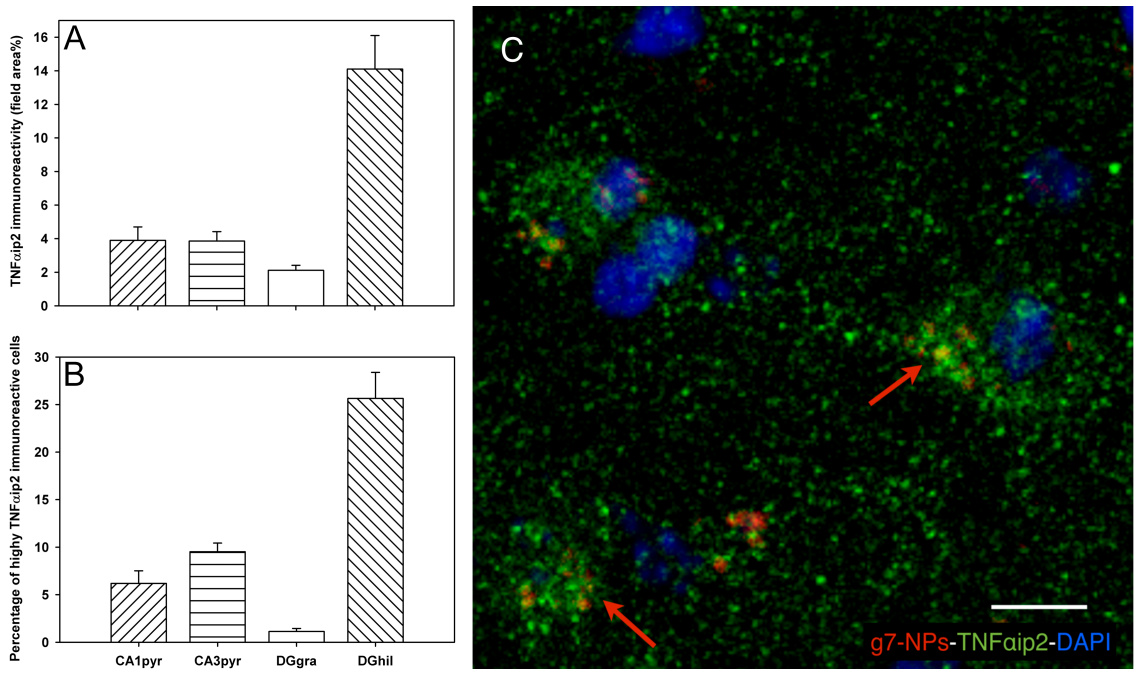


Fig.15 Correlation between TNFαip2 immunoreactivity and g7-NP labeling Confocal microscopy image of brain cryosection labeled with DAPI (blue), rabbit anti-TNFαip2 immunoreactivity (green) or g7-NPs (red) of the dentate gyrus from a mouse sacrificed 48 h after an i.p. injection of 300ag/300µl/mouse of g7-NPs. A, B) semiquantitative analysis of TNFαip2 immunoreactivity (expressed as field area%) and percentage of highly TNFαip2-ir cells in hippocampal sub-regions (pyr: pyramidal; gra: granule; hil: hilus; DG: dentate gyrus). C) Colocalization of g7-NPs with TNT formation marker. g7-NPs and highly TNFαip2-ir spots co-localized within some putative neuronal cells (see red arrows).
Scale bar = 10 µm

Therefore, we decided to assess the percentage of cells that are intensely stained for TNFαip2 in each of the sampled regions by cell count on confocal images (Fig.15b). In the DG hilar region, roughly 1 out of 4 cells was intensely stained. This figure was 9, 6 and 2% in CA3 and CA1 pyramidal layers and DG granule layer, respectively.

The cells showing intense TNFαip2 immunoreactivity often appeared to have a high accumulation of g7-NPs. We also evaluated the percentage of cells that have both high levels of TNFαip2 and high accumulation of g7-NPs. We performed this analysis in the hilus of DG since only in this region the cells are relatively isolated and allow a safe attribution of the two signals to the same cell. The analysis showed that 72.1 ± 5.6% of the highly TNFαip2-ir cells also accumulate high levels of g7-NPs, whereas 62.2 ± 6.7% of the cells that accumulate high levels of g7-NPs show also high levels of TNFαip2 immunoreactivity. However, while very often the same cell has high levels of both TNFαip2 and g7-NP, very rarely *g7*-NP labeling co-localizes with TNFαip2-

ir spots (Fig.14c). This suggests that the two markers are highly concentrated in the same cells, but label different sub-cellular structures.

6. Engineered Ab-modified g7-NP accumulation in brain areas and cell types: *in vivo* evidence

In a previous paper (Grabrucker et al 2011), it was shown that engineering of g7-NPs with cell-type specific Abs allowed a cell-type-specific targeting of NPs *in vitro*. To investigate whether the function of the Ab moiety to drive g7-NPs to the targeted cell is maintained *in vivo* we analyzed CD44-g7-NPs and NCAM-g7-NP accumulation within the brain after a peripheral administration by using IF and Abs specific for the different cell types: NeuN, GFAP and Iba1.

Representative images illustrate the confocal analysis of brain sections (Fig. 16a-i) comparing the cellular accumulation of g7-NPs, CD44-g7-NPs and NCAM-g7-NPs, respectively. As also described before, *g7*-NPs very rarely colocalized with astrocytes (Fig.16a), while they were often found associated with microglial cells (Fig.16b).

Besides this selectivity for specific non-neuronal cell populations, the main target of *g7*-NPs appeared to be neurons (Fig.16c). Again, g7-NP targeting appeared cell-type selective with NPs especially accumulating in some neuronal sub-populations that include NPY positive and glutamic acid decarboxylase (GAD) positive interneurons (not shown) of the Cx and hippocampal formation, in particular the interneurons of the hilar region of the DG.

Regarding Ab-modified g7-NPs, confocal images did not show altered selectivity of CD44-g7-NPs and NCAM-g7-NPs to astrocytes (Fig.16d,g), microglia (Fig.16e,h) or neuronal cells (Fig.16f,i), compared to g7-NPs. Interestingly, as previously shown for g7-NPs, we observed a tendency of both Ab-modified g7-NPs to display a tropism for NPY or GAD positive interneurons (not shown), that seems to be, therefore, maintained notwithstanding the surface engineering of NPs with Ab. Moreover, the *in vivo* preferential tropism to specific interneurons (GAD or NPY positive) of any kind of modified g7-NPs, independently from the presence of Ab modified g7-NPs, tallies well with the *in vitro* results on a preferential tropism for NPY/GABAergic interneurons (Tosi et al 2014).

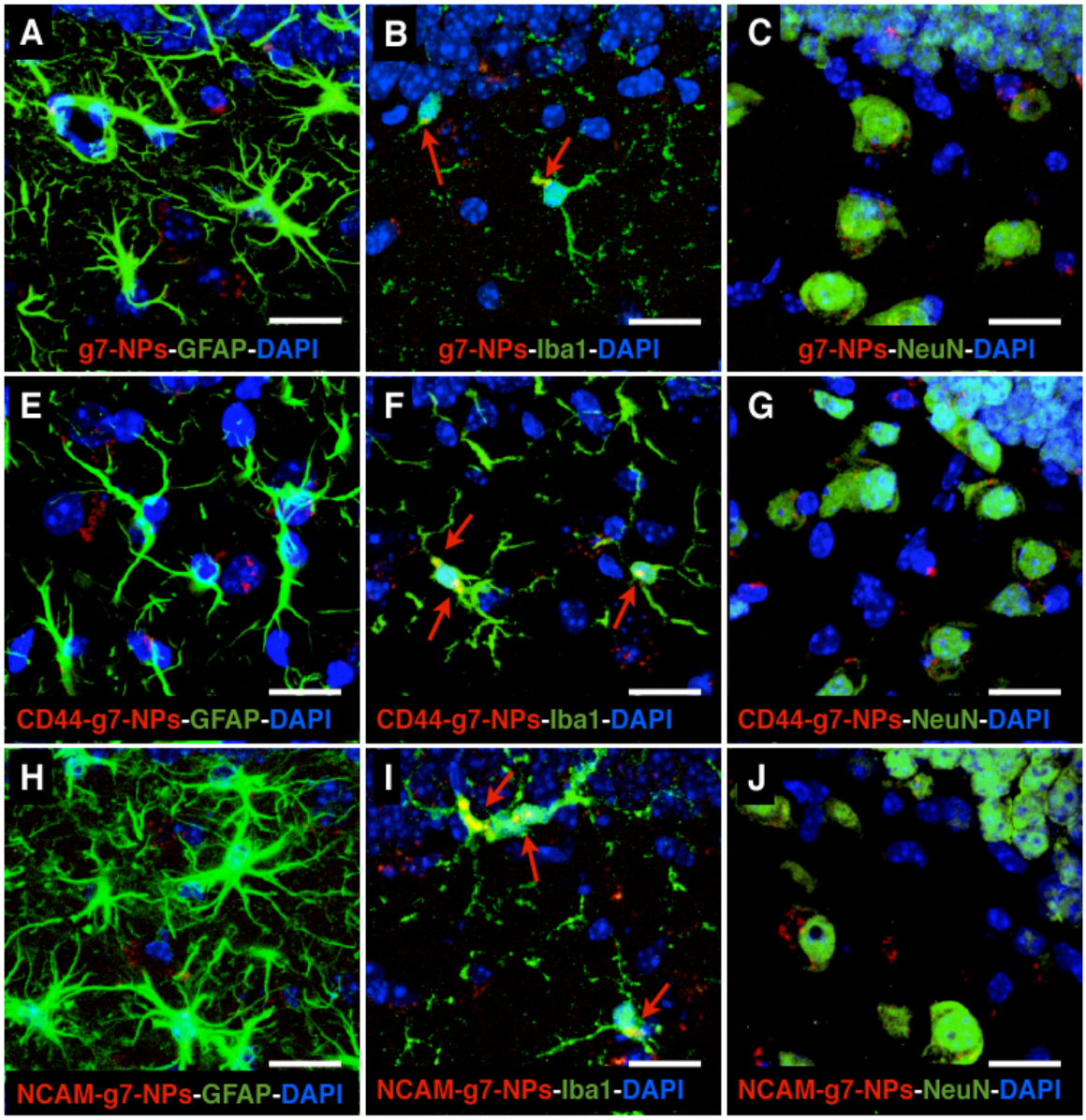


Fig.16 Cell type-specific accumulation of g7-NPs and antibody-modified g7-NPs in vivo
Confocal microscopy images of cell type-specific accumulation of g7-NPs, NCAM-g7-NPs and CD44-g7-NPs 30 min after an i.p. injection of 300ag/300µl/mouse of NPs.
(A-J) Brain cryosections labeled with DAPI (blue), labeled g7-NPs (red) and, in green, rabbit anti-GFAP (A,E,H), rabbit anti-Iba1 (B,F,I) or rabbit anti-NeuN (C,G,J) from hippocampal dentate gyrus of mice. 30 min after i.p. injections, g7-NPs, CD44-g7-NPs and NCAM-g7-NPs, respectively, accumulated in both, microglial cells (B, F, I) and neuronal cells (C,G,J) in the dentate gyrus hilus. Only rarely GFAP-ir astrocyte were positive (A,E,H).
Scale bar = 20 µm

DISCUSSION

In the last few years, an increasing number of studies has been performed to develop efficient therapies for brain diseases such as cancer, HIV-dementia, stroke, ischemia, AD and PD (Hawkins & Davis 2005, Ricci et al 2006, Soppimath et al 2001).

In this perspective, the development of nanocarriers, such as Lps and NPs, able to reach brain cells after having crossed the BBB represents an important topic of the pharmaceutical research (De Jong & Borm 2008, Lim et al 2012, Moghimi et al 2005). Many attempts to use NPs as a DDS for CNS were performed with a certain success; among the various non-invasive approaches, nanoparticulate carriers and particularly NPs seem to be the most interesting strategies (Edwards 2001, Peer et al 2007).

Different strategies were proposed to allow BBB crossing of the NPs. Most of them are based on the physical adsorption of a hydrophilic polymer, i.e., the surfactant polysorbate 80, on the surface of polycyanoacrylate (PCA)-NPs; alternatively, NPs able to cross the BBB were prepared using amphiphilic copolymers, like the block copolymer of polyethylenglycol and n-hexadecylcyanoacrylate (PEG-PHDCA), in which the hydrophilic part remains on the surface (Calvo et al 2001). These carriers were shown to be effective in delivering to the brain a variety of drugs such as dalargin, Lop, NMDA-receptor antagonists or doxorubicin (Ambruosi et al 2006, Chen et al 2008, Tosi et al 2007) as well as nucleic acid constructs (Miller 2008, Yamamoto et al 2012).

The mechanism of BBB crossing of surfactant-coated NPs appears to be the absorption of ApoE or A-1 on NPs during their passage through the blood stream, followed by RME via the low density lipoprotein (LDL) receptor by the brain capillary endothelial cells (Kim et al 2007, Kreuter et al 2002). This hypothesis was supported by the finding that covalent coupling of ApoE or A1 to human serum albumin NPs (HSA NPs) leads to similar effects (Kreuter et al 2007, Michaelis et al 2006, Petri et al 2007).

On the basis of these findings, a common strategy for NP targeting to the brain seems to be represented by the possibility to modify the surface of NPs modulating the interaction of the NP surface ligand (*Trojan horse molecule*) with a specific receptor expressed by the BBB allowing the BBB crossing by receptor mediated transport (transcytosis).

Specific receptors can be targeted with suitable ligands: receptors of the BBB endothelium were identified for LDL (Dehouck et al 1997), insulin (Frank et al 1986), lactoferrin (Lf) (Fillebeen et al 1999), IGF-I and IGF-II (Duffy et al 1988), interleukin-1 (IL-1), folic acid (FA) (Wu & Pardridge 1999) and Tf (Descamps et al 1996). The mechanism of uptake of Tf, LDL, Lf, melanotransferrin (MTf) ligands is represented by transcytosis. Among them, TfR represents the most widely studied receptor for BBB targeting. The receptor is highly expressed by brain capillaries to mediate the delivery of iron to the brain and is also expressed by neurons (Jones & Shusta 2007). Thus, a single ligand targeted to TfR can not only mediate the transport of nanocarriers across the BBB but also help to increase intracellular delivery into neurons; moreover, TfR is over-expressed in many tumors. Although many studies have demonstrated that Tf increases brain delivery of nanocarriers *in vitro* and *in vivo*, the specific brain uptake mechanism of Tf modified nanocarriers has not yet been clearly defined. For example, caveolae-mediated transcytosis of Tf was shown to occur in an *in vitro* model of co-colture of endothelial cells and astrocytes (Candela et al 2008) but the same mechanism was not confirmed in other models of culture, in which endocytosis was shown to occur through the clathrin pathway (Pang et al 2011, Visser et al 2004).

Most of the evidence on NP uptake mechanisms reported in the literature about NP intracellular pathways and processes involved, is based on *in vitro* studies (Kuo & Chung 2012, Luther et al 2013, Thomsen et al 2012, Wagner et al 2012). Nowadays, a particular attention is devoted to increasing the knowledge of the rate of *in vivo* BBB crossing of nanocarriers and their subsequent exocytosis in the brain compartments, their fate and trafficking in the brain.

In fact, in most of the *in vivo* studies, only the capability of NPs to cross the BBB and accumulate within the brain were assessed without considering either the specificity of the NP-cell interaction or the modulation of response in a time and dose dependent manner; no studies about specific cellular targeting of NPs, as well as their distribution over time and the mechanism of selective transport inside and between neural cells were investigated.

For example, the capability of Lf-NPs and Tf-NPs to cross the BBB *in vivo* was demonstrated investigating the fluorescent probe coumarin-6 signal within the brain. The Cx, the periventricular region of the lateral ventricles and the third ventricle were positive to coumarin-6 labeled Tf-NPs; Cx, substantia nigra (SN)

and striatum regions incorporated coumarin-6 Lf-NPs 1 h after i.v. injection (Hu et al 2011). No information was provided about the mechanism of transport *in vivo*: authors only demonstrated Tf-NP or Lf-NP uptake mechanism *in vitro*, using b.End3 cells (the immortalized mouse brain endothelial cell line) via RME.

Our first aim was to assess the capability of g7-NPs, designed for brain delivery, to cross the BBB, preserving its integrity, after different administration routes. The i.v. route is clearly one of the most successful, since it assures an immediate and fast circulation within the blood stream and therefore a short time to reach brain capillaries. O.a. and i.p. (Fig.5) routes allow the g7-NPs to interact with the BBB and reach the CNS after a longer period, owing to the time necessary to cross other barriers (intestinal walls or peritoneal walls).

The capability of g7-NPs to reach the brain after o.a. is an important finding as, to the best of our knowledge, until now only few papers (Das & Lin 2005, Schroeder et al 1998) have dealt with CNS targeting after this administration route (Lalatsa et al 2012). However, before proposing the o.a. of the g7-NPs for brain targeting, an important drawback should be underlined. Notwithstanding g7-NPs are capable to reach the CNS, orally administered g7-NPs charged with Lop, an opioid receptor agonist unable to cross the BBB by itself, did not have any significant analgesic effect. Since previous papers (Tosi et al 2010) demonstrated that i.v. administration of g7-NPs charged with Lop have analgesic activity, a reasonable interpretation of the failure of Lop targeting to the CNS is the release of Lop (low MW, close to 500 Da) into the gastric environment. Thus, g7-NPs cannot be applied to the CNS targeting of low MW drugs, though this administration route could be reserved to the administration of high MW macromolecules (macropeptides, proteins and gene materials) that would otherwise be unstable after an o.a.

Notwithstanding the failure to target low MW drugs to the brain, the observation that g7-NPs reach the brain after o.a. is of relevance, as it gives evidence of the g7 stability in the acid medium of the stomach and to the proteolytic enzymes along the route from the mouth to the blood. The g7 stability is due to the presence in the glycopeptide molecule of D-Thr more resistant to proteases than L-amino acids. Indeed, g7 stability is not surprising as the parent glycopeptide MMP-2200 (the Tyr in MMP2200 was substituted in g7 by Phe in order to avoid a potential opioid effect (Do Carmo et al 2008, Li et al 2012,

Lowery et al 2011, Polt et al 2005, Polt et al 1994), demonstrated a higher stability in the bloodstream with respect to native opioid peptides.

I.n. administration offers an alternative strategy for non-invasive delivery of large molecules, such as IGF-I, nerve growth factor (NGF) and vasoactive intestinal peptide (VIP) to the brain, with the advantage to bypass the BBB and transport directly drugs to the CNS (Graff & Pollack 2005). The poor membrane permeability of standard NPs, as for example polyethyleneglycol-PLGA NPs (PEG-PLGA-NPs) and polyethyleneglycol-polylactic acid NPs (PEG-PLA-NPs), that allows limited endocytosis at nasal mucosa, still restricts the application of this route for brain drug delivery. An approach to enhance nasal adsorption of NPs is the surface modification with biorecognitive ligands such as Solanum tuberosum lectin (STL), a glycoprotein that selectively binds to N-acetylglucosamine, abundant on the nasal epithelial membrane. STL-PEG-PLGA NPs loaded with radiolabelled basic FGF (bFGF), ^{125}I-bFGF (STL-bFGF-NP) i.n. administered to AD model rats (i.c.v. injected with β-amyloid$_{25-35}$ and ibotenic acid) are able to cross the BBB and distribute within different brain areas. The peak concentration of released bFGF occurred at 30 min in the olfactory bulb and at 2.4 h in other brain tissues, such as cerebrum and cerebellum. AD rats treated with STL-bFGF-NP showed improvements in spatial learning and memory (Zhang et al 2014).

We reported that g7-NPs are able to cross the olfactory mucosal barrier and be uptaken by neurons and supporting cells through a number of endocytic mechanisms before reaching the brain via an intra-axonal route (Illum 2003, Mistry et al 2009). As reported in Fig.6, g7-NPs were found to be localized in the CNS 60 min after i.n. administration: a number of cells were positive to Rhod-red spots (g7-NPs) in different brain areas.

Proven the capability of g7-NPs to reach the brain after o.a., i.n. or i.p. administration, we selected the easiest i.p. injection to perform a more detailed study about cell uptake and brain distribution of unmodified and Ab-modified g7-NPs *in vivo*.

The study of NP accumulation in specific brain areas and cell populations was carried out injecting different doses of NPs and analyzing samples at different time points. Six hours after the injection, g7-NPs were largely distributed across brain regions, with higher concentrations in grey matter areas

than in white matter areas (Fig.7). Within all these regions, cellular accumulation of g7-NPs appeared to be highly heterogeneous (Fig.7e-h).

The regional analysis indicates that NPs are able to reach multiple levels of the neuraxis but are not homogeneously distributed within the CNS. White matter areas that are poor in neurons and rich in glia are less intensely labeled than the neuron rich grey matter areas, suggesting a tropism of NPs towards neurons that is confirmed by the analysis at cellular level. The BBB does not seem to be a crucial factor in determining the fate of g7-NPs since the SFO, an area devoid of BBB, shows the same level of NP labeling as other grey matter areas. Indeed, the CP epithelium, that is located outside the BBB, shows a low level of NP accumulation. Overall, these data suggest that cell-specific targeting features of g7-NPs more than their simple capability to cross the BBB determine the distribution of g7-NPs inside the CNS.

Among the brain areas positive to g7-NP accumulation, we focused our analysis on the hippocampal region and, using specific Abs against neurons, microglia and astrocytes, demonstrated that g7-NPs are accumulated inside NeuN immunoreactivity neurons and Iba1 immunoreactivity microglia; whereas g7-NPs can only rarely be attributed to GFAP-ir astroglia as reported in Fig.8.

g7-NP accumulation in hippocampal neurons was heterogeneous. In fact, we found a preferential accumulation of NPs in interneurons of stratum oriens and lacunosum-molecolare of CA subfields and in the NPY interneurons (Fig.8c), especially, of the hilus of the DG. Regarding the other major classes of hippocampal neurons, the g7-NP labeling was clearly present in CA3 pyramidal neurons, though at a level lower than that present in NPY interneurons, but labeling was almost undetectable in granule cells of the DG or CA1 pyramidal neurons.

No qualitative change in g7-NP signal accumulation in the different cell types was recorded over time from 10 min to 5 days, as shown in Fig.9; yet, the amount of g7-NP accumulation per cell was time-dependent, with minimal accumulation at 10 min, a peak at 30 min, and a subsequent decrease (Fig.9p). These kinetics were similar in hilar NPY interneurons and CA3 pyramidal neurons, being g7-NP accumulation in the former cells always higher than that in the latter cells. The initial increase in NP accumulation is likely due to the progressive arrival of NPs into the brain extracellular fluid after the i.p. administration and the passage through the BBB. The subsequent modest

decrease in the intracellular NP signal may be due to a release of part of the NPs or their redistribution within the cellular network as suggested by the role of TNTs in intercellular transport of NPs (see below). Most importantly, from 2 hr to 5 days NP signal remains substantially stable, suggesting the slow degradation rate of g7-NPs accumulated within the target cells.

Independently from both the time point and the dose used (Fig.10), the accumulation of g7-NPs in neuronal populations changed in relation to the injected dose as illustrated in Fig.10. On the contrary, NPs devoid of g7 (C-NPs) were always unable to cross the BBB and reach the brain compartment after i.p. injection in mice. This phenomenon confirms the notion that if the surface of the NPs is not modified, they are opsonized, then removed rapidly from the bloodstream by monocytes and usually concentrated in the liver and spleen (Panagi et al 2001).

A quantitative analysis of the dose-response study, performed on hilar NPY interneurons, DG granule cells and CA3 pyramidal neurons, showed that, on the one hand, saturation of g7-NP accumulation was reached at the dose of 300fg/ 300μL/mouse, and, on the other hand, that the rank order of NP accumulation between neuronal cell types (NPY interneurons > CA3 pyramidal neurons >> DG granule cells) was maintained at all NP doses tested (Fig.10g). This evidence is of main interest since it demonstrates that the mechanism that leads to g7-NP accumulation within neurons is saturable and specific of each neuronal subtype. A likely candidate for this saturable mechanism is the initial uptake of NPs into neurons that is thought to be mediated by clathrin-mediated endocytosis (see below).

In addition, at all times and doses studied, no morphological changes suggestive of toxic phenomena were observed in glial cells confirming that g7-PLGA preparations are biocompatible, non-toxic and free of poly (vinyl alcohol) PVA surfactant (less than 3% of starting dose, see below). The morphological evidence is also supported by the absence of behavioral signs of toxicity in NP-treated mice, such as tremor, spontaneous seizures and hyperactivity after different injection routes.

Contrary to PLGA polymers, cationic polymers are reported to induce certain cell damage through their interaction with anionic components, like sialic acid (SA), of glycoproteins on the surface of epithelial cells (Fischer et al 2003). NPs made of PLGA polymer offer a non-toxic and efficient carrier system for the

delivery of drugs within the cell (Weissenbock et al 2004); also chitosan was found to be less toxic than other cationic polymers such as poly-L-Lysine and PEI *in vivo* and *in vitro* (Richardson et al 1999). The toxicity of chitosan-modified NPs was measured by assessing cellular damage indicated by reduction in metabolic activity (3-(4,5-dimethylthiazol-2yl)-2,5-diphenyltetrazolium bromide (MTT) and adenosine triphosphate (ATP) assay) or leakage of plasma membrane (lactate dehydrogenase, LDH release). Nafee and colleagues (2009) demonstrated that in COS-1 cells but not in A549 cells, cytotoxicity of chitosan-NPs was found to be dose-dependent. Nevertheless, the toxicity is underestimated due to the colloidal instability in culture media, reduction in effective NP concentration on the nanosize range, in addition to adsorption of medium components to the NP surface. Slight shift of the surrounding pH allows ionization of chitosan and increases in surface charge of the NPs, which as a consequence leads to more pronounced loss of membrane integrity of the cells (Nafee et al 2009).

Another factor that seems to influence NP-induced toxicity is the use of stabilizers to avoid the aggregation of NPs during solvent evaporation process, a notable problem regardless of the different preparation methods. Polymer stabilizers are often used for their function of coating the surface of NPs and prevent aggregation. Many of them, as PVA (Abdelwahed et al 2006), poly (vinyl pyrrolidone) (PVP), Tween 80 (Alyautdin et al 1997) are excellent stabilizer candidates. However, they are difficult to be removed even through thorough washing and some of them can be toxic to the BBB.

Oliver and colleagues demonstrated, in fact, that the drug delivery targeting using polysorbate 80-coated polymeric n-butyl-2-cyanoacrylate (PBCA)-NPs cause toxicity. They loaded dalargin in PBCA-NPs and in PS-NPs and added polysorbate 80 to NPs to induced a complete removal. Dalargin a Leu-enkephalin analogue (Tyr-D Ala-Gly-Phe-Leu-Arg), containing D-Ala in second position in order to prevent enzymatic destruction, shows good stability in the blood stream. Normally, the i.c.v. injection of this peptide has analgesic effect whereas its systemic administration has no analgesic effect. Nevertheless, dalargin associated with PBCA-NPs and polysorbate 80 induced a potent and prolonged analgesia, evaluated using the tail-flick test, which could not be obtained using PS-NPs in place of PBCA-NPs. In addition, PBCA-NPs, but not PS-NPs, caused a dramatic decrease in locomotor activity and occasional mortality in mice. As, *in vitro* PBCA-NPs (10 μg/mL) induced a permeabilization of the BBB model, they

concluded that a non specific permeabilization of the BBB, probably related to the toxicity of the carrier, may account for the CNS penetration of dalargin associated with PBCA-NPs and polysorbate 80 (Olivier et al 1999). Similarly to polysorbate 80, demonstrated a strong toxic effect of Tween 20-NPs supported by a dramatic increase in [^{14}C]sucrose paracellular passage in cell culture.

Clathrin-mediated endocytosis represents the **"**classical route**"** of cellular entry, which is present and inherently active in all mammalian cells. For instance, it is responsible for uptake of essential nutrients like cholesterol carried into cells by LDL via the LDL receptor (LDLr), or iron carried by Tf via the TfR (Sahay et al 2010).

In the literature on cellular uptake of NPs the discussion is only restricted to clathrin-mediated and caveolae-mediated endocytosis (Iversen et al 2011) without any consideration about transport inside and between cells. Recent studies reported that LDH-NP internalization in neurons is mediated by clathrin-dependent endocytosis (Wong et al 2010) and that NPs are targeted mainly to the clathrin endocytotic machinery (Harush-Frenkel et al 2008).

On the basis of the results obtained in *in vitro* experiments (Vilella et al 2014), we investigated whether the same uptake mechanisms of g7-NPs are active also *in vivo* in the mouse brain upon peripheral g7-NP administration. The endocytic mechanism responsible for cellular uptake of g7-NPs within the brain was studied, in more detail, using pharmacological inhibitors. Thus, the unilateral infusion within mouse hippocampus of chlorpromazine hydrochloride or staurosporine, inhibitors of clathrin-dependent and caveolin-dependent endocytosis, respectively, results in a marked decrease of g7-NP signal accumulation within hippocampal neurons in chlorpromazine-treated hippocampus (Fig.13c,d) but not in staurosporine-treated hippocampus (Fig. 13a,b).

Accordingly, g7-NPs co-localized impressively with clathrin-related Rab5 (Fig.12a,b), and minimally with caveola-related EAA1, early endosome markers (Fig.12c,d) in hippocampal interneurons. Therefore, we analyzed the immunoreactivity distribution of Rab5 within the hippocampus. Only few hilar cells showed high levels of Rab5 immunoreactivity, whereas granule cells demonstrated low level of Rab5 expression; likewise, pyramidal neurons in CA3 and CA1 fields showed moderate and low Rab5 immunoreactivity, respectively as represented in Fig.14. In addition, a high magnification single cell analysis of

highly intense Rab5-ir cells in the hilus of DG demonstrates that these cells correspond to the interneurons that accumulate the highest levels of g7-NPs after peripheral administration (Fig.14f).

Interestingly, Rab5 expression correlated with NP accumulation also in the case of astroglia, since astroglial cells in culture show high Rab5 immunoreactivity and accumulate high levels of g7-NPs (Fig.14j-k), whereas astroglial cells in the brain express very low levels of Rab5 immunoreactivity and do not accumulate g7-NPs *in vivo* (Fig.14l). This difference could be explained by the fact that, in the *in vitro* environment, the ability of astrocytes in phagocyting and accumulating materials (including NPs) is greatly enhanced (Amundson et al 1992, Guillemin et al 1997, Rinaman et al 1991, Rutka et al 1987). *In vivo*, astrocyte activation is rare, or even connected to serious pathological conditions such as insults, traumas or ischemia (Czlonkowska & Kurkowska-Jastrzebska 2011, Rodriguez et al 2009). Thus, since our animal model were healthy wildtype mice, astrocytes are not activated and have no phagocytotic activity. As a consequence, g7-NPs or Ab-modified g7-NPs (see below) are not accumulated within astrocytes after *in vivo* administration, thus being free to move and interact with neurons, where they display a higher accumulation.

EECs are the first major sorting station of the endosomal-lysosomal pathway (ELP) and the site of internalization and initial processing of different biological mediators and proteins. In neurons, the ELP performs a multiplicity of integral functions including internalization of nutrients and neurotrophic factors, degradation and recycling of receptors and integration of signaling information to relevant intracellular pathways.

Endosomal Rab5 localized in EEs, is known to play important roles in regulating the various stages of endosomal trafficking and fusion and its function in neuronal endocytosis has received much recent attention.

Grimes and colleagues (1996) reported that NGF binding to its cognate neurotrophic tyrosine kinase receptor type 1 (TrkA) results in signaling activities from cell surface. NGF signaling is initiated when it binds to its TrkA at the cell surface, leading to transient activation of the Ras/MAP(Mitogen-activated protein kinase) pathway and phosphoinositide 3-kinase (PIK3) that promotes cell survival (Zhang et al 2000). The NGF–TrkA complex is then endocytosed into the cell and found in the so-called signaling endosomes (Grimes et al 1996)

where TrkA is suggested to recruit new adaptors and to activate additional signaling processes to induce neurite outgrowth (Meakin et al 1999, York et al 1998). The biogenesis of signaling endosomes is not well understood. Although signaling endosomes contain EE markers such as Rab5, they are involved in long-distance retrograde transport of NGF in axons and have a much longer lifetime than conventional EEs, implying that Rab5 activity needs to be suppressed at this stage to avoid fusion with endosomes (Delcroix et al 2003). Rink and colleagues (2005) recently described a model on the dynamic nature of the EE network (EEN) and the transition to LEs. Rab5-dependent EE fusion is necessary for the entry to the EEN where cargoes are concentrated before the progression to LEs (Rink et al 2005).

In another report, Deinhardt and colleagues (2006) demonstrated that Rab5 is essential for the sorting step of tetanus toxin heavy chain (TeNT-H_c) conjugated to paramagnetic beads that precedes axonal transport. GFP-tagged Rab5 is found largely in TeNT-H_c containing vesicles that exhibit short-range bidirectional movements, but not those undergoing long-range retrograde transports (Deinhardt et al 2006). Therefore, Rab5 may function to keep the size of synaptic vesicles uniform by preventing their homotypic fusion via mechanisms that are yet unknown; in fact, studies in Drosophila indicated that the dominant negative mutant of Rab5, Rab5-N142I, induces a peculiar phenotype of enlarged synaptic vesicle in fly photoreceptor cells. This enlargement could be suppressed by enhancing synaptic vesicle recycling (Shimizu et al 2003).

Neuronal activity-dependent insertion or removal of AMPA receptors from the postsynaptic plasma membrane underlies the phenomenon of both long-term potentiation (LTP) and long-term depression (LTD), which are experimental manifestations of synaptic plasticity (Malinow & Malenka 2002). Removal of AMPA receptors from the postsynaptic plasma membrane in LTD would involve endocytosis; the endosomal Rab5 protein is therefore predictably a prime regulator of at least part of this process. Rab5 activation drives the specific internalization of synaptic AMPA receptors in a clathrin-dependent manner, and this activity is required for LTD, as a dominant-negative Rab5 inhibits LTD induction. However, Rab5 does not participate in the constitutive cycling of AMPA receptors. Although the details remain elusive, the emerging picture is that synaptic activity activates Rab5, which in turn drives the removal of both

AMPA receptor subunit glutamate receptor 1 (GluA1) and 2 (GluA2) from synaptic membrane into endosomes (Brown et al 2007, Gerges et al 2005).

Endosomal-lysosomal system dysfunction is one of the earliest disturbances observed in AD and may be one of the fundamental mechanisms underlying neurodegenerative changes during the progression of AD (Cataldo et al 1994, Grbovic et al 2003). Increases in Rab5 regulates EE enlargement that is a pathological feature that precedes cerebral and vascular amyloid-beta peptide (Aβ) deposition, neurofibrillary tangle (NFT) formation and is selective for AD (Cataldo et al 1997). Many vulnerable cell types within the basal forebrain, frontal cortex and hippocampus demonstrate enlarged endosomes and increased Rab5 immunoreactivity in human AD as well as in animal models of AD that display endosomal disturbances (Ginsberg et al 2010).

Overall, present data confirm that, similarly to other types of NP, clathrin-dependent endocytosis mediates g7-NP uptake. In addition, we could identify, for the first time, Rab5-positive intermediate endosomes as an intracellular store of g7-NPs. Most interestingly, our data on the heterogeneity of Rab5 expression in different brain cell populations *in vivo* and its correlation with g7-NP accumulation, suggest that the activity of clathrin-dependent endocytosis mechanisms is different in different cell types and that this cellular feature is a principal determinant of g7-NP targeting to specific brain cells *in vivo*.

A further objective of present research was to investigate the mechanisms of g7-NP transport between cells, taking into consideration the recent discovery of TNT.

This type of cell-to-cell communication was discovered to be enabled by the formation of membranous F-actin-rich structures between cells. TNTs mediate the intercellular transport of various cellular components through the generation of membrane continuity between cells (Gurke et al 2008). In that way, the direct transfer of cargos between cells in cell-to-cell communication is possible. Intriguingly, previous findings on qD-NPs showed that these systems are actively transported in membrane nanotubes between cardiac myocytes in a bidirectional fashion (with a mean velocity of 1.23 μm/s).

Regarding the mechanism of NP cell-to-cell exchange *in vivo*, g7-NPs were shown to be enriched in cells that are enriched in M-Sec (a marker of TNT), also called TNFαip2, in accordance with *in vitro* data. In more detail, TNFαip2 immunoreactivity, as for Rab5, shows different expression levels within the

hippocampus: highest amount of signal was detected on DG hilar cells (1 out of 4 cells was intensely stained), whereas CA3 and CA1 pyramidal layers (9 and 6% of total cells respectively) showed a moderate level of immunoreactivity and DG granule layer a low level of immunoreactivity (2% of total cells) (Fig.15a). In CA1 and CA3 pyramidal layers as well as in DG granule layer a restricted sub-population of cells showed a very high level of signal whereas the large majority of cells showed a much lower and substantially homogeneous level of signal.

By correlating the expression level of TNFαip2 and the accumulation of g7-NPs in the same cells, we found that 72.1 ± 5.6% of the highly TNFαip2-ir cells also accumulate high levels of g7-NPs, whereas 62.2 ± 6.7% of the cells that accumulate high levels of g7-NPs show also high levels of TNFαip2 immunoreativity. However, while very often the same cell has high levels of both TNFαip2 and g7-NP, very rarely g7-NP labeling co-localizes with TNFαip2-ir spots (Fig.15c).These data suggest that the presence of high levels of TNTs is correlated with the accumulation of g7-NPs although g7-NPs are rarely contained by TNT structures, possibly because of a fast passage through these sub-cellular structures or their short length *in vivo*. Here we showed that g7-NPs are strongly co-localized with Rab5 immunoreactivity. Since Rab5 is a marker of clathrin-related EE, we may hypothesize that following their entry into the brain g7-NPs are accumulated in specific cell sub-populations, mostly cortical and hippocampal interneurons, either after direct uptake or through TNT-mediated intercellular transfer, where they are permanently stored in a specific endosomal compartment (Fig.17).

Finally, we demonstrated the loss of Ab-related selectivity of Ab-modified g7-NPs, namely NCAM-g7-NPs and CD44-g7-NPs, *in vivo*. In fact, while in hippocampal culture Ab-modified g7-NPs demonstrated preferential accumulation in neurons (N-CAM) or astroglial cells (CD44) the *in vivo* accumulation profile of Ab-modified g7-NPs in different cell types within the hippocampus remains the same as that of g7-NPs (Fig.16a-i). As shown *in vitro* (Tosi et al 2014), the Ab surface modification loses its specific activity in driving NPs to the cell target if NPs are surrounded by a vesicle, especially considering neuron and glia transfer and dynamics. Unfortunately, the dynamics of extracellular NP loading inside vesicles are still poorly studied *in vivo* and need further investigations. Due to the lack of specific data on BBB dynamics and transcytosis, several hypothesis could be proposed including the adsorption of blood proteins onto NP surface that cover Abs influencing the trafficking

(Chaudhari et al 2012) and the possibility of a degradation of the Abs located onto NP surface during the transport across the BBB, the release of cargo after BBB crossing and NP loading into vesicles, the role of exosomes (Kramer-Albers et al 2013). Some of these are better documented.

The exosomes represent a way by which neurons, microglia, astrocytes and oligodendrocytes secrete molecules into the extracellular environment of the CNS. Neuronal exosomes carry the adhesion molecule L1, the C-terminal glycophosphatidyl-inositol (GPI)-anchored prion protein and have been implicated in synaptic plasticity. Enhanced glutamatergic activity stimulates the release of exosomes carrying GluR2 from the somatodendritic postsynaptic compartment (Lachenal et al 2011). In the context of CNS pathology, it appears that pathogenic proteins such as Aβ, prion protein, α-synuclein, tau and superoxide dismutase are released from cells in association with exosomes (Fruhbeis et al 2012). These proteins have in common the property to form aggregates (amyloid, prionoids) that escape the normal cellular degradation machinery.

Furthermore, particles in the nanometer range have easy accessibility in the body, being transported to different parts of the body via the blood circulation. Particles with a diameter below 100 nm with hydrophilic surface have been found to have longer circulation time in the blood (Moghimi et al 2001). The interaction of the colloidal carriers with blood plasma proteins (opsonins) and with the membranes of macrophages (opsonizations) is believed to be the major mechanisms for the clearance of these DDS from the bloodstream (Owens & Peppas 2006). On the other hand, opsonization is thought to allow brain specific targeting via ApoE adsorption (Kim et al 2007).

Despite their loss of selectivity for neurons (N-CAM) or astroglial cells (CD44), a tendency of both Ab-modified g7-NPs to display a tropism for NPY or GAD positive interneurons (not shown), as previously shown for g7-NPs, was observed.

Moreover, the *in vivo* preferential tropism to specific interneurons (GAD or NPY positive) of any kind of modified g7-NPs, independently from the presence of Ab modification, tallies well with the *in vitro* results on a preferential tropism for NPY/GABAergic interneurons.

GABAergic neurons contribute to the orchestration of pyramidal neuron firing by releasing GABA on $GABA_A$ and $GABA_B$ receptors ($GABA_A$r and

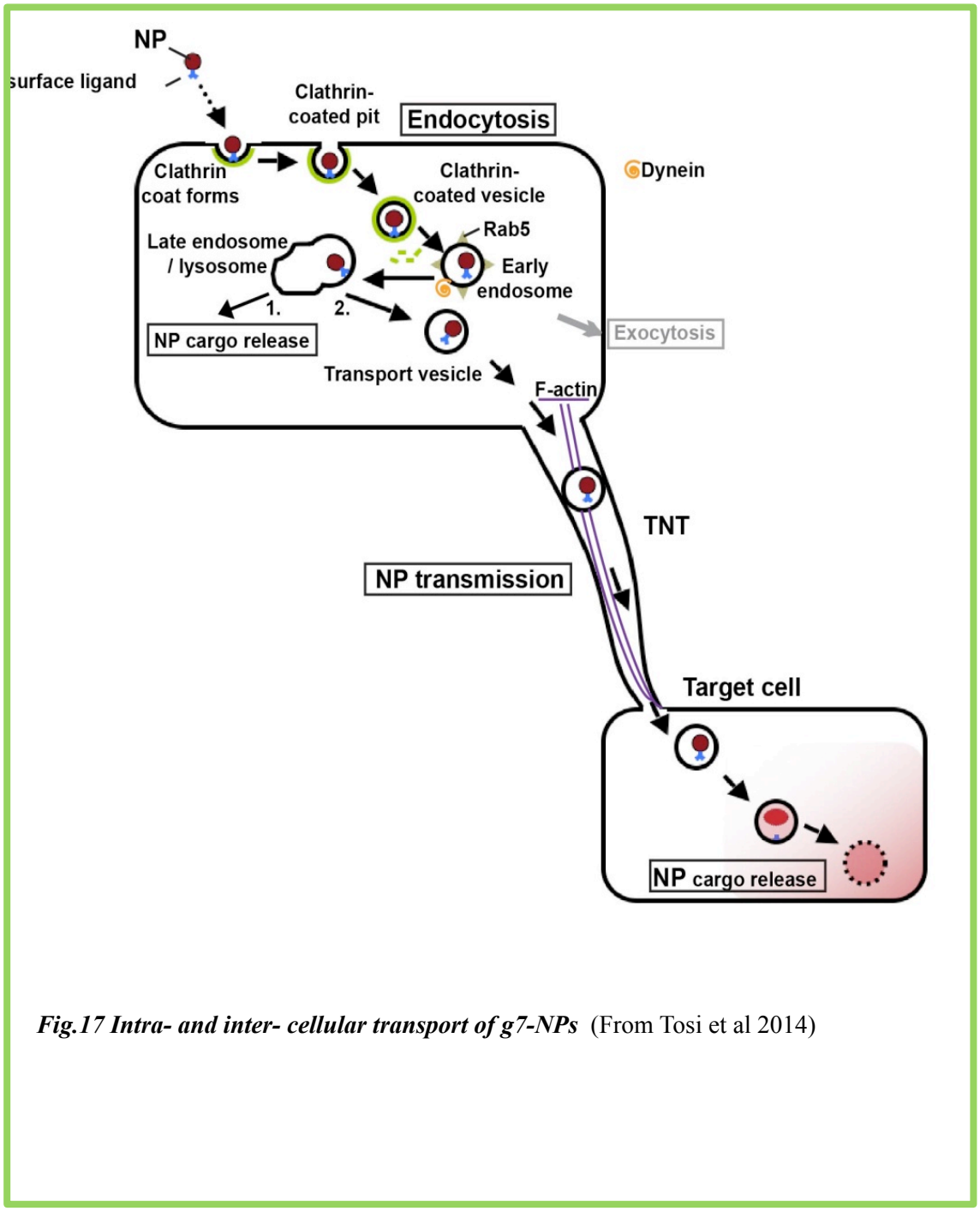


Fig.17 Intra- and inter- cellular transport of g7-NPs (From Tosi et al 2014)

$GABA_BR$) and releasing reelin (Reln) in the proximity of integrin receptors located on cortical pyramidal neuron dendritic spines and, through Reln, contributing to the regulation of dendritic spine plasticity by modulating dendritic resident mRNA translation (Guidotti et al 2005).

GABAergic interneurons are the only source of GABA and the main source of inhibition in the mammalian CNS (Le Magueresse & Monyer 2013). GABA is synthesized by two isoforms of GAD, GAD65 and GAD67. Both isoforms are present in most GABA-containing neurons, but GAD67 appears to be distributed

throughout the cell cytoplasm, whereas GAD 65 is specially targeted to membrane and nerve endings. It has been suggested that GAD67 preferentially synthesizes cytoplasmic GABA, while GAD65 ensures GABA synthesis destined for vesicular release (Soghomonian & Martin 1998).

A deficit or an excess of GABA release from inhibitory interneuron axon terminals on $GABA_Ar$ or $GABA_Br$ subtypes located in dendritic shaft, somata or initial axon segments of pyramidal neurons influence their rhythmic excitability and their functional output. Several neuropsychiatric diseases, including seizures, PD, neuropathic pain, stroke, psychosis and anxiety, may be considered at least in part developmental disorders of the GABAergic systems.

In fact, all these pathologies share a dysfunction of the basal GABAergic inhibitory activity; GAD67 and Reln resulted downregulated in prefrontal cortex (PFC) GABAergic neurons of schizophrenia (SZ) or bipolar disorder (BPD) patients (Akbarian et al 1995, Guidotti et al 2000, Impagnatiello et al 1998). This downregulation has been associated with pyramidal neuron hypoplasticity, a reduction of dendritic spine density, an alteration of high speed synchronous cortical neuron population firing and a working memory deficit. Reln is constitutively released from GABAergic interneurons into the extracellular matrix and plays a role in the regulation of extrasomatic protein synthesis (Dong et al 2003). Parvalbumin (PV) and Calretinin (CR) are not released intracellularly and their functional role in GABAergic transmission at the molecular level is not precisely known. Because PV and CR are calcium-binding proteins, they likely contribute to intracellular Ca^{2+} homeostasis and probably modulate the activity of transcription factors in cooperation with RNA polymerase II. When recombinant Reln is applied to rat hippocampal slices, it enhances the induction of LTP (Weeber et al 2002); however, when applied to dissociated neuronal cultures of heterozygous reeler mouse hippocampus characterized by dendritic hypoplasticity, it normalizes the expression of dendritic arborization (Niu et al 2004).

Czeh and colleagues (2005) demonstrated that chronic psychosocial stress resulted in significantly fewer PV-ir cells in the DG and in the CA2 and CA3 regions of the Ammon's horn, whereas the CA1 subfield was not affected (Czeh et al 2005). Disturbances in the anatomy and function of the GABAergic system have been implicated in various stress-related psychiatric disorders (Brambilla et al 2003, Sanacora et al 1999). Changes in the number of local inhibitory neurons

have been reported, especially in the anterior cingulate and PFC, and in the hippocampi of SZ and BPD patients (Beasley et al 2002, Benes & Berretta 2001, Lewis et al 2005). These observations are often interpreted as a consequence of altered neurodevelopment, but the contribution of stressful experiences, especially in the perinatal period, should be also taken into account (Benes 1999, Vaid et al 1997). A recent post-mortem study comparing densities of different subpopulations of GABAergic interneurons revealed a significant and profound deficit in the relative density of PV-ir neurons in all hippocampal subfields of SZ patients, but they did not reveal any changes in patients with a depressive disorder (Zhang & Reynolds 2002).

Changes of hippocampal GABA interneuronal circuits are known to play a central role also in epileptogenesis (Esclapez & Houser 1999, Houser 1991, Loup et al 2000). Although the majority of non-principal neurons seem to be resistant, so that GABAergic neurons are present in large numbers in the epileptic human hippocampus (Babb et al 1989, Sloviter et al 1991), a subset of GABAergic inhibitory cells containing CR was shown to be vulnerable to ischaemic and epileptic injury both in animal models and humans (Andre et al 2001, Knopp et al 2008, Magloczky & Freund 2005, Taylor et al 2014).

Dinocourt and colleagues and Kobayashi and Buckmaster (2003) analyzed respectively interneuron loss in the CA1 region and DG of the hippocampus of pilocarpine-treated rat as a model of temporal lobe epilepsy (Dinocourt et al 2003, Kobayashi et al 2003). The two studies provide independent lines of evidence that specific groups of GABAergic interneurons, including somatostatin (SS) and PV neurons, are lost shortly after severe status epilepticus. Because the number of GABAergic interneurons also was reduced many months later, the loss appears to be permanent.

AD is characterized neuropathologically by extracellular aggregates of Aβ derived from the amyloid precursor protein (APP), intracellular NFT, and synapse and neuron loss. Deficits in GABAergic transmission seem to play an important role in the cognitive and behavioral symptoms of AD (Lanctot et al 2004). In the hippocampus, which is severely affected in AD (Cummings & Cole 2002, Hof & Morrison 2004), inhibition is mediated by largely non-overlapping subsets of GABAergic interneurons that can be identified by the presence of PV, CR or calbindin (CB) (Freund & Buzsaki 1996, Maccaferri & Lacaille 2003). These proteins can be used as markers of selective neuronal degeneration (Hof et

al 1991) since depletion of calcium-binding proteins deprives neurons of the ability to maintain intracellular calcium levels and renders them vulnerable to pathological processes (Popovic et al 2008).

Magarinos and colleagues also demonstrated that PV-positive interneurons are subjected to the deleterious effect of excessive excitatory amino acid release from the mossy fiber terminals during stress exposure (Magarinos et al 1997).

Two principal strategies should be considered to correct the primary GABAergic neuron deficit observed in the pathologies just described: targeting abnormalities in nuclear epigenetic mechanism (Costa et al 2004) and enhancing the defective GABAergic transmission with drugs acting as direct or indirect $GABA_Ar$ agonist or as selective positive allosteric modulators of GABA action at pertinent $GABA_Ar$ subtypes. To treat these forms of neuropsychiatric diseases, systemic drugs are used that enhance the inhibitory mechanisms mediated by the neurotransmitter GABA, whose long-term use, however, can lead to unwanted side effects in behavior or cognition. Not to mention that about a third of patients are refractory to therapy anyway. Despite new researches about the mechanisms leading to the development of abnormalities in GABA interneurons, these neuropsychiatric diseases remain mostly untreatable due the inability of the majority of drugs to reach the brain parenchyma and be effectively delivered into the brain, when intravenously administered.

Good results were obtained using invasive strategies based on the injection of GABAergic interneuron progenitors within the brain (Tyson & Anderson 2014). Several studies have shown that interneuron precursor transplantation into neonatal or adult neocortex or hippocampus can ameliorate both the development of seizure activity and the intensity of seizure already established (Zipancic et al 2010) and even attenuate behavioral phenotypes in rodent seizure models (Hunt et al 2013). Accordingly, medial ganglionic eminence (MGE)-interneuron progenitors transplanted into rats that had received unilateral SN lesions with 6-hydroxydopamine (6-OHDA) differentiated into interneuron and glial subclasses and partially rescued motor behavior in lesioned animals. Although the physiological relationships between the transplants and the motor behaviors are unclear, this study highlights the capability of MGE progenitor transplants to affect complex neuronal circuits and improve deficits in a diseased brain (Martinez-Cerdeno et al 2010). In addition, interneuron-based therapies may enhance recovery after stroke. MGE progenitors were transplanted into multiple

cortical regions in a rat model of stroke induced by transient middle cerebral artery occlusion (Daadi et al 2009). Cells were delivered focally to regions surrounding the infarction two weeks after the occlusion, and grafted animals displayed reduced motor deficits compared to sham- and fibroblast-transplanted controls. Curiously, unlike many of the other transplant studies reviewed herein, the authors reported that only 20% of MGE-derived cells differentiated into GABAergic neurons in the occluded animals, suggesting that the stroke environment may alter transplant fate.

By exploiting the spontaneous tropism of g7-NPs for GABAergic cells, it is plausible to think that opportunely encapsulated g7-NPs may be used to develop new cell-targeted therapies for different aims:

(I) To deliver trophic neuromodulators, such as Reln or bFGF, or neurotrophins by overcoming their inability to cross the BBB. Today, purified neurotrophins can be directly infused into the brain by i.c.v. injection. NGF that is infused into the lateral ventricle can act on the TrkA receptor located at the axonal terminals to retrogradely transmit trophic support signal for basal forebrain cholinergic neurons (BFCNs). This approach has been proven especially effective in preventing loss of BFCNs in lesioned and aged rodents. Clinical trials with NGF infusion showed that, although long-term NGF administration by i.c.v. injection may cause certain potentially beneficial effects, the i.c.v. route of administration is associated with significant side effects, such as hyperinnervation of cerebral blood vessels, hypophagia, Schwann cell hyperplasia, sprouting of sensory and sympathetic neurons, and neuropathic pain (Apfel 2002, Eriksdotter Jonhagen et al 1998, Isaacson et al 1990, Jonhagen et al 1998, Winkler et al 1997). As such, these side effects may cause serious concerns in limiting the dose of infused NGF, thus providing only little therapeutic benefit. To circumvent the lack of significant therapeutic benefits in combination with serious adverse effects associated with the infusion approach, g7-NP delivery represents a new method to achieve more targeted delivery of trophic neuromodulators and neurotrophins directly to those populations of neurons affected in the disease.

(II) To deliver substances with known neuroprotective and cytoprotectant effects such as curcumin and urocortin (UCN), respectively, that have poor or no brain bioavailability. Curcumin, a natural polyphenol product derived from the rhizome of the Indian spice turmeric (Curcuma longa), possesses pleiotropic

biological and pharmacological properties. Curcumin provides neuroprotection in cellular and animal models of neuropsychiatric disorders including AD, PD, Huntington's disease (HD), multiple sclerosis, depression, and SZ (Hickey et al 2012, Mishra & Palanivelu 2008, Mythri & Bharath 2012, Xie et al 2011). Curcumin exerts neuroprotection due to its antioxidant properties and by activating the nuclear erythroid 2-related transcription factor (Nrf2), a master regulator of the antioxidant response (Yang et al 2009). Curcumin inhibits Aβ-oligomerization and tau-phosphorylation in the brain and protects dopaminergic (DA) neurons against 1-methyl-4-phenyl-1,2,3,6,tetrahydropyridine (MPTP) and 6-OHDA-induced neurotoxicity (Szwed & Milowska 2012). Curcuminoids potentiate spatial memory in an Aβ-induced rat model of AD (Ahmed et al 2010), promote neurite outgrowth and proliferation of neural stem cells *in vitro* and *in vivo* through activation of the extracellular signal-regulated kinases (ERK) and MAPK pathways (Kim et al 2008, Liao et al 2012) and increase the number of neurons in chronically stressed rats (Xu et al 2007) and cognition in aged rats (Dong et al 2012). In addition, curcumin plays a role in neurogenesis, synaptogenesis, and migration of neural progenitor cells *in vitro* (Kang et al 2006). Altogether, these studies suggest a potential neuroprotective role of curcumin. However, the neuroprotective efficacy of curcumin is limited by its poor brain bioavailability due to poor absorption, rapid metabolism, systemic elimination, and limited BBB permeability (Tsai et al 2011). Also UCN, a corticotrophin releasing hormone related peptide, has recently been proposed as cytoprotectant for cultured hippocampal neurons, cerebellar granule cells and GABAergic neurons (Choi et al 2006, Facci et al 2003, Pedersen et al 2002). Abuirmeileh and colleagues (2007) demonstrated that UCN arrests the development of Parkinsonian like features in the 6-OHDA lesioned hemiparkinsonian rat (Abuirmeileh et al 2007). UCN substantially reverses apomorphine-induced circling, loss of tissue DA, loss of nigral and striatal tyrosine hydroxylase (TH) activity and loss of TH protein levels (Abuirmeileh et al 2009). Although the 6-OHDA model of PD is well established, it has significant physiological limitations. Evidence suggests that systemic inflammation can predispose or be causative in the genesis of PD (Whitton 2007). Therefore, exposure to conditions leading to neuroinflammation, a condition to which the SN is particularly susceptible, constitutes a realistic mechanism by which the disease may be initiated. The observations with UCN suggest that under neuroinflammatory conditions it is able to elicit a functional recovery in nigrostriatal neurotransmission. Abuirmeileh and colleagues

reported that i.c.v. injection of 20 fmol of UCN was able to arrest the development of PD like features in rat 6-OHDA and lipopolysaccharide (LPS) paradigms of PD disease, indicating substantial therapeutic utility of UCN.

(III) To deliver RNAs blocking the translation of specific mRNAs or deliver specific molecules able to recognize and destroy unsafe protein aggregates as the amyloid plaques for AD;

(IV) To deliver inhibitors of specific deacethylase enzymes to increase the expression of specific genes such as Reln, GAD67, GluA1, TrkB, GAT-1, nicotinic receptors and PV known to be epigenetically downregulated in Cx and other brain regions of post mortem SZ patients. This idea is supported by data from SZ and BPD patients that showed (1) an increased number of cortical GABAergic neurons that stain positive for DNA-methyltransferase 1 (DNMT1) and 3a (DNMT3a) mRNA and protein (Veldic et al 2004, Zhubi et al 2009); (2) an increased PFC level of S-adenosyl-methionine (SAM), the universal methyl donor utilized by DNMTs (Guidotti et al 2007); and (3) the promoter hypermethylation in Reln and other genes observed in GABAergic neurons (Abdolmaleky et al 2005, Chen et al 2002, Grayson et al 2005, Mill et al 2008). DNA methylation (5-methylcytosine [5mC]) is one of several epigenetic markers altered in AD brain. More recently, attention has been given to DNA hydroxymethylation (5-hydroxymethylcytosine [5hmC]), the oxidized form of 5mC. Whereas 5mC is generally associated with the inhibition of gene expression, 5hmC has been associated with increased gene expression and is involved in cellular processes such as differentiation, development, and aging. Coppieters and colleagues demonstrated that in control and AD brains, levels of 5mC and 5hmC were low in astrocytes and microglia but were elevated in neurons. Different findings point toward a role for 5hmC in the development of diseases including AD, potentially opening new pathways for treating AD through correcting methylation and hydroxymethylation alterations (Coppieters et al 2013). Because epigenetic processes are known to be dynamic and reversible, future treatment strategies directly targeting epigenetic regulation may provide powerful means for pharmacological and/or behavioral intervention strategies in neurodegenerative disorders like AD.

(V) In general, to deliver drugs that are not able to pass easily the BBB thus representing an effective strategy to solve the most important problem for neuro-pharmacological research. In fact, the clinical failure of many potentially

effective therapeutic agents is often not due to the lack of drug potency but rather to shortcomings in the methods by which the drug is delivered.

The results of this thesis convincingly indicated that g7-NPs can cross the BBB, are endocytosed through clathrin-dependent mechanism and accumulate in specific neurons and microglia within Rab5 positive endosomes suggesting that these NPs can be promising carriers for the treatment of neuropsychiatric and neurodegenerative disease where these cells are involved.

REFERENCE LIST

Abdelwahed W, Degobert G, Stainmesse S, Fessi H. 2006. Freeze-drying of nanoparticles: formulation, process and storage considerations. *Advanced drug delivery reviews* 58: 1688-713

Abdolmaleky HM, Cheng KH, Russo A, Smith CL, Faraone SV, et al. 2005. Hypermethylation of the reelin (RELN) promoter in the brain of schizophrenic patients: a preliminary report. *American journal of medical genetics. Part B, Neuropsychiatric genetics : the official publication of the International Society of Psychiatric Genetics* 134B: 60-6

Abuirmeileh A, Harkavyi A, Kingsbury A, Lever R, Whitton PS. 2009. The CRF-like peptide urocortin greatly attenuates loss of extracellular striatal dopamine in rat models of Parkinson's disease by activating CRF(1) receptors. *European journal of pharmacology* 604: 45-50

Abuirmeileh A, Harkavyi A, Lever R, Biggs CS, Whitton PS. 2007. Urocortin, a CRF-like peptide, restores key indicators of damage in the substantia nigra in a neuroinflammatory model of Parkinson's disease. *Journal of neuroinflammation* 4: 19

Ahmed T, Enam SA, Gilani AH. 2010. Curcuminoids Enhance Memory in an Amyloid-Infused Rat Model of Alzheimer's Disease. *Neuroscience* 169: 1296-306

Akbarian S, Kim JJ, Potkin SG, Hagman JO, Tafazzoli A, et al. 1995. Gene-Expression for Glutamic-Acid Decarboxylase Is Reduced without Loss of Neurons in Prefrontal Cortex of Schizophrenics. *Arch Gen Psychiat* 52: 258-66

Akerman ME, Chan WCW, Laakkonen P, Bhatia SN, Ruoslahti E. 2002. Nanocrystal targeting in vivo. *P Natl Acad Sci USA* 99: 12617-21

Alyautdin RN, Petrov VE, Langer K, Berthold A, Kharkevich DA, Kreuter J. 1997. Delivery of loperamide across the blood-brain barrier with polysorbate 80-coated polybutylcyanoacrylate nanoparticles. *Pharmaceutical research* 14: 325-8

Ambruosi A, Khalansky AS, Yamamoto H, Gelperina SE, Begley DJ, Kreuter J. 2006. Biodistribution of polysorbate 80-coated doxorubicin-loaded [14C]-poly(butyl cyanoacrylate) nanoparticles after intravenous administration to glioblastoma-bearing rats. *Journal of drug targeting* 14: 97-105

Amundson RH, Goderie SK, Kimelberg HK. 1992. Uptake of [H-3] Serotonin and [H-3] Glutamate by Primary Astrocyte Cultures .2. Differences in Cultures Prepared from Different Brain-Regions. *Glia* 6: 9-18

Andre V, Marescaux C, Nehlig A, Fritschy JM. 2001. Alterations of hippocampal GAbaergic system contribute to development of spontaneous recurrent seizures in the rat lithium-pilocarpine model of temporal lobe epilepsy. *Hippocampus* 11: 452-68

Apfel SC. 2002. Nerve growth factor for the treatment of diabetic neuropathy: What went wrong, what went right, and what does the future hold? *Int Rev Neurobiol* 50: 393-413

Babb TL, Pretorius JK, Kupfer WR, Crandall PH. 1989. Glutamate decarboxylase-immunoreactive neurons are preserved in human epileptic hippocampus. *J Neurosci* 9: 2562-74

Bawarski WE, Chidlowsky E, Bharali DJ, Mousa SA. 2008. Emerging nanopharmaceuticals. *Nanomedicine : nanotechnology, biology, and medicine* 4: 273-82

Beasley CL, Cotter DR, Everall IP. 2002. Density and distribution of white matter neurons in schizophrenia, bipolar disorder and major depressive disorder: no evidence for abnormalities of neuronal migration. *Mol Psychiatr* 7: 564-70

Beddell CR, Clark RB, Hardy GW, Lowe LA, Ubatuba FB, et al. 1977. Structural requirements for opioid activity of analogues of the enkephalins. *Proceedings of the Royal Society of London. Series B, Containing papers of a Biological character. Royal Society* 198: 249-65

Begley DJ. 1996. The blood-brain barrier: principles for targeting peptides and drugs to the central nervous system. *The Journal of pharmacy and pharmacology* 48: 136-46

Benes FM. 1999. A reduction of nonpyramidal cells in sector CA2 of schizophrenics and manic depressives - Reply. *Biol Psychiat* 45: 1529-30

Benes FM, Berretta S. 2001. GABAergic interneurons: Implications for understanding schizophrenia and bipolar disorder (vol 25, pg 1, 2001). *Neuropsychopharmacol* 25: 453-53

Bhaskar S, Tian F, Stoeger T, Kreyling W, de la Fuente JM, et al. 2010. Multifunctional Nanocarriers for diagnostics, drug delivery and targeted treatment across blood-brain barrier: perspectives on tracking and neuroimaging. *Particle and fibre toxicology* 7: 3

Blasberg RG, Patlak C, Fenstermacher JD. 1975. Intrathecal chemotherapy: brain tissue profiles after ventriculocisternal perfusion. *J Pharmacol Exp Ther* 195: 73-83

Bondi ML, Craparo EF. 2010. Solid lipid nanoparticles for applications in gene therapy: a review of the state of the art. *Expert opinion on drug delivery* 7: 7-18

Brambilla P, Nicoletti MA, Sassi RB, Mallinger AG, Frank E, et al. 2003. Magnetic resonance imaging study of corpus callosum abnormalities in patients with bipolar disorder. *Biol Psychiat* 54: 1294-97

Brightman MW. 1968. The intracerebral movement of proteins injected into blood and cerebrospinal fluid of mice. *Progress in brain research* 29: 19-40

Brown TC, Correia SS, Petrok CN, Esteban JA. 2007. Functional compartmentalization of endosomal trafficking for the synaptic delivery of AMPA receptors during long-term potentiation. *J Neurosci* 27: 13311-15

Brown TC, Tran IC, Backos DS, Esteban JA. 2005. NMDA receptor-dependent activation of the small GTPase Rab5 drives the removal of synaptic AMPA receptors during hippocampal LTD. *Neuron* 45: 81-94

Bucci C, Parton RG, Mather IH, Stunnenberg H, Simons K, et al. 1992. The small GTPase rab5 functions as a regulatory factor in the early endocytic pathway. *Cell* 70: 715-28

Calvo P, Gouritin B, Chacun H, Desmaele D, D'Angelo J, et al. 2001. Long-circulating PEGylated polycyanoacrylate nanoparticles as new drug carrier for brain delivery. *Pharmaceutical research* 18: 1157-66

Candela P, Gosselet F, Miller F, Buee-Scherrer V, Torpier G, et al. 2008. Physiological pathway for low-density lipoproteins across the blood-brain barrier: transcytosis through brain capillary endothelial cells in vitro. *Endothelium : journal of endothelial cell research* 15: 254-64

Cataldo AM, Barnett JL, Pieroni C, Nixon RA. 1997. Increased neuronal endocytosis and protease delivery to early endosomes in sporadic Alzheimer's disease: Neuropathologic evidence for a mechanism of increased beta-amyloidogenesis. *J Neurosci* 17: 6142-51

Cataldo AM, Hamilton DJ, Nixon RA. 1994. Lysosomal Abnormalities in Degenerating Neurons Link Neuronal Compromise to Senile Plaque Development in Alzheimer-Disease. *Brain Res* 640: 68-80

Chang J, Jallouli Y, Kroubi M, Yuan XB, Feng W, et al. 2009. Characterization of endocytosis of transferrin-coated PLGA nanoparticles by the blood-brain barrier. *International journal of pharmaceutics* 379: 285-92

Chaudhari KR, Ukawala M, Manjappa AS, Kumar A, Mundada PK, et al. 2012. Opsonization, Biodistribution, Cellular Uptake and Apoptosis Study of PEGylated PBCA Nanoparticle as Potential Drug Delivery Carrier. *Pharmaceutical research* 29: 53-68

Chen Y, Sharma RP, Costa RH, Costa E, Grayson DR. 2002. On the epigenetic regulation of the human reelin promoter. *Nucleic acids research* 30: 2930-9

Chen Y, Siddalingappa B, Chan PH, Benson HA. 2008. Development of a chitosan-based nanoparticle formulation for delivery of a hydrophilic hexapeptide, dalargin. *Biopolymers* 90: 663-70

Choi JS, Pham TT, Jang YJ, Bui BC, Lee BH, et al. 2006. Corticotropin-releasing factor (CRF) and urocortin promote the survival of cultured cerebellar GABAergic neurons through the type 1 CRF receptor. *Journal of Korean medical science* 21: 518-26

Cleal K, He L, Watson PD, Jones AT. 2013. Endocytosis, intracellular traffic and fate of cell penetrating peptide based conjugates and nanoparticles. *Current pharmaceutical design* 19: 2878-94

Clemente-Casares X, Santamaria P. 2014. Nanomedicine in autoimmunity. *Immunology letters* 158: 167-74

Coppieters N, Dieriks BV, Lill C, Faull RL, Curtis MA, Dragunow M. 2013. Global changes in DNA methylation and hydroxymethylation in Alzheimer's disease human brain. *Neurobiology of aging*

Costa E, Davis JM, Dong E, Grayson DR, Guidotti A, et al. 2004. A GABAergic cortical deficit dominates schizophrenia pathophysiology. *Critical reviews in neurobiology* 16: 1-23

Costantino L, Gandolfi F, Bossy-Nobs L, Tosi G, Gurny R, et al. 2006. Nanoparticulate drug carriers based on hybrid poly(D,L-lactide-co-glycolide)-dendron structures. *Biomaterials* 27: 4635-45

Costantino L, Gandolfi F, Tosi G, Rivasi F, Vandelli MA, Forni F. 2005. Peptide-derivatized biodegradable nanoparticles able to cross the blood-brain barrier. *J Control Release* 108: 84-96

Costantino U, Bugatti V, Gorrasi G, Montanari F, Nocchetti M, et al. 2009. New polymeric composites based on poly(-caprolactone) and layered double hydroxides containing antimicrobial species. *ACS applied materials & interfaces* 1: 668-77

Cummings JL, Cole G. 2002. Alzheimer disease. *JAMA : the journal of the American Medical Association* 287: 2335-8

Czeh B, Simon M, van der Hart MGC, Schmelting B, Hesselink MB, Fuchs E. 2005. Chronic stress decreases the number of parvalbumin-immunoreactive Interneurons in the hippocampus: Prevention by treatment with a substance P receptor (NK1) antagonist. *Neuropsychopharmacol* 30: 67-79

Czlonkowska A, Kurkowska-Jastrzebska I. 2011. Inflammation and gliosis in neurological diseases - clinical implications. *J Neuroimmunol* 231: 78-85

Daadi MM, Lee SH, Arac A, Grueter BA, Bhatnagar R, et al. 2009. Functional Engraftment of the Medial Ganglionic Eminence Cells in Experimental Stroke Model. *Cell transplantation* 18: 815-26

Dahan M, Levi S, Luccardini C, Rostaing P, Riveau B, Triller A. 2003. Diffusion dynamics of glycine receptors revealed by single-quantum dot tracking. *Science* 302: 442-45

Danhier F, Ansorena E, Silva JM, Coco R, Le Breton A, Preat V. 2012. PLGA-based nanoparticles: an overview of biomedical applications. *J Control Release* 161: 505-22

Das D, Lin S. 2005. Double-coated poly (butylcynanoacrylate) nanoparticulate delivery systems for brain targeting of dalargin via oral administration. *Journal of pharmaceutical sciences* 94: 1343-53

De Jong WH, Borm PJ. 2008. Drug delivery and nanoparticles:applications and hazards. *International journal of nanomedicine* 3: 133-49

De Rosa G, Salzano G, Caraglia M, Abbruzzese A. 2012. Nanotechnologies: a strategy to overcome blood-brain barrier. *Current drug metabolism* 13: 61-9

Dehouck B, Fenart L, Dehouck MP, Pierce A, Torpier G, Cecchelli R. 1997. A new function for the LDL receptor: transcytosis of LDL across the blood-brain barrier. *The Journal of cell biology* 138: 877-89

Deinhardt K, Salinas S, Verastegui C, Watson R, Worth D, et al. 2006. Rab5 and Rab7 control endocytic sorting along the axonal retrograde transport pathway. *Neuron* 52: 293-305

Delcroix JD, Valletta JS, Wu CB, Hunt SJ, Kowal AS, Mobley WC. 2003. NGF signaling in sensory neurons: Evidence that early endosomes carry NGF retrograde signals. *Neuron* 39: 69-84

Denora N, Trapani A, Laquintana V, Lopedota A, Trapani G. 2009. Recent advances in medicinal chemistry and pharmaceutical technology--strategies for drug delivery to the brain. *Current topics in medicinal chemistry* 9: 182-96

Descamps L, Dehouck MP, Torpier G, Cecchelli R. 1996. Receptor-mediated transcytosis of transferrin through blood-brain barrier endothelial cells. *The American journal of physiology* 270: H1149-58

Dinocourt C, Petanjek Z, Freund TF, Ben-Ari Y, Esclapez M. 2003. Loss of interneurons innervating pyramidal cell dendrites and axon initial segments in the CA1 region of the hippocampus following pilocarpine-induced seizures. *J Comp Neurol* 459: 407-25

Do Carmo GP, Polt R, Bilsky EJ, Rice KC, Negus SS. 2008. Behavioral pharmacology of the mu/delta opioid glycopeptide MMP2200 in rhesus monkeys. *The Journal of pharmacology and experimental therapeutics* 326: 939-48

Dong E, Caruncho H, Liu WS, Smalheiser NR, Grayson DR, et al. 2003. A reelin-integrin receptor interaction regulates Arc mRNA translation in synaptoneurosomes. *Proc Natl Acad Sci U S A* 100: 5479-84

Dong SZ, Zeng QW, Mitchell ES, Xiu J, Duan Y, et al. 2012. Curcumin Enhances Neurogenesis and Cognition in Aged Rats: Implications for Transcriptional Interactions Related to Growth and Synaptic Plasticity. *Plos One* 7

Duffy KR, Pardridge WM, Rosenfeld RG. 1988. Human blood-brain barrier insulin-like growth factor receptor. *Metabolism: clinical and experimental* 37: 136-40

Edwards RH. 2001. Drug delivery via the blood-brain barrier. *Nature neuroscience* 4: 221-2

Eriksdotter Jonhagen M, Nordberg A, Amberla K, Backman L, Ebendal T, et al. 1998. Intracerebroventricular infusion of nerve growth factor in three patients with Alzheimer's disease. *Dementia and geriatric cognitive disorders* 9: 246-57

Esclapez M, Houser CR. 1999. Up-regulation of GAD65 and GAD67 in remaining hippocampal GABA neurons in a model of temporal lobe epilepsy. *J Comp Neurol* 412: 488-505

Facci L, Stevens DA, Pangallo M, Franceschini D, Skaper SD, Strijbos PJ. 2003. Corticotropin-releasing factor (CRF) and related peptides confer neuroprotection via type 1 CRF receptors. *Neuropharmacology* 45: 623-36

Feng Y, Press B, Wandinger-Ness A. 1995. Rab 7: an important regulator of late endocytic membrane traffic. *The Journal of cell biology* 131: 1435-52

Fessi H, Puisieux F, Devissaguet JP, Ammoury N, Benita S. 1989. Nanocapsule Formation by Interfacial Polymer Deposition Following Solvent Displacement. *Int J Pharm* 55: R1-R4

Fillebeen C, Mitchell V, Dexter D, Benaissa M, Beauvillain J, et al. 1999. Lactoferrin is synthesized by mouse brain tissue and its expression is enhanced after MPTP treatment. *Brain research. Molecular brain research* 72: 183-94

Fiori A, Cardelli P, Negri L, Savi MR, Strom R, Erspamer V. 1997. Deltorphin transport across the blood-brain barrier. *P Natl Acad Sci USA* 94: 9469-74

Fischer D, Li Y, Ahlemeyer B, Krieglstein J, Kissel T. 2003. In vitro cytotoxicity testing of polycations: influence of polymer structure on cell viability and hemolysis. *Biomaterials* 24: 1121-31

Flessner MF. 2005. The transport barrier in intraperitoneal therapy. *Am J Physiol-Renal* 288: F433-F42

Fontaine M, Elmquist WF, Miller DW. 1996. Use of rhodamine 123 to examine the functional activity of P-glycoprotein in primary cultured brain microvessel endothelial cell monolayers. *Life Sci* 59: 1521-31

Frank HJ, Pardridge WM, Morris WL, Rosenfeld RG, Choi TB. 1986. Binding and internalization of insulin and insulin-like growth factors by isolated brain microvessels. *Diabetes* 35: 654-61

Freund TF, Buzsaki G. 1996. Interneurons of the hippocampus. *Hippocampus* 6: 347-470

Fruhbeis C, Frohlich D, Kramer-Albers EM. 2012. Emerging roles of exosomes in neuron-glia communication. *Frontiers in physiology* 3: 119

Gabathuler R. 2010. Approaches to transport therapeutic drugs across the blood-brain barrier to treat brain diseases. *Neurobiology of disease* 37: 48-57

Gerges NZ, Brown TC, Correia SS, Esteban JA. 2005. Analysis of Rab protein function in neurotransmitter receptor trafficking at hippocampal synapses. *Method Enzymol* 403: 153-66

Ginsberg SD, Mufson EJ, Counts SE, Wuu J, Alldred MJ, et al. 2010. Regional Selectivity of rab5 and rab7 Protein Upregulation in Mild Cognitive Impairment and Alzheimer's Disease. *J Alzheimers Dis* 22: 631-39

Gorvel JP, Chavrier P, Zerial M, Gruenberg J. 1991. rab5 controls early endosome fusion in vitro. *Cell* 64: 915-25

Grabrucker AM, Garner CC, Boeckers TM, Bondioli L, Ruozi B, et al. 2011. Development of novel Zn2+ loaded nanoparticles designed for cell-type targeted drug release in CNS neurons: in vitro evidences. *PloS one* 6: e17851

Graff CL, Pollack GM. 2005. Nasal drug administration: potential for targeted central nervous system delivery. *Journal of pharmaceutical sciences* 94: 1187-95

Grant BD, Donaldson JG. 2009. Pathways and mechanisms of endocytic recycling. *Nature reviews. Molecular cell biology* 10: 597-608

Grayson DR, Jia X, Chen Y, Sharma RP, Mitchell CP, et al. 2005. Reelin promoter hypermethylation in schizophrenia. *Proc Natl Acad Sci U S A* 102: 9341-6

Grbovic OM, Mathews PM, Jiang Y, Schmidt SD, Dinakar R, et al. 2003. Rab5-stimulated up-regulation of the endocytic pathway increases intracellular beta-cleaved amyloid precursor protein carboxyl-terminal fragment levels and A beta production. *J Biol Chem* 278: 31261-68

Grimes ML, Zhou J, Beattie EC, Yuen EC, Hall DE, et al. 1996. Endocytosis of activated TrkA: Evidence that nerve growth factor induces formation of signaling endosomes. *J Neurosci* 16: 7950-64

Guidotti A, Auta J, Davis JM, Di-Giorgi-Gerevini V, Dwivedi Y, et al. 2000. Decrease in reelin and glutamic acid decarboxylase67 (GAD67) expression in schizophrenia and bipolar disorder: a postmortem brain study. *Arch Gen Psychiatry* 57: 1061-9

Guidotti A, Auta J, Davis JM, Dong EB, Grayson DR, et al. 2005. GABAergic dysfunction in schizophrenia: new treatment strategies on the horizon. *Psychopharmacology* 180: 191-205

Guidotti A, Ruzicka W, Grayson DR, Veldic M, Pinna G, et al. 2007. S-adenosyl methionine and DNA methyltransferase-1 mRNA overexpression in psychosis. *Neuroreport* 18: 57-60

Guillemin G, Boussin FD, Croitoru J, FranckDuchenne M, LeGrand R, et al. 1997. Obtention and characterization of primary astrocyte and microglial cultures from adult monkey brains. *J Neurosci Res* 49: 576-91

Gurke S, Barroso JFV, Gerdes HH. 2008. The art of cellular communication: tunneling nanotubes bridge the divide. *Histochem Cell Biol* 129: 539-50

Hardman R. 2006. A toxicologic review of quantum dots: Toxicity depends on physicochemical and environmental factors. *Environ Health Persp* 114: 165-72

Harush-Frenkel O, Rozentur E, Benita S, Altschuler Y. 2008. Surface charge of nanoparticles determines their endocytic and transcytotic pathway in polarized MDCK cells. *Biomacromolecules* 9: 435-43

Hawkins BT, Davis TP. 2005. The blood-brain barrier/neurovascular unit in health and disease. *Pharmacological reviews* 57: 173-85

Hickey MA, Zhu C, Medvedeva V, Lerner RP, Patassini S, et al. 2012. Improvement of neuropathology and transcriptional deficits in CAG 140 knock-in mice supports a beneficial effect of dietary curcumin in Huntington's disease. *Mol Neurodegener* 7

Hof PR, Cox K, Young WG, Celio MR, Rogers J, Morrison JH. 1991. Parvalbumin-immunoreactive neurons in the neocortex are resistant to degeneration in Alzheimer's disease. *Journal of neuropathology and experimental neurology* 50: 451-62

Hof PR, Morrison JH. 2004. The aging brain: morphomolecular senescence of cortical circuits. *Trends Neurosci* 27: 607-13

Houser CR. 1991. Gaba Neurons in Seizure Disorders - a Review of Immunocytochemical Studies. *Neurochem Res* 16: 295-308

Howarth M, Liu WH, Puthenveetil S, Zheng Y, Marshall LF, et al. 2008. Monovalent, reduced-size quantum dots for imaging receptors on living cells. *Nat Methods* 5: 397-99

Hu K, Shi Y, Jiang W, Han J, Huang S, Jiang X. 2011. Lactoferrin conjugated PEG-PLGA nanoparticles for brain delivery: preparation, characterization and efficacy in Parkinson's disease. *International journal of pharmaceutics* 415: 273-83

Hunt RF, Girskis KM, Rubenstein JL, Alvarez-Buylla A, Baraban SC. 2013. GABA progenitors grafted into the adult epileptic brain control seizures and abnormal behavior. *Nat Neurosci* 16: 692-+

Huwyler J, Wu DF, Pardridge WM. 1996. Brain drug delivery of small molecules using immunoliposomes. *P Natl Acad Sci USA* 93: 14164-69

Illum L. 2003. Nasal drug delivery--possibilities, problems and solutions. *Journal of controlled release : official journal of the Controlled Release Society* 87: 187-98

Impagnatiello F, Guidotti AR, Pesold C, Dwivedi Y, Caruncho H, et al. 1998. A decrease of reelin expression as a putative vulnerability factor in schizophrenia. *P Natl Acad Sci USA* 95: 15718-23

Isaacson LG, Saffran BN, Crutcher KA. 1990. Intracerebral NGF infusion induces hyperinnervation of cerebral blood vessels. *Neurobiology of aging* 11: 51-5

Iversen TG, Skotland T, Sandvig K. 2011. Endocytosis and intracellular transport of nanoparticles: Present knowledge and need for future studies. *Nano Today* 6: 176-85

Jones AR, Shusta EV. 2007. Blood-brain barrier transport of therapeutics via receptor-mediation. *Pharmaceutical research* 24: 1759-71

Jonhagen ME, Nordberg A, Amberla K, Backman L, Ebendal T, et al. 1998. Intracerebroventricular infusion of nerve growth factor in three patients with Alzheimer's disease. *Dement Geriatr Cogn* 9: 246-57

Kabanov AV, Batrakova EV. 2004. New technologies for drug delivery across the blood brain barrier. *Curr Pharm Design* 10: 1355-63

Kang SK, Cha SH, Jeon HG. 2006. Curcumin-induced histone hypoacetylation enhances caspase-3-dependent glioma cell death and neurogenesis of neural progenitor cells. *Stem Cells Dev* 15: 165-74

Kim HI, Huang H, Cheepala S, Huang S, Chung J. 2008. Curcumin Inhibition of Integrin (alpha(6)beta(4))-Dependent Breast Cancer Cell Motility and Invasion. *Cancer Prev Res* 1: 385-91

Kim HR, Andrieux K, Gil S, Taverna M, Chacun H, et al. 2007. Translocation of poly(ethylene glycol-co-hexadecyl)cyanoacrylate nanoparticles into rat brain endothelial cells: Role of apolipoproteins in receptor-mediated endocytosis. *Biomacromolecules* 8: 793-99

Knopp A, Frahm C, Fidzinski P, Witte OW, Behr J. 2008. Loss of GABAergic neurons in the subiculum and its functional implications in temporal lobe epilepsy. *Brain* 131: 1516-27

Kobayashi M, Wen X, Buckmaster PS. 2003. Reduced inhibition and increased output of layer II neurons in the medial entorhinal cortex in a model of temporal lobe epilepsy. *J Neurosci* 23: 8471-9

Kramer-Albers EM, Fruhbeis C, Frohlich D, Kuo WP. 2013. Delivery on Call: The Role of Exosomes in Neuron-Glia Communication. *Glia* 61: S40-S40

Kreuter J, Hekmatara T, Dreis S, Vogel T, Gelperina S, Langer K. 2007. Covalent attachment of apolipoprotein A-I and apolipoprotein B-100 to albumin nanoparticles enables drug transport into the brain. *Journal of controlled release : official journal of the Controlled Release Society* 118: 54-8

Kreuter J, Shamenkov D, Petrov V, Ramge P, Cychutek K, et al. 2002. Apolipoprotein-mediated transport of nanoparticle-bound drugs across the blood-brain barrier. *Journal of drug targeting* 10: 317-25

Kumari A, Yadav SK, Yadav SC. 2010. Biodegradable polymeric nanoparticles based drug delivery systems. *Colloids and surfaces. B, Biointerfaces* 75: 1-18

Kuo YC, Chung CY. 2012. Transcytosis of CRM197-grafted polybutylcyanoacrylate nanoparticles for delivering zidovudine across human brain-microvascular endothelial cells. *Colloids and surfaces. B, Biointerfaces* 91: 242-9

Lachenal G, Pernet-Gallay K, Chivet M, Hemming FJ, Belly A, et al. 2011. Release of exosomes from differentiated neurons and its regulation by synaptic glutamatergic activity. *Mol Cell Neurosci* 46: 409-18

Lalatsa A, Lee V, Malkinson JP, Zloh M, Schatzlein AG, Uchegbu IF. 2012. A prodrug nanoparticle approach for the oral delivery of a hydrophilic peptide, leucine(5)-enkephalin, to the brain. *Molecular pharmaceutics* 9: 1665-80

Lam CW, James JT, McCluskey R, Hunter RL. 2004. Pulmonary toxicity of single-wall carbon nanotubes in mice 7 and 90 days after intratracheal instillation. *Toxicol Sci* 77: 126-34

Lanctot KL, Herrmann N, Mazzotta P, Khan LR, Ingber N. 2004. GABAergic function in Alzheimer's disease: Evidence for dysfunction and potential as a therapeutic target for the treatment of behavioural and psychological symptoms of dementia. *Can J Psychiat* 49: 439-53

Le Magueresse C, Monyer H. 2013. GABAergic Interneurons Shape the Functional Maturation of the Cortex. *Neuron* 77: 388-405

Lewis DA, Hashimoto T, Volk DW. 2005. Cortical inhibitory neurons and schizophrenia. *Nat Rev Neurosci* 6: 312-24

Li Y, Lefever MR, Muthu D, Bidlack JM, Bilsky EJ, Polt R. 2012. Opioid glycopeptide analgesics derived from endogenous enkephalins and endorphins. *Future medicinal chemistry* 4: 205-26

Liao KK, Wu MJ, Chen PY, Huang SW, Chiu SJ, et al. 2012. Curcuminoids Promote Neurite Outgrowth in PC12 Cells through MAPK/ERK- and PKC-Dependent Pathways. *J Agr Food Chem* 60: 433-43

Lim SB, Banerjee A, Onyuksel H. 2012. Improvement of drug safety by the use of lipid-based nanocarriers. *Journal of controlled release : official journal of the Controlled Release Society* 163: 34-45

Liu MJ, Kono K, Frechet JMJ. 2000. Water-soluble dendritic unimolecular micelles: Their potential as drug delivery agents. *J Control Release* 65: 121-31

Liu Z, Chen K, Davis C, Sherlock S, Cao QZ, et al. 2008. Drug delivery with carbon nanotubes for in vivo cancer treatment. *Cancer Res* 68: 6652-60

Lo EH, Singhal AB, Torchilin VP, Abbott NJ. 2001. Drug delivery to damaged brain. *Brain Res Rev* 38: 140-48

Lombardi D, Soldati T, Riederer MA, Goda Y, Zerial M, Pfeffer SR. 1993. Rab9 Functions in Transport between Late Endosomes and the Trans Golgi Network. *Embo Journal* 12: 677-82

Loup F, Wieser HG, Yonekawa Y, Aguzzi A, Fritschy JM. 2000. Selective alterations in GABAA receptor subtypes in human temporal lobe epilepsy. *J Neurosci* 20: 5401-19

Lowery JJ, Raymond TJ, Giuvelis D, Bidlack JM, Polt R, Bilsky EJ. 2011. In vivo characterization of MMP-2200, a mixed delta/mu opioid agonist, in mice. *The Journal of pharmacology and experimental therapeutics* 336: 767-78

Luther EM, Petters C, Bulcke F, Kaltz A, Thiel K, et al. 2013. Endocytotic uptake of iron oxide nanoparticles by cultured brain microglial cells. *Acta biomaterialia* 9: 8454-65

Maccaferri G, Lacaille JC. 2003. Interneuron Diversity series: Hippocampal interneuron classifications--making things as simple as possible, not simpler. *Trends Neurosci* 26: 564-71

Magarinos AM, Verdugo JM, McEwen BS. 1997. Chronic stress alters synaptic terminal structure in hippocampus. *Proc Natl Acad Sci U S A* 94: 14002-8

Magloczky Z, Freund TF. 2005. Impaired and repaired inhibitory circuits in the epileptic human hippocampus. *Trends Neurosci* 28: 334-40

Makadia HK, Siegel SJ. 2011. Poly Lactic-co-Glycolic Acid (PLGA) as Biodegradable Controlled Drug Delivery Carrier. *Polymers-Basel* 3: 1377-97

Malinow R, Malenka RC. 2002. AMPA receptor trafficking and synaptic plasticity. *Annu Rev Neurosci* 25: 103-26

Martinez-Cerdeno V, Noctor SC, Espinosa A, Ariza J, Parker P, et al. 2010. Embryonic MGE Precursor Cells Grafted into Adult Rat Striatum Integrate and Ameliorate Motor Symptoms in 6-OHDA-Lesioned Rats. *Cell Stem Cell* 6: 238-50

McLauchlan H, Newell J, Morrice N, Osborne A, West M, Smythe E. 1998. A novel role for Rab5-GDI in ligand sequestration into clathrin-coated pits. *Current biology : CB* 8: 34-45

Meakin SO, MacDonald JIS, Gryz EA, Kubu CJ, Verdi JM. 1999. The signaling adapter FRS-2 competes with Shc for binding to the nerve growth factor receptor TrkA - A model for discriminating proliferation and differentiation. *J Biol Chem* 274: 9861-70

Michaelis K, Hoffmann MM, Dreis S, Herbert E, Alyautdin RN, et al. 2006. Covalent linkage of apolipoprotein e to albumin nanoparticles strongly enhances drug transport into the brain. *The Journal of pharmacology and experimental therapeutics* 317: 1246-53

Mill J, Tang T, Kaminsky Z, Khare T, Yazdanpanah S, et al. 2008. Epigenomic profiling reveals DNA-methylation changes associated with major psychosis. *American journal of human genetics* 82: 696-711

Miller AD. 2008. Towards safe nanoparticle technologies for nucleic acid therapeutics. *Tumori* 94: 234-45

Mishra S, Palanivelu K. 2008. The effect of curcumin (turmeric) on Alzheimer's disease: An overview. *Ann Indian Acad Neur* 11: 13-19

Misra A, Ganesh S, Shahiwala A, Shah SP. 2003. Drug delivery to the central nervous system: a review. *Journal of pharmacy & pharmaceutical sciences : a publication of the Canadian Society for Pharmaceutical Sciences, Societe canadienne des sciences pharmaceutiques* 6: 252-73

Mistry A, Stolnik S, Illum L. 2009. Nanoparticles for direct nose-to-brain delivery of drugs. *International journal of pharmaceutics* 379: 146-57

Moghimi SM, Hunter AC, Murray JC. 2001. Long-circulating and target-specific nanoparticles: theory to practice. *Pharmacological reviews* 53: 283-318

Moghimi SM, Hunter AC, Murray JC. 2005. Nanomedicine: current status and future prospects. *FASEB journal : official publication of the Federation of American Societies for Experimental Biology* 19: 311-30

Moulari B, Pertuit D, Pellequer Y, Lamprecht A. 2008. The targeting of surface modified silica nanoparticles to inflamed tissue in experimental colitis. *Biomaterials* 29: 4554-60

Mulder WJ, Fayad ZA. 2008. Nanomedicine captures cardiovascular disease. *Arteriosclerosis, thrombosis, and vascular biology* 28: 801-2

Mythri RB, Bharath MMS. 2012. Curcumin: A Potential Neuroprotective Agent in Parkinson's Disease. *Curr Pharm Design* 18: 91-99

Nabeshima S, Reese TS, Landis DM, Brightman MW. 1975. Junctions in the meninges and marginal glia. *The Journal of comparative neurology* 164: 127-69

Nafee N, Schneider M, Schaefer UF, Lehr CM. 2009. Relevance of the colloidal stability of chitosan/ PLGA nanoparticles on their cytotoxicity profile. *International journal of pharmaceutics* 381: 130-9

Nagayama S, Ogawara K, Fukuoka Y, Higaki K, Kimura T. 2007. Time-dependent changes in opsonin amount associated on nanoparticles alter their hepatic uptake characteristics. *Int J Pharm* 342: 215-21

Newton HB. 2006. Advances in strategies to improve drug delivery to brain tumors. *Expert review of neurotherapeutics* 6: 1495-509

Ng EL, Tang BL. 2008. Rab GTPases and their roles in brain neurons and glia. *Brain research reviews* 58: 236-46

Niu S, Renfro A, Quattrocchi CC, Sheldon M, D'Arcangelo G. 2004. Reelin promotes hippocampal dendrite development through the VLDLR/ApoER2-Dab1 pathway. *Neuron* 41: 71-84

Olivier JC, Fenart L, Chauvet R, Pariat C, Cecchelli R, Couet W. 1999. Indirect evidence that drug brain targeting using polysorbate 80-coated polybutylcyanoacrylate nanoparticles is related to toxicity. *Pharmaceutical research* 16: 1836-42

Owens DE, 3rd, Peppas NA. 2006. Opsonization, biodistribution, and pharmacokinetics of polymeric nanoparticles. *International journal of pharmaceutics* 307: 93-102

Panagi Z, Beletsi A, Evangelatos G, Livaniou E, Ithakissios DS, Avgoustakis K. 2001. Effect of dose on the biodistribution and pharmacokinetics of PLGA and PLGA-mPEG nanoparticles. *International journal of pharmaceutics* 221: 143-52

Pang Z, Gao H, Yu Y, Chen J, Guo L, et al. 2011. Brain delivery and cellular internalization mechanisms for transferrin conjugated biodegradable polymersomes. *International journal of pharmaceutics* 415: 284-92

Pang ZQ, Lu W, Gao HL, Hu KL, Chen J, et al. 2008. Preparation and brain delivery property of biodegradable polymersomes conjugated with OX26. *J Control Release* 128: 120-27

Parton RG, Simons K. 2007. The multiple faces of caveolae. *Nature reviews. Molecular cell biology* 8: 185-94

Patabendige A, Skinner RA, Morgan L, Abbott NJ. 2013. A detailed method for preparation of a functional and flexible blood-brain barrier model using porcine brain endothelial cells. *Brain research* 1521: 16-30

Patel MM, Goyal BR, Bhadada SV, Bhatt JS, Amin AF. 2009. Getting into the Brain Approaches to Enhance Brain Drug Delivery. *Cns Drugs* 23: 35-58

Pedersen WA, Wan RQ, Zhang PS, Mattson MP. 2002. Urocortin, but not urocortin II, protects cultured hippocampal neurons from oxidative and excitotoxic cell death via corticotropin-releasing hormone receptor type I. *J Neurosci* 22: 404-12

Peer D, Karp JM, Hong S, Farokhzad OC, Margalit R, Langer R. 2007. Nanocarriers as an emerging platform for cancer therapy. *Nature nanotechnology* 2: 751-60

Petri B, Bootz A, Khalansky A, Hekmatara T, Muller R, et al. 2007. Chemotherapy of brain tumour using doxorubicin bound to surfactant-coated poly(butyl cyanoacrylate) nanoparticles: revisiting the role of surfactants. *Journal of controlled release : official journal of the Controlled Release Society* 117: 51-8

Polt R, Dhanasekaran M, Keyari CM. 2005. Glycosylated neuropeptides: a new vista for neuropsychopharmacology? *Medicinal research reviews* 25: 557-85

Polt R, Porreca F, Szabo LZ, Bilsky EJ, Davis P, et al. 1994. Glycopeptide enkephalin analogues produce analgesia in mice: evidence for penetration of the blood-brain barrier. *Proceedings of the National Academy of Sciences of the United States of America* 91: 7114-8

Popovic M, Caballero-Bleda M, Kadish I, Van Groen T. 2008. Subfield and layer-specific depletion in calbindin-D28K, calretinin and parvalbumin immunoreactivity in the dentate gyrus of amyloid precursor protein/presenilin 1 transgenic mice. *Neuroscience* 155: 182-91

Prokop A, Davidson JM. 2008. Nanovehicular intracellular delivery systems. *Journal of pharmaceutical sciences* 97: 3518-90

Ricci M, Blasi P, Giovagnoli S, Rossi C. 2006. Delivering drugs to the central nervous system: a medicinal chemistry or a pharmaceutical technology issue? *Current medicinal chemistry* 13: 1757-75

Ricci-Junior E, Marchetti JM. 2006. Zinc(II) phthalocyanine loaded PLGA nanoparticles for photodynamic therapy use. *International journal of pharmaceutics* 310: 187-95

Richardson SC, Kolbe HV, Duncan R. 1999. Potential of low molecular mass chitosan as a DNA delivery system: biocompatibility, body distribution and ability to complex and protect DNA. *International journal of pharmaceutics* 178: 231-43

Rinaman L, Milligan CE, Levitt P. 1991. Persistence of Fluorogold Following Degeneration of Labeled Motoneurons Is Due to Phagocytosis by Microglia and Macrophages. *Neuroscience* 44: 765-76

Rink J, Ghigo E, Kalaidzidis Y, Zerial M. 2005. Rab conversion as a mechanism of progression from early to late endosomes. *Cell* 122: 735-49

Roberts RL, Fine RE, Sandra A. 1993. Receptor-Mediated Endocytosis of Transferrin at the Blood-Brain-Barrier. *J Cell Sci* 104: 521-32

Rodriguez JJ, Olabarria M, Chvatal A, Verkhratsky A. 2009. Astroglia in dementia and Alzheimer's disease. *Cell Death Differ* 16: 378-85

Rutka JT, Giblin JR, Balkissoon R, Wen D, Myatt CA, et al. 1987. Characterization of Fetal Human-Brain Cultures - Development of a Potential Model for Selectively Purifying Human Glial-Cells in Culture. *Dev Neurosci-Basel* 9: 154-73

Sadeque AJ, Wandel C, He H, Shah S, Wood AJ. 2000. Increased drug delivery to the brain by P-glycoprotein inhibition. *Clinical pharmacology and therapeutics* 68: 231-7

Sahay G, Alakhova DY, Kabanov AV. 2010. Endocytosis of nanomedicines. *J Control Release* 145: 182-95

Sanacora G, Mason GF, Rothman DL, Behar KL, Hyder F, et al. 1999. Reduced cortical gamma-aminobutyric acid levels in depressed patients determined by proton magnetic resonance spectroscopy. *Arch Gen Psychiat* 56: 1043-47

Schroeder U, Sommerfeld P, Sabel BA. 1998. Efficacy of oral dalargin-loaded nanoparticle delivery across the blood-brain barrier. *Peptides* 19: 777-80

Seju U, Kumar A, Sawant KK. 2011. Development and evaluation of olanzapine-loaded PLGA nanoparticles for nose-to-brain delivery: In vitro and in vivo studies. *Acta Biomater* 7: 4169-76

Semmler-Behnke M, Kreyling WG, Lipka J, Fertsch S, Wenk A, et al. 2008. Biodistribution of 1.4-and 18-nm Gold Particles in Rats. *Small* 4: 2108-11

Shan Y, Ma S, Nie L, Shang X, Hao X, et al. 2011. Size-dependent endocytosis of single gold nanoparticles. *Chemical communications* 47: 8091-3

Shi NY, Boado RJ, Pardridge WM. 2001. Receptor-mediated gene targeting to tissues in vivo following intravenous administration of pegylated immunoliposomes. *Pharmaceutical research* 18: 1091-95

Shi NY, Pardridge WM. 2000. Noninvasive gene targeting to the brain. *P Natl Acad Sci USA* 97: 7567-72

Shimizu H, Kawamura S, Ozaki K. 2003. An essential role of Rab5 in uniformity of synaptic vesicle size. *J Cell Sci* 116: 3583-90

Siegal T, Zylber-Katz E. 2002. Strategies for increasing drug delivery to the brain - Focus on brain lymphoma. *Clin Pharmacokinet* 41: 171-86

Sloviter RS, Sollas AL, Barbaro NM, Laxer KD. 1991. Calcium-binding protein (calbindin-D28K) and parvalbumin immunocytochemistry in the normal and epileptic human hippocampus. *J Comp Neurol* 308: 381-96

Soghomonian JJ, Martin DL. 1998. Two isoforms of glutamate decarboxylase: why? *Trends in pharmacological sciences* 19: 500-5

Soppimath KS, Aminabhavi TM, Kulkarni AR, Rudzinski WE. 2001. Biodegradable polymeric nanoparticles as drug delivery devices. *Journal of controlled release : official journal of the Controlled Release Society* 70: 1-20

Stenmark H. 2009. Rab GTPases as coordinators of vesicle traffic. *Nat Rev Mol Cell Bio* 10: 513-25

Stenmark H, Valencia A, Martinez O, Ullrich O, Goud B, Zerial M. 1994. Distinct structural elements of rab5 define its functional specificity. *The EMBO journal* 13: 575-83

Sundar S, Prajapati VK. 2012. Drug targeting to infectious diseases by nanoparticles surface functionalized with special biomolecules. *Current medicinal chemistry* 19: 3196-202

Svenson S, Tomalia DA. 2005. Dendrimers in biomedical applications--reflections on the field. *Advanced drug delivery reviews* 57: 2106-29

Szwed A, Milowska K. 2012. The role of proteins in neurodegenerative disease. *Postep Hig Med Dosw* 66: 187-95

Tabernero A, Velasco A, Granda B, Lavado EM, Medina JM. 2002. Transcytosis of albumin in astrocytes activates the sterol regulatory element-binding protein-1, which promotes the synthesis of the neurotrophic factor oleic acid. *J Biol Chem* 277: 4240-46

Taylor SF, Demeter E, Phan KL, Tso IF, Welsh RC. 2014. Abnormal GABAergic function and negative affect in schizophrenia. *Neuropsychopharmacol* 39: 1000-8

Thomsen LB, Lichota J, Eskehave TN, Linemann T, Mortensen JH, et al. 2012. Brain delivery systems via mechanism independent of receptor-mediated endocytosis and adsorptive-mediated endocytosis. *Current pharmaceutical biotechnology* 13: 2349-54

Thorne RG, Emory CR, Ala TA, Frey WH. 1995. Quantitative-Analysis of the Olfactory Pathway for Drug-Delivery to the Brain. *Brain research* 692: 278-82

Tosi G, Bondioli L, Ruozi B, Badiali L, Severini GM, et al. 2011. NIR-labeled nanoparticles engineered for brain targeting: in vivo optical imaging application and fluorescent microscopy evidences. *J Neural Transm* 118: 145-53

Tosi G, Bortot B, Ruozi B, Dolcetta D, Vandelli MA, et al. 2013. Potential Use of Polymeric Nanoparticles for Drug Delivery Across the Blood-Brain Barrier. *Curr Med Chem* 20: 2212-25

Tosi G, Costantino L, Rivasi F, Ruozi B, Leo E, et al. 2007. Targeting the central nervous system: in vivo experiments with peptide-derivatized nanoparticles loaded with Loperamide and Rhodamine-123. *Journal of controlled release : official journal of the Controlled Release Society* 122: 1-9

Tosi G, Vergoni AV, Ruozi B, Bondioli L, Badiali L, et al. 2010. Sialic acid and glycopeptides conjugated PLGA nanoparticles for central nervous system targeting: In vivo pharmacological evidence and biodistribution. *Journal of controlled release : official journal of the Controlled Release Society* 145: 49-57

Tosi G, Vilella A, Chhabra R, Schmeisser MJ, Boeckers TM, et al. 2014. Insight on the fate of CNS-targeted nanoparticles. Part II: Intercellular neuronal cell-to-cell transport. *J Control Release* 177C: 96-107

Tsai CJ, Zheng J, Aleman C, Nussinov R. 2006. Structure by design: from single proteins and their building blocks to nanostructures. *Trends Biotechnol* 24: 449-54

Tsai YM, Chien CF, Lin LC, Tsai TH. 2011. Curcumin and its nano-formulation: The kinetics of tissue distribution and blood-brain barrier penetration. *Int J Pharmaceut* 416: 331-38

Tyson JA, Anderson SA. 2014. GABAergic interneuron transplants to study development and treat disease. *Trends Neurosci*

Ulbrich W, Lamprecht A. 2010. Targeted drug-delivery approaches by nanoparticulate carriers in the therapy of inflammatory diseases. *Journal of the Royal Society, Interface / the Royal Society* 7 Suppl 1: S55-66

Ullrich O, Reinsch S, Urbe S, Zerial M, Parton RG. 1996. Rab11 regulates recycling through the pericentriolar recycling endosome. *The Journal of cell biology* 135: 913-24

Vaid RR, Yee BK, Shalev U, Rawlins JNP, Weiner I, et al. 1997. Neonatal nonhandling and in utero prenatal stress reduce the density of NADPH-diaphorase-reactive neurons in the fascia dentata and Ammon's horn of rats. *J Neurosci* 17: 5599-609

Vandersluijs P, Hull M, Zahraoui A, Tavitian A, Goud B, Mellman I. 1991. The Small Gtp-Binding Protein Rab4 Is Associated with Early Endosomes. *P Natl Acad Sci USA* 88: 6313-17

Veldic M, Caruncho HJ, Liu WS, Davis J, Satta R, et al. 2004. DNA-methyltransferase 1 mRNA is selectively overexpressed in telencephalic GABAergic interneurons of schizophrenia brains. *P Natl Acad Sci USA* 101: 348-53

Vergoni AV, Tosi G, Tacchi R, Vandelli MA, Bertolini A, Costantino L. 2009. Nanoparticles as drug delivery agents specific for CNS: in vivo biodistribution. *Nanomed-Nanotechnol* 5: 369-77

Vij N, Min T, Marasigan R, Belcher CN, Mazur S, et al. 2010. Development of PEGylated PLGA nanoparticle for controlled and sustained drug delivery in cystic fibrosis. *Journal of nanobiotechnology* 8: 22

Vilella A, Tosi G, Grabrucker AM, Ruozi B, Belletti D, et al. 2014. Insight on the fate of CNS-targeted nanoparticles. Part I: Rab5-dependent cell-specific uptake and distribution. *J Control Release* 174: 195-201

Vinogradov SV, Bronich TK, Kabanov AV. 2002. Nanosized cationic hydrogels for drug delivery: preparation, properties and interactions with cells. *Advanced drug delivery reviews* 54: 135-47

Visser CC, Stevanovic S, Heleen Voorwinden L, Gaillard PJ, Crommelin DJ, et al. 2004. Validation of the transferrin receptor for drug targeting to brain capillary endothelial cells in vitro. *Journal of drug targeting* 12: 145-50

Vitelli R, Santillo M, Lattero D, Chiariello M, Bifulco M, et al. 1997. Role of the small GTPase Rab7 in the late endocytic pathway. *The Journal of biological chemistry* 272: 4391-7

Wagner S, Zensi A, Wien SL, Tschickardt SE, Maier W, et al. 2012. Uptake mechanism of ApoE-modified nanoparticles on brain capillary endothelial cells as a blood-brain barrier model. *PloS one* 7: e32568

Wagner V, Dullaart A, Bock AK, Zweck A. 2006. The emerging nanomedicine landscape. *Nature biotechnology* 24: 1211-7

Wang F, Bronich TK, Kabanov AV, Rauh RD, Roovers J. 2005. Synthesis and evaluation of a star amphiphilic block copolymer from poly(epsilon-caprolactone) and poly(ethylene glycol) as a potential drug delivery carrier. *Bioconjugate Chem* 16: 397-405

Wang J, Liu Y, Jiao F, Lao F, Li W, et al. 2008. Time-dependent translocation and potential impairment on central nervous system by intranasally instilled TiO(2) nanoparticles. *Toxicology* 254: 82-90

Wang N, Wu XS, Li C, Feng MF. 2000. Synthesis, characterization, biodegradation, and drug delivery application of biodegradable lactic/glycolic acid polymers I. Synthesis and characterization. *J Biomat Sci-Polym E* 11: 301-18

Warheit DB, Laurence BR, Reed KL, Roach DH, Reynolds GAM, Webb TR. 2004. Comparative pulmonary toxicity assessment of single-wall carbon nanotubes in rats. *Toxicol Sci* 77: 117-25

Weeber EJ, Beffert U, Jones C, Christian JM, Forster E, et al. 2002. Reelin and ApoE receptors cooperate to enhance hippocampal synaptic plasticity and learning. *J Biol Chem* 277: 39944-52

Weissenbock A, Wirth M, Gabor F. 2004. WGA-grafted PLGA-nanospheres: preparation and association with Caco-2 single cells. *Journal of controlled release : official journal of the Controlled Release Society* 99: 383-92

Whitton PS. 2007. Inflammation as a causative factor in the aetiology of Parkinson's disease. *Brit J Pharmacol* 150: 963-76

Wilcke M, Johannes L, Galli T, Mayau V, Goud B, Salamero J. 2000. Rab11 regulates the compartmentalization of early endosomes required for efficient transport from early endosomes to the trans-golgi network. *The Journal of cell biology* 151: 1207-20

Winkler J, Ramirez GA, Kuhn HG, Peterson DA, DayLollini PA, et al. 1997. Reversible Schwann cell hyperplasia and sprouting of sensory and sympathetic neurites after intraventricular administration of nerve growth factor. *Ann Neurol* 41: 82-93

Witt KA, Gillespie TJ, Huber JD, Egleton RD, Davis TP. 2001. Peptide drug modifications to enhance bioavailability and blood-brain barrier permeability. *Peptides* 22: 2329-43

Witt KA, Huber JD, Egleton RD, Davis TP. 2000. Insulin enhancement of opioid peptide transport across the blood-brain barrier and assessment of analgesic effect. *J Pharmacol Exp Ther* 295: 972-78

Wong YY, Markham K, Xu ZP, Chen M, Lu GQ, et al. 2010. Efficient delivery of siRNA to cortical neurons using layered double hydroxide nanoparticles. *Biomaterials* 31: 8770-79

Wu D, Pardridge WM. 1999. Blood-brain barrier transport of reduced folic acid. *Pharmaceutical research* 16: 415-9

Xie L, Li XK, Takahara S. 2011. Curcumin has bright prospects for the treatment of multiple sclerosis. *Int Immunopharmacol* 11: 323-30

Xu Y, Ku B, Cui L, Li XJ, Barish PA, et al. 2007. Curcumin reverses impaired hippocampal neurogenesis and increases serotonin receptor 1A mRNA and brain-derived neurotrophic factor expression in chronically stressed rats. *Brain Res* 1162: 9-18

Yadav KS, Chuttani K, Mishra AK, Sawant KK. 2011. Effect of Size on the Biodistribution and Blood Clearance of Etoposide-Loaded PLGA Nanoparticles. *PDA journal of pharmaceutical science and technology / PDA* 65: 131-9

Yamamoto H, Tahara K, Kawashima Y. 2012. Nanomedical system for nucleic acid drugs created with the biodegradable nanoparticle platform. *Journal of microencapsulation* 29: 54-62

Yang CH, Zhang XJ, Fan HG, Liu Y. 2009. Curcumin upregulates transcription factor Nrf2, HO-1 expression and protects rat brains against focal ischemia. *Brain Res* 1282: 133-41

Yang H, Kao WYJ. 2006. Dendrimers for pharmaceutical and biomedical applications. *J Biomat Sci-Polym E* 17: 3-19

Yang S, Zhu J, Lu Y, Liang B, Yang C. 1999. Body distribution of camptothecin solid lipid nanoparticles after oral administration. *Pharmaceutical research* 16: 751-7

Ye J, Wang Q, Zhou X, Zhang N. 2008. Injectable actarit-loaded solid lipid nanoparticles as passive targeting therapeutic agents for rheumatoid arthritis. *Int J Pharm* 352: 273-79

York RD, Yao H, Dillon T, Ellig CL, Eckert SP, et al. 1998. Rap1 mediates sustained MAP kinase activation induced by nerve growth factor. *Nature* 392: 622-26

Zerial M, McBride H. 2001. Rab proteins as membrane organizers. *Nat Rev Mol Cell Bio* 2: 107-17

Zhang C, Chen J, Feng C, Shao X, Liu Q, et al. 2014. Intranasal nanoparticles of basic fibroblast growth factor for brain delivery to treat Alzheimer's disease. *International journal of pharmaceutics* 461: 192-202

Zhang SL, Li J, Lykotrafitis G, Bao G, Suresh S. 2009. Size-Dependent Endocytosis of Nanoparticles. *Adv Mater* 21: 419-+

Zhang Y, Calon F, Zhu CN, Boado RJ, Pardridge WM. 2003a. Intravenous nonviral gene therapy causes normalization of striatal tyrosine hydroxylase and reversal of motor impairment in experimental parkinsonism. *Hum Gene Ther* 14: 1-12

Zhang Y, Schlachetzki F, Pardridge WM. 2003b. Global non-viral gene transfer to the primate brain following intravenous administration. *Mol Ther* 7: 11-18

Zhang Y, Schlachetzki F, Zhang YF, Boado RJ, Pardridge WM. 2004. Normalization of striatal tyrosine hydroxylase and reversal of motor impairment in experimental parkinsonism with intravenous nonviral gene therapy and a brain-specific promoter. *Hum Gene Ther* 15: 339-50

Zhang YZ, Moheban DB, Conway BR, Bhattacharyya A, Segal RA. 2000. Cell surface Trk receptors mediate NGF-induced survival while internalized receptors regulate NGF-induced differentiation. *J Neurosci* 20: 5671-78

Zhang ZJ, Reynolds GP. 2002. A selective decrease in the relative density of parvalbumin-immunoreactive neurons in the hippocampus in schizophrenia. *Schizophr Res* 55: 1-10

Zhubi A, Veldic M, Puri NV, Kadriu B, Caruncho H, et al. 2009. An upregulation of DNA-methyltransferase 1 and 3a expressed in telencephalic GABAergic neurons of schizophrenia patients is also detected in peripheral blood lymphocytes. *Schizophr Res* 111: 115-22

Zipancic I, Calcagnotto ME, Piquer-Gil M, Mello LE, Alvarez-Dolado M. 2010. Transplant of GABAergic precursors restores hippocampal inhibitory function in a mouse model of seizure susceptibility. *Cell transplantation* 19: 549-64

Zoli M, Guidolin D, Agnati LF. 1992. Morphometric Evaluation of Populations of Neuronal Profiles (Cell-Bodies, Dendrites, and Nerve-Terminals) in the Central-Nervous-System. *Microsc Res Techniq* 21: 315-37